A DYNAMIC STUDY OF STRUCTURAL CONCRETE

A thesis presented for the
degree of Master of Engineering in Civil Engineering
in the University of Canterbury,
Christchurch, New Zealand.

by

D. S. HUNT.

December, 1966.

SYNOPSIS

The properties of prestressed concrete beams under the action of loading similar to that produced in the components of a structural frame during an earthquake have been studied. A Dynamic Loading Unit was designed and built to test three similar pretensioned prestressed concrete beams under transverse reversed cyclic loading. Static load tests were also carried out on two similar beams to provide a comparison. The parameters of particular interest were the stiffness, ductility and mode of failure of the beams and these parameters have been studied and conclusions reached.

ACKNOWLEDGEMENTS

The author wishes to thank the following:

Professor H.J. Hopkins for his overall guidance and support throughout the project.

Mr. J.I. Glanville for his supervision and guidance during the early stages of the project, and Dr. R. Park for his help and constructive criticism during the testing and writing of this thesis.

Mr. H.T. Watson for his technical assistance,

Messrs. A.R. Banks and K.L. Marrion for their efforts in building the Dynamic Loading Unit, and the other members of the technical staff who assisted on this project.

The University Grants Committee for the financial assistance to build the Dynamic Loading Unit.

TABLE OF CONTENTS.

LIST OF PLATES

NOTATION.

The notation used in the text of this thesis is outlined below and in addition is also defined where it appears in the text.

A_s	areas of steel in bottom half and top half of beams (in^2).
b	width of beam (in).
C	compressive force in concrete of beams(Kips).
C'	coefficient for determining the modal frequencies of the beams.
$\bar{C}$	coefficient of speed variation of flywheels.
D'	depth to bottom steel from top compressive fibres (in).
e	strain in concrete or steel(in/in).
E	modulus of elasticity of concrete (p.s.i.).
f_n	frequency of n^{th} mode of vibration of beams (c.p.s.).
F	testing frequency of beams (c.p.s.).
I	second moment of area of cross section of beams (in^4).
I_f	moment of inertia of flywheels ($lb\text{-}in/sec^2$).
M	bending moment (kip-ins).
M_u	estimated ultimate bending moment of beams (kip-ins).
m	mass of beam per unit length ($lb\text{-}sec/in^2$).

$k_u.d$ depth to neutral axis from extreme compressive fibre (in).

L length of beam between supports (in).

P_i total inertial load on beam (lbs).

R reaction at one support of a beam(kips).

T_1, T_2 tensile forces in lower upper pairs of wires respection (kips).

T total tensile force in wires (kips)

$\bar{W}$ weight per unit volume of beam (lbs/ft^2).

w angular velocity of flywheels (rad./sec).

x distance of point considered from nearest support (in).

y deflection at x (in).

ϕ curvature

Subscripts

First subscript	c	concrete
	s	steel
Second subscript	d	dynamic
	s	static
	1,2,---n.	refers to the number of the cycle considered.

1. INTRODUCTION AND SCOPE OF RESEARCH

1.1 Introduction

The true structural response of a multi-storey building to earthquake ground motion is a function of the load-deformation properties of the structural elements, the damping properties of the structure and the gound motion. Nevertheless the analysis of the response is a long and complex problem for which it is necessary, even with the use of large, high-speed computers, to make numerous simplifications. One such simplification is the adoption of either a linear or bi-linear load-deformation relationship for the components of the structure. However at the Third World Conference on Earthquake Engineering Housner[1] reported that there was little known of the true physical properties of the elements of frame structures under strong earthquake conditions. As it is generally accepted that in the more highly stressed regions yielding or cracking of the components will occur during strong earthquakes it was felt that a great deal of further research was needed on the action of structural members under large repeated loads beyond the linear range and also on the resulting failure process.

Although throughout the world prestressed concrete is becoming increasingly popular in structural design, there are doubts in the minds of some architects and engineers of its ability to withstand the reversals of load imposed by earthquakes. Despeyroux[2] reports that there are objections that prestressed concrete has insufficient ductility and that the

energy absorbing capacity is rather low for use in aseismic design. There is a further problem that very little is known of the dynamic load-deformation properties and how they are affected by repeated reversals of load. Previous research on the properties of prestressed concrete under cyclic loading has not considered high intensities of loading, nor has the effect of reversal of loading been considered.

1.2 Scope of Research.

The object of the Experimental Programme was to test a number of similar prestressed concrete beams under forced cyclic loading similar to the type of loading which could be experienced during an earthquake. Three pretensioned prestressed beams were subjected to reversed cyclic loading by a Dynamic Loading Unit which was designed and built specifically for the project. The tests on each beam were divided into three sections:

1. Loading within the linear range at speeds of $\frac{1}{2}$-2 c.p.s. to determine the effects of speed of testing and cyclic loading on the stiffness.
2. A fatigue test where constant maximum and minimum loads greater than the cracking loads were applied to determine the overall stiffness and ductility under cyclic loading.
3. A static test to failure to assess the effect of the cyclic loading on the beam and the resulting mode of failure.

Two similar beams were tested statically for the purpose of comparing the results of the dynamically tested beams, one

of these beams being loaded directly to failure and the other was loaded through $2\frac{1}{4}$ cycles to failure.

2. REVIEW OF PREVIOUS RESEARCH

2.1 Introduction

A material may be said to have failed in fatigue if it has failed under the action of repeated cycles of load, the magnitude of the applied loads being less than the magnitude of the single static load required to cause failure. Van Ornum[3] in 1903 stated "tests of concretes led to the conclusion that brittle engineering materials, of which cement mixtures are a fair type, possess the property of progressive failure or "gradual fracture" which finally becomes complete under the repetition of a load well within the ultimate strength of the material". Since Van Ornum there has been a great deal of further research on fatigue of concrete, (much of which has been published in foreign publications or publications not easily obtained), and this work has been reviewed extensively by Nordby[4] (1958) and Bate[5] (1956). Consequently some of the references to foreign publications may be attributed to one of these sources.

2.2. Plain Concrete.

Nordby attributes the first investigations on "concrete fatigue" to Considerè and De Joly who began work on mortar specimens and published their results in 1898.

Van Ornum[6] tested concrete prisms and over reinforced concrete beams, and his results showed that the stress-strain curve for concrete exhibited the four stages of behaviour shown in fig. 2.1. On the first application of load a convex curve was obtained which was subsequently straightened by the

2nd application of load, i.e. 1st repetition, giving a line almost parallel to the linear portion of the first. The second stage was characterized by a gradual decrease in slope, i.e. decrease in the modulus of the concrete, with the rate of change being related to the maximum load applied. The third stage began relatively near failure and was characterized by the lower portion of the curve becoming concave upwards; this was thought to indicate the initial breakdown of the internal structure. The final stage exhibited a convex curvature at the higher stresses in the specimen. If the prism was tested at a load less than that necessary to cause failure then only the first two stages of loading were produced.

An extensive investigation on concrete under fatigue loading was directed and summarized* by Probst[7] who verified the first three stages of behaviour of the stress-strain curve for prisms under compressive cyclic loading as shown in fig. 2.2. However, there was no evidence of the fourth stage found by Van Ornum but this could be due to a difference in the testing techniques and the type of concrete. The fatigue strength for an indefinite number of cycles was in the range of 47-60% of the ultimate strength and was found to be identical with the stress above which the stress-strain curve would become concave upwards. The static ultimate load was also found to be increased slightly by repetitions of load below the fatigue strength of the concrete, a result which many subsequent investigations have also found.

* The original publications were in German; Nordby reports that important portions of Probst's work remains unpublished in English.

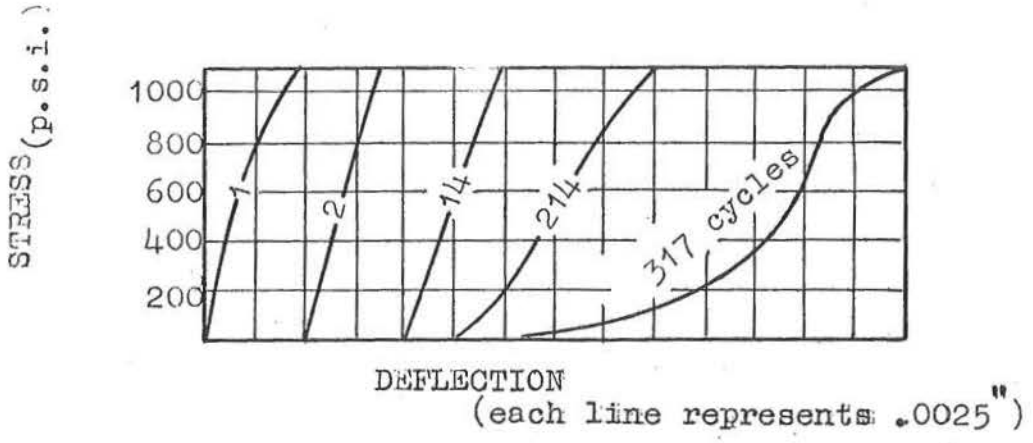

Fig. 2.1 STRESS-STRAIN CURVES for CONCRETE
(Van Ornum[4])

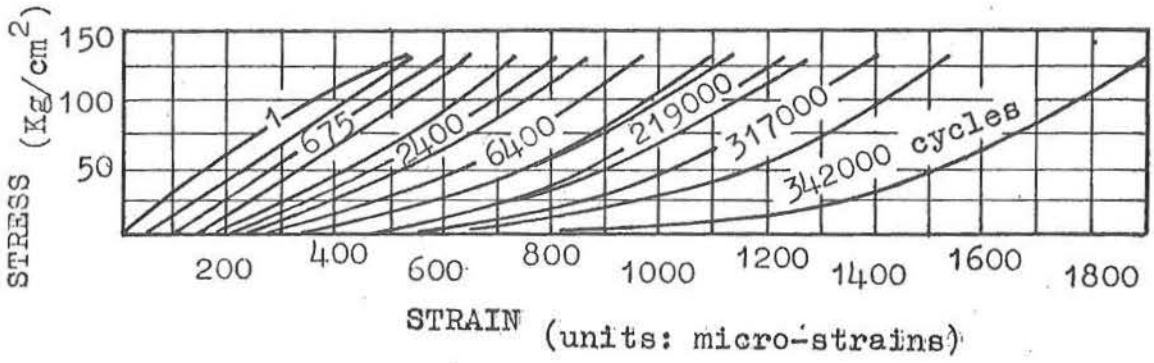

Fig. 2.2 STRESS-STRAIN CURVES for a CONCRETE SPECIMEN LOADED ABOVE the ENDURANCE LIMIT (Probst[7])

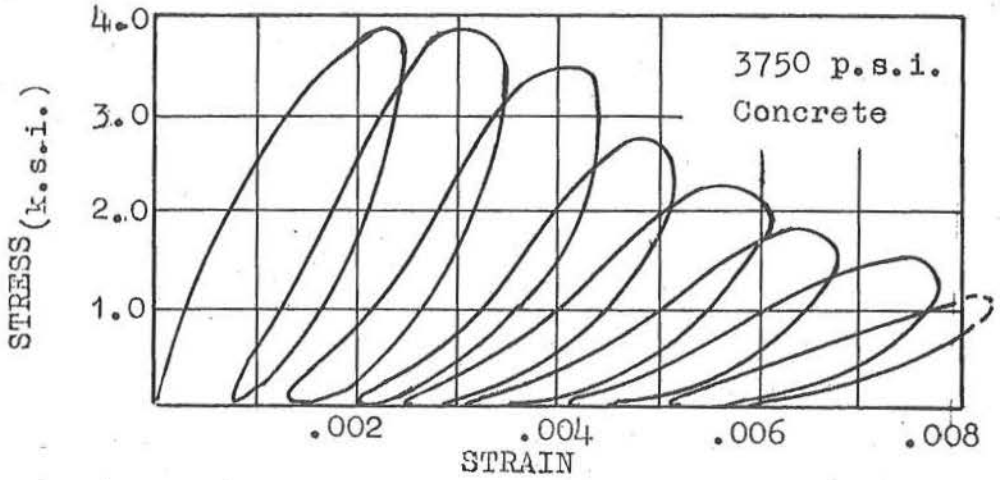

Fig. 2.3 EXPERIMENTAL STRESS-STRAIN CURVES for CONCRETE (Sinha, Gertsle & Tulin[8])

Although the concretes tested by Van Ornum and Probst were inferior to present day concretes, an investigation of the stress-strain properties of plain concrete under cyclic loading by Sinha, Gertsle, and Tulin[8] verified that the stress-strain curve does become concave upwards as shown in fig. 2.3. As the tests were carried out at a speed of 1 cycle/min and at high loads for less than a hundred cycles. the reversal of the stress-strain curve would appear to indicate the degree of micro-cracking and internal damage.

Nordby[3] has summarized the work of Graf & Brenner (originally published in German) who introduced the "modified Goodman Diagram" which is drawn for a nominated number of cycles of load and illustrates the effect of the minimum and maximum stresses on the fatigue strength. Graf and Brenner's results from tests on prisms loaded for 2 million cycles, and shown in fig.2.4, illustrate that as the minimum stress increases the maximum stress also increases. The speed of testing within the range 260-480 c.p.m. had negligible effect on the results but at 10 c.p.m. there was a slight decrease in strength. It was noticed that cracks forming on the side of the prisms did not always result in immediate failure.

Kesler[9] tested small concrete beams in flexure at speeds of 70, 230, 440 c.p.m. and verified that, as for tests in pure compression, the speed of testing had negligible influence on the results. No evidence of an endurance limit for concrete was found, the endurance limit being the stress below which failure will not occur regardless of the number of repetitions of load.

At 10 million cycles the fatigue strength was 55% of the static strength. Subsequent investigations have not indicated the existance of an endurance limit for concrete. In general the fatigue strength of concrete for two million cycles has been found to be 55-65% of the static ultimate strength.

Ople and Hubsbos[10] tested plain concrete prisms in compression with a stress gradient which was produced by applying an axial load to the prism at a known eccentricity. In their results there was a wide range of scatter which tended to decrease as the maximum stress level increased and consequently the results were analysed statistically. The results are shown in fig 2.5. It was stated: "A significant difference in fatigue strength exists between uniformly stressed speciments and non-uniformly stressed specimens, the fatigue strength of the latter being higher". Although this statement implies that the maximum load necessary to produce failure was greater for the non-uniformly stressed specimens the results show the contrary. It is likely that the intended meaning was that the maximum fatigue stress was greater for the non-uniformly stressed specimens. Nevertheless the increase of the maximum stress will not be as great as shown since no account was taken of the stress redistribution across the section at high stress levels. If plane sections remain plane then as the creep rate and permanent deformations are likely to be improportionately greater for the highly stressed fibres, it follows that there will be a stress redistribution. A photograph of a typical fatigue failure of a non-uniformly stressed specimen shows evidence of a stress redistribution

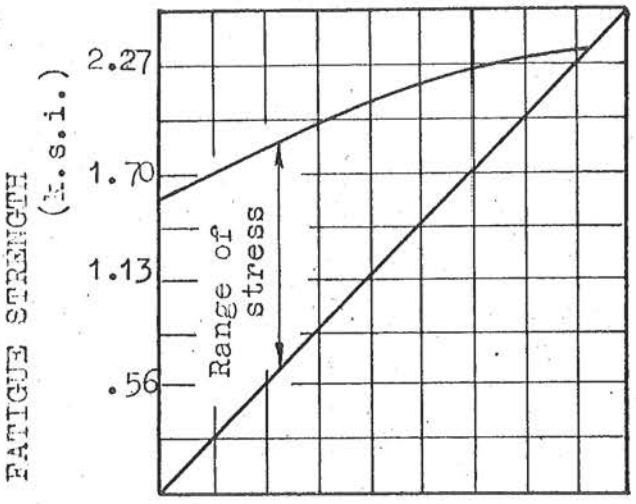

The minimum stress is the 45° line and the maximum stress is the upper curve. Therefore the vertical intercept between the two lines shows the range of stress which may be taken repetitively for a specified number of cycles

Fig. 2.4 MODIFIED GOODMAN DIAGRAM FOR CONCRETE COMPRESSION SPECIMENS (Nordby[4])

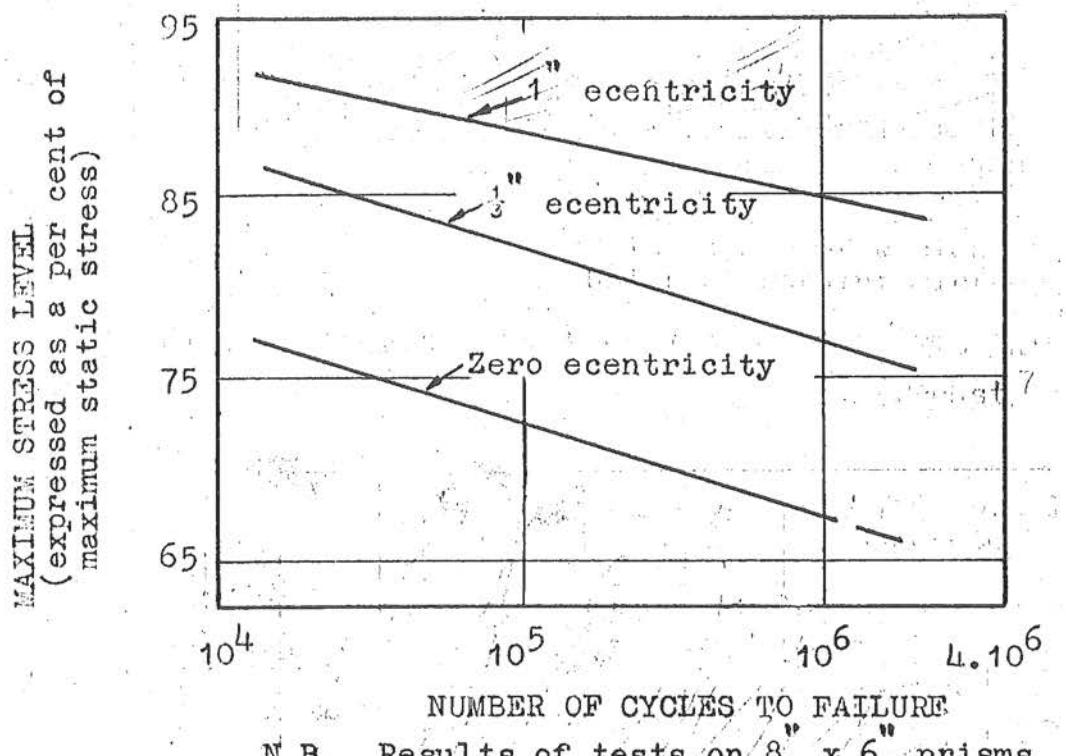

N.B. Results of tests on 8" x 6" prisms

Fig. 2.5 MAXIMUM STRESS VERSUS FATIGUE LIFE (Ople and Hulsbos[10])

due to a wide tension crack in the prism after failure. However the results illustrate that for a particular maximum stress level the fatigue life, i.e. the number of cycles of load necessary to cause failure, increases as the stress gradient increases. Therefore the application of results from uniformly stressed specimens in the design of reinforced and prestressed concrete members will lead to a lower bound result.

2.3 Bond.

Van Ornum was one of the first to study the effect of fatigue loading on the bond between concrete and steel. When testing the "over-reinforced" concrete beams diagonal cracks formed and it was stated "it appears that the gradual and progressive destruction of the adhesive bond of the concrete to the steel produced a vital influence upon the phenomenon". During the test, and starting in the centre of the beam, the bond was destroyed and slip occurred causing small striations on the steel.

In 1940 Lea[11] tested the pull-out strength of $\frac{1}{2}$" dia bars embedded in concrete such that at failure the concrete as well as the steel was in tension. After 10 million cycles, at 2000 c.p.m., the fatigue bond stress was 300 p.s.i. which was 50% of the static pull-out bond stress.

Muhlenbruch[12,13] investigated the pull-out strength of (a) $\frac{5}{8}$" dia hot rolled deformed bars (b) $\frac{5}{8}$" dia bars with a smooth surface, embedded in concrete (f'_c = 3000 p.s.i.) The results showed that the plain reinforcing bars slipped considerably

more at lower repeated loads than the deformed bars. The effect of the repeated loads on the bond strength is shown in fig. 2.6, and illustrates the reduction of the static pull-out bond stress for deformed bars when preceded by repeated pull-out loads. The higher the ratio of the repeated pull-out load to the static pull-out load the lower the pull-out stress after such repetitions. The results of tests on plain bars were variable and the investigation indicated that the performance of the deformed bars was superior.

Nordby in a more comprehensive summary reports that failures at low stresses are possible and that until that time (1958) the results had shown a wide degree of divergence.

2.4 Reinforced Concrete.

Van Ornum[6] probably made the most valuable early investigation of the fatigue characteristics of reinforced concrete when he tested 82 beams specifically designed to collapse by compression failure alone; the testing speed was 2-4 c.p.m. Failure was initiated by tension cracks which were followed by diagonal shear cracks and these led to a compression failure of the concrete near the loading point.

Probst[7] and associates investigated the formation and propogation of cracks in reinforced concrete beams and their influence on the static ultimate load. In the fatigue tests the load at which cracks developed after a million cycles was half that necessary to cause cracking in a single static load test. During the test the cracks breathed, i.e. they opened and partially closed during each cycle. A range of differently aged

beams was tested and the deflections of the older beams became stable after a lower number of cycles than did their younger counterparts. It was found that providing the steel stresses during the fatigue loading did not exceed the yield stresses the static ultimate load remained practically unchanged.

Saliger[14] tested concrete beams reinforced by various types of steel to determine the effect of the steel properties on the behaviour of the beams. The cracks in beams reinforced by steel with a high yield point did not penetrate as rapidly as beams with normal reinforcement and the elastic range was also greater because of the reduced elongation of the steel. For beams given a preliminary fatigue test the total and permanent deformations produced in a subsequent static test were less than those for beams tested statically without being subjected to previous testing. This was probably due to the effect of the permanent strains in the concrete being removed by the preliminary testing. From the translated summary it would appear that the performance of the beams was improved by the use of high strength bars as reinforcing. After several million cycles of load, the maximum being 55% of the static ultimate load, there was no reduction of the static ultimate load, nor of the bond or shear resistance.

Bate[4] summarized the work of Le Camus who tested beams specifically designed to fail in (a) fatigue of the longitudinal reinforcement, (b) fatigue crushing of the concrete, (c) fatigue of the concrete in shear. The ranges of loading were: (a) 6-60%, (b) 5-68%, (c) 6-48% of the static ultimate loads respectively.

The increase of the static strength after one million cycles was (a) slight, (b) 6-10%, (c) nil. These results would appear to verify a strain-hardening effect for concrete subjected to repeated loads of intermediate intensity.

Chang & Kesler[15] tested 39 small reinforced concrete beams in fatigue. Three types of failure were produced:

1. 23 beams failed by destruction of the compression zone at the end of a diagonal tension crack which started in the shear span and developed towards the loading point.
2. 11 beams failed by diagonal cracking, the beams failing immediately after the crack developed.
3. 2 beams failed by fatigue of the reinforcement in the region of pure flexure. The two beams which did not fail by fatigue were tested statically, the results showing that neither the diagonal tension cracking load nor the ultimate load were affected. The fatigue strength was approximately 60% of the static strength at a million cycles.

In a second paper[16] 25 similar reinforced concrete beams, designed to fail in flexure at a load only slightly less than the load causing a shear failure, were tested. Fourteen beams failed by fatigue of the tensile reinforcement in the region of pure flexure; four beams failed simultaneously by diagonal cracking and shear compression after the development of a few tensile cracks; four beams failed by shear compression failure following the development of diagonal tension cracks; and three beams did not fail. The type of failure was found to be dependent on the magnitude of the applied load and generally high fatigue loads

led to shear failures while lower loads tended to cause flexural failures. This may have been caused by a change in the ratio of the stresses in the concrete and steel, and their different fatigue strengths.

Verna and Stelson[17] tested a range of 60 reinforced concrete beams to determine the modes of failure for static and fatigue loading. Beams weak in bond were found to be susceptible to fatigue damage and failure after a relatively low number of cycles and the type of beam which failed by bond statically always failed by bond in fatigue. A bond failure could be readily identified by a rapid early increase in the deflection. If a beam failed statically by either a tension, compression, or diagonal tension failure then in a fatigue test the mode of failure would have been found to be dependent on the load level, as found by Chang & Kesler, as well as on the static failure mode. In a second test series[18], four groups of four reinforced concrete beams were designed for three different modes of failure. The object was to assess the effect on the static ultimate load of fatigue loading for 10,000, 33,000, and 100,000 cycles at a peak load which normally would have produced a 40-55% decrease in the beam strength "after 1,000,000 or more cycles". The reinforcement was "intermediate grade steel" and the results are shown in fig. 2.7. Unfortunately although the investigation was made by a Ph.D candidate no suggestions were given for the large increases in the tensile strength. Nor were there any suggestions why smaller increases followed by decreases for the diagonal tension strength should have occurred.

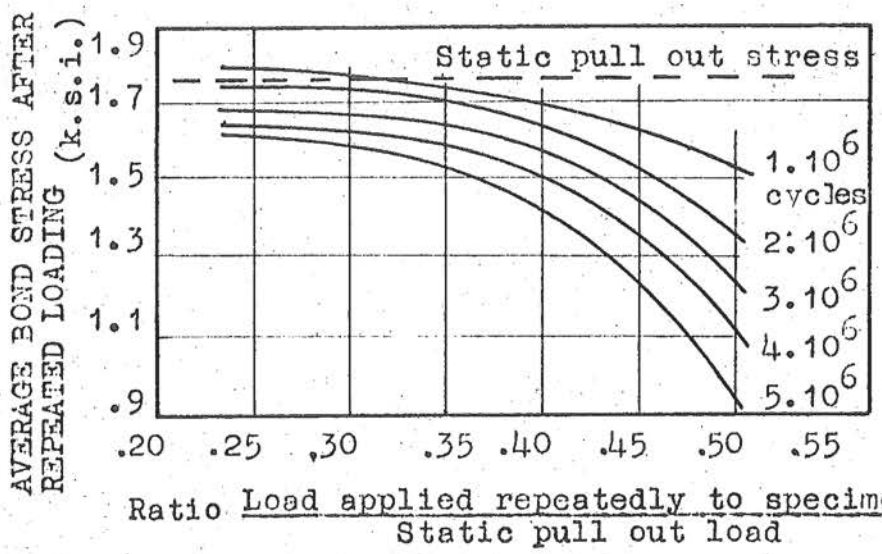

Results of pull out tests on deformed bars.

Fig. 2.6 EFFECT OF REPEATED LOAD ON BOND STRENGTH (Muhlenbruch [13])

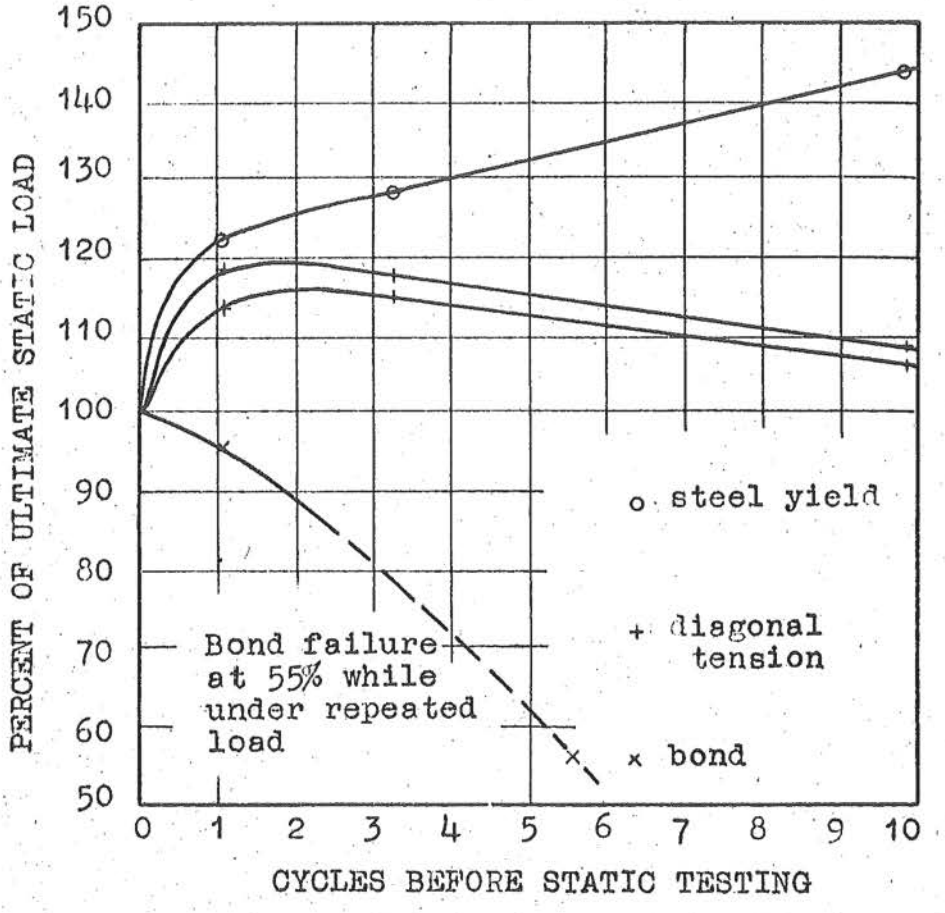

Fig. 2.7 EFFECT OF CYCLES OF LOAD ON ULTIMATE STRENGTH (Verna and Stelson[18])

2.5 Prestessed Concrete.

Freyssinet[19] conducted the first fatigue tests on Prestressed Concrete when he tested two telegraph posts with similar ultimate loads, one being prestressed concrete and the other reinforced concrete. In the fatigue test the maximum load was 50% of the static ultimate load and the load was completely reversed during each cycle. It is reported that the reinforced concrete post had failed after "a few thousand cycles" whereas the prestressed post was still in a good condition after 500,000 cycles. However, the results are merely of historical interest.

Abeles[20] compared the performance of prestressed concrete railway sleepers which had been in use for $2\frac{1}{2}$ years and in that time subjected to an estimated 4 million cycles of loading (150,000 being at "larger" loads), with similar unused sleepers. No significant difference was found between the performance of the old and new sleepers and the steel concrete bond was not affected in any way. However there is no indication of the stresses produced while the sleepers were in use. Bate[5], reports that Le Camus; Jacquemenin; and Thomas while testing prestressed concrete railways sleepers found that the use of embedded positive anchorages gave better resistance under repeated loading than when the bond between the steel wires and concrete was relied on alone. Results of tests on sleepers prestressed by plain or indented wires show little difference in the performance of the sleeper; at failure the indented wires fractured and the plain wires slipped.

Abeles[21] tested 3 partially prestressed concrete beams

in fatigue. The beams were loaded statically prior to the fatigue test to produce cracks which "breathed" in the fatigue tests, but which become invisible during rest periods; fatigue failures occurred when the wire fractured. As failure was approached the bond and friction adjacent to the cracks were destroyed and on opposite sides of the beam there were differences in the crack widths.

Hanson[22] tested pretensioned concrete beams prestressed by either clean or rusted wires. The results showed that all beams in the fatigue test failed through loss of bond although the maximum observed bond stresses were greater for the rusted wires. For the clean wires the fatigue life, i.e. the number of cycles to failure, decreased greatly for a relatively small increase in the maximum load and the flexural bond always failed before the prestress transfer bond failed. Low amplitude, high frequency vibrations to 10 million cycles did not produce any significant changes of the bond stresses along the wires.

Ozell and Ardaman[23] tested beams prestressed by seven wire strands with compression reinforcement to ensure a tension failure of the strand. Examination of the fractured surface of the wires showed that only one or two failed in fatigue, the remainder being essentially static failures because of the resulting imposed overloads.

Bate [24-25] investigated the properties of (a) beams prestessed by wires with various surface conditions to determine the effect on the fatigue strength (b) beams prestressed by strand subjected to either static or dynamic loading (c) Pre-

stressed and Reinforced concrete beams to compare their relative abilities to withstand fatigue loading. In the first section of the investigation, on composite Tee Beams, the use of deformed wires led to the development of higher stresses in the steel at failure than were obtained with plain rust free wires. However, the range of the fatigue stress at one million cycles was greater for the plain rust free wires than for the deformed wires and the range of stress for the plain wires was unchanged by rusting sufficient to improve the bond.

In the second section of tests, also on composite Tee Beams, it was found that the fatigue resistance at 1,000,000 cycles of beams stressed with strand was inferior to that for beams stressed with plain wire but slightly superior for beams with deformed wires. Had the comparisons been made at 100,000 cycles the results would have been more favourable to the strand but at 10,000,000 cycles the results would have been less favourable to the strand. Although no reason is given for this observation it is possible that it may be connected with the bond and the bond slip. An examination of the fractured wires in the strand after the tests did not reveal any evidence of fretting corrosion.

For both the reinforced concrete and prestressed concrete beams during fatigue loading the total deflections were slightly greater than in the static tests and for the reinforced concrete beams the increase in the size of the cracks was insignificant. Nevertheless for the prestressed concrete beams prior to cracking the stiffness, as shown by the range of deflection,

tended to be greater for beams subjected to repeated loadings. After the prestressed concrete beams cracked during fatigue tests the development of the cracks was more rapid than for similarly overloaded reinforced concrete beams. The average maximum applied load for the prestressed concrete beams, rectangular in section, which survived 3,000,000 cycles, ranged from 65-85% (average 73%) of the estimated static ultimate strength, with the failure load in the subsequent static test ranging from 92-104% (average 99%) of the estimated ultimate load. The prestressed concrete beams with smaller percentages of steel failed by fracture of the steel and those with greater percentages by crushing of the concrete.

Venuti[27] fatigue tested 90/$4\frac{1}{2}$" x 6" pretensioned prestressed concrete beams with 2/$\frac{3}{8}$" dia seven wire strands to failure. If after five million cycles failure had not occurred the test was stopped and the beam tested to failure statically. The predominant mode of failure for beams tested in fatigue at 60% and 70% of the static ultimate load was a tension failure, i.e. fracture of the strands, whereas for the beams tested at 80% or 90% of the ultimate load the predominant mode of failure became a compression failure of the concrete. Of the beams tested at a maximum load of 50% eleven out of eighteen had not failed after 5,000,000 cycles and these beams exhibited only a very slightly decreased ultimate load at failure. At all load levels those beams which failed in compression showed a faster rate of decrease of flexural stiffness and the fatigue life was generally shorter than for the beams failing in tension. A statistical analysis showed that the variability of fatigue

life increased as the maximum applied load increased. The fatigue strengths, at a million cycles, of the beams tested by Venuti and those tested by Bate, in the third section of his investigation, were not equal since the stresses produced in the concrete and steel at equal relative load levels were different. Hence the results of the two investigations may only be compared if it is kept in mind that the ratio of the stresses in the steel and concrete in each series of beams were different.

2.6 Summary.

Many of the early investigations were made on concretes which are inferior to present day concretes and it is therefore necessary to exercise care when interpreting the results of early research. For fatigue loading:

(a) The stress-strain curve for plain concrete changes in shape.

(b) The speed of testing does not influence the results except when the testing speed is slow.

(c) The bond strength for plain wires is reduced substantially and is also variable. The condition of the bond greatly influences the fatigue life and mode of failure. (An extensive investigation of bond under fatigue is required).

(d) The mode of failure of reinforced and prestressed concrete is influenced by the static mode of failure and the magnitude of the repeated load. The probable reason is a change in the ratio of stresses in both the concrete and the steel as the load increases.

(e) The fatigue strength of reinforced concrete and prestressed

concrete beams is dependent on the properties of the section i.e. the steel properties, the area of steel, the prestressing forces, the shape of the section and the crushing strength of the concrete.

(f) To compare the results of different tests it is necessary to analyse the stresses within the concrete and steel, before making the comparison.

3. DESIGN OF APPARATUS FOR DYNAMIC TESTS.

3.1. Introduction

The testing of prestressed concrete beams under loading similar to that produced in the components of a structure during an earthquake required a machine for applying reversed cyclic loadings at frequencies within the range of .5 - 5 c.p.s. As the seismic motion of a building is generally assumed to be sinusoidal it was necessary that the machine (which will be referred to as the Dynamic Loading Unit) subject the beams to sinusoidal or approximately sinusoidal motion with approximately equal maximum positive and negative loads. A further requirement was that it should be possible to vary the magnitude of the maximum loads without stopping or slowing down the Unit. The Dynamic Loading Unit was designed to apply maximum loads of up to 4 tons.

As the normal methods of measuring the load could not be used it was necessary to incorporate a load-cell in the Dynamic Loading Unit and record the output from the cell automatically on an oscilloscript. Deflection gauges for measuring the maximum and minimum deflections were also required and the output from the gauges was also recorded by the oscilloscript.

3.2. Dynamic Loading Unit.

3.2.1. General Principles.

A general plan of the Dynamic Loading Unit is shown in fig 3.1 and general views of the Unit are shown in Plates 1 and 2. The Unit consisted of an eccentric "Crankpin" mounted on the "Main Disc" and connected to the beam by the linkage system shown in fig 3.4. The main disc is shown in Plate 3.

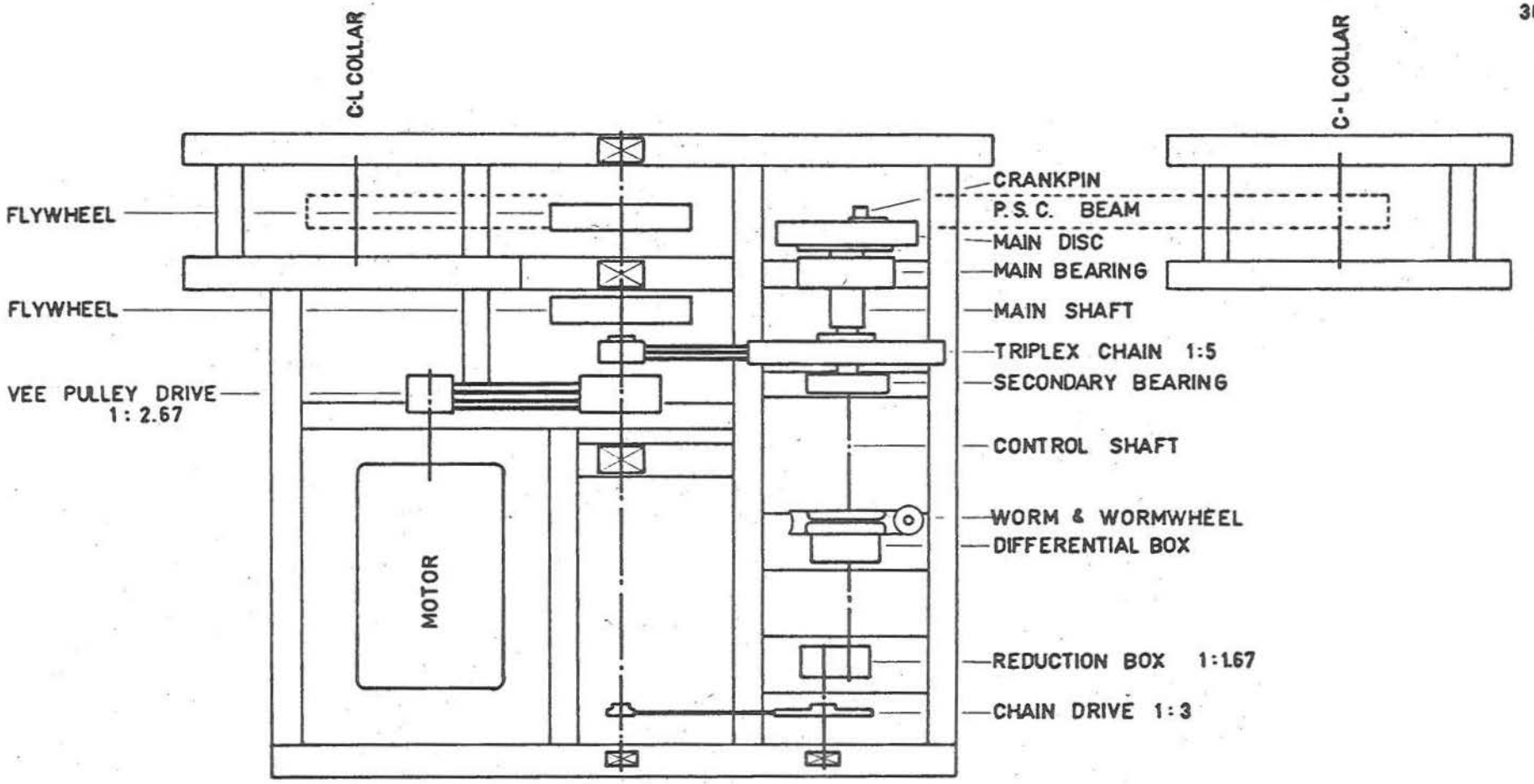

FIG. 31 PLAN OF DYNAMIC LOADING UNIT

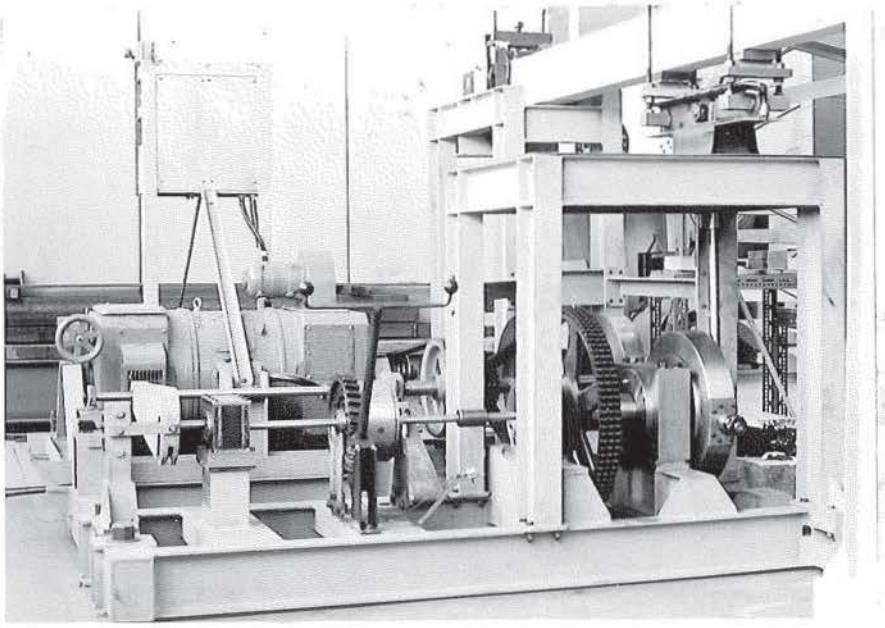

Plate 1. DYNAMIC LOADING UNIT. General view showing the general layout and Beam 3 prior to testing.

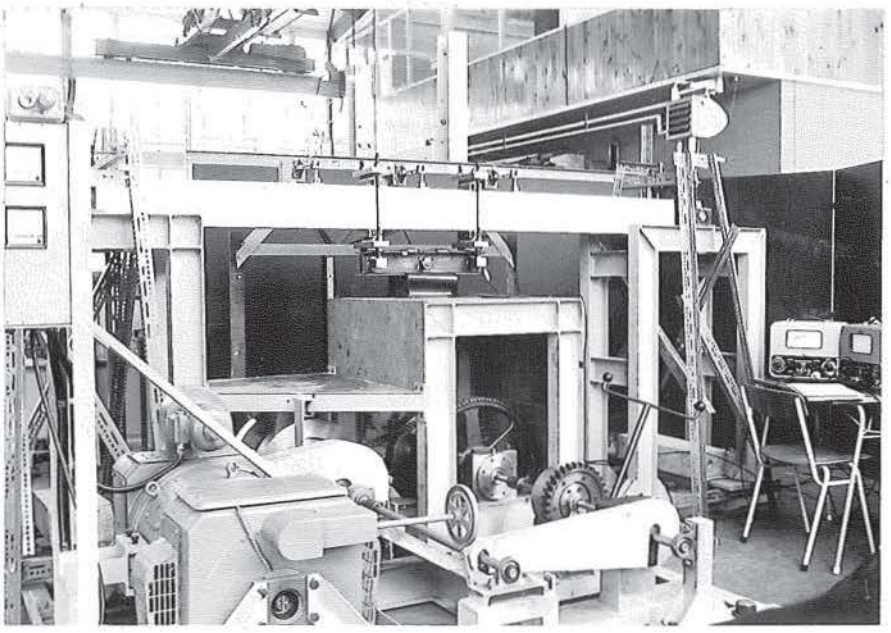

Plate 2. DYNAMIC LOADING UNIT. General view showing main dis and shaft, main bearing housing, triplex chain, differential box and reduction box with motor behind

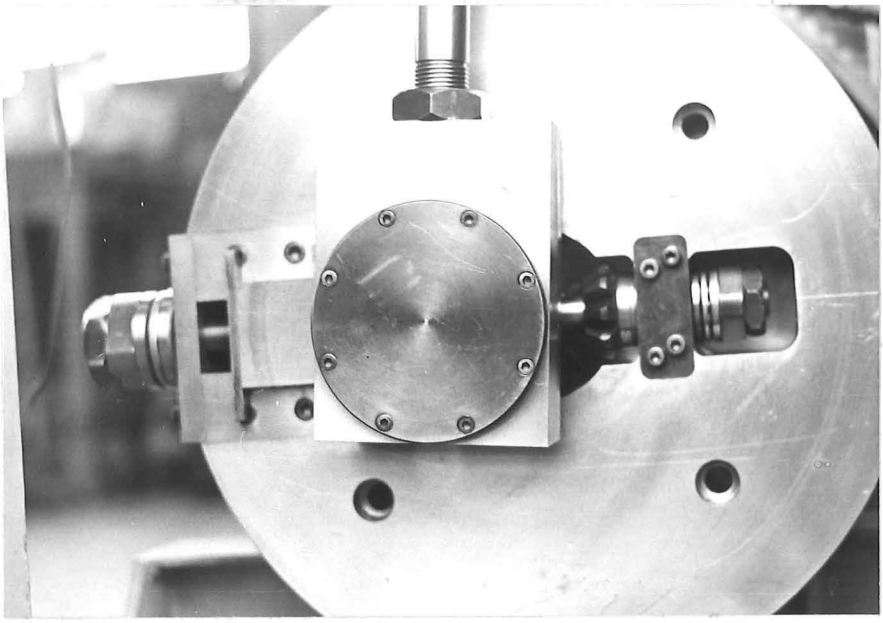

Plate 3. MAIN DISC. Side view showing the main screw together with the thrust bearings and the small bevel gear. Also shown are the conrod and mild steel bearing housing and a small portion of the slide.

The throw, i.e. the ecentricity, of the crankpin could be changed without altering the speed of the machine by rotating the "Differential Box" with the worm and worm-wheel. Hence the maximum loads applied could be varied during a test because the throw of the crankpin and the maximum displacement of the beam at the loading points were the same. The Unit was driven by a 15 H.P. variable speed motor. The drive from the motor to the main shaft was through vee belt and triplex chain drives and the overall speed reduction from the motor to the main shaft was 13.3.

The maximum throw of the crankpin was 3 inches and the maximum allowable torque in the main shaft was limited to 4.9

ton inches by the tensile capacity of the main driving chain. The applied torque was proportional to the maximum applied load, the maximum deflection of the beam and a Beam Factor which was a function of the load deflection curve and was less than unity. For the design the load-deflection curves of the prestressed beams were assumed to be cubic parabolas for which the Beam Factor was .76.

Where the stress of a component was critical a load factor against failure of 5 was adopted except for the main driving chain where the manufacturer recommended a minimum load factor of 20.

3.2.2. Main Assembly.

The "Main Assembly" of the Dynamic Loading Unit is shown in fig. 3.2. The crankpin and slide were machined from a 6" x 4" high tensile strength bar as fabrication of the two parts and welding were undesirable. The slide and crankpin were mounted in the milled slot of the 17½" dia. "Main Disc" shown in Plate 3. The main disc was bolted to the flange of the "Main Shaft" which was fabricated from mild steel bars and plate as shown in the figure. It was specified that the welds should be of radiographic (i.e. very high) standard because they occurred in regions of high stress where pockets of slag or blowholes could have caused stress raisers and fatigue failure. High tensile steel was used for the shoulders of the slot to reduce wear and to take the impulsive transverse loads from the crankpin and slide.

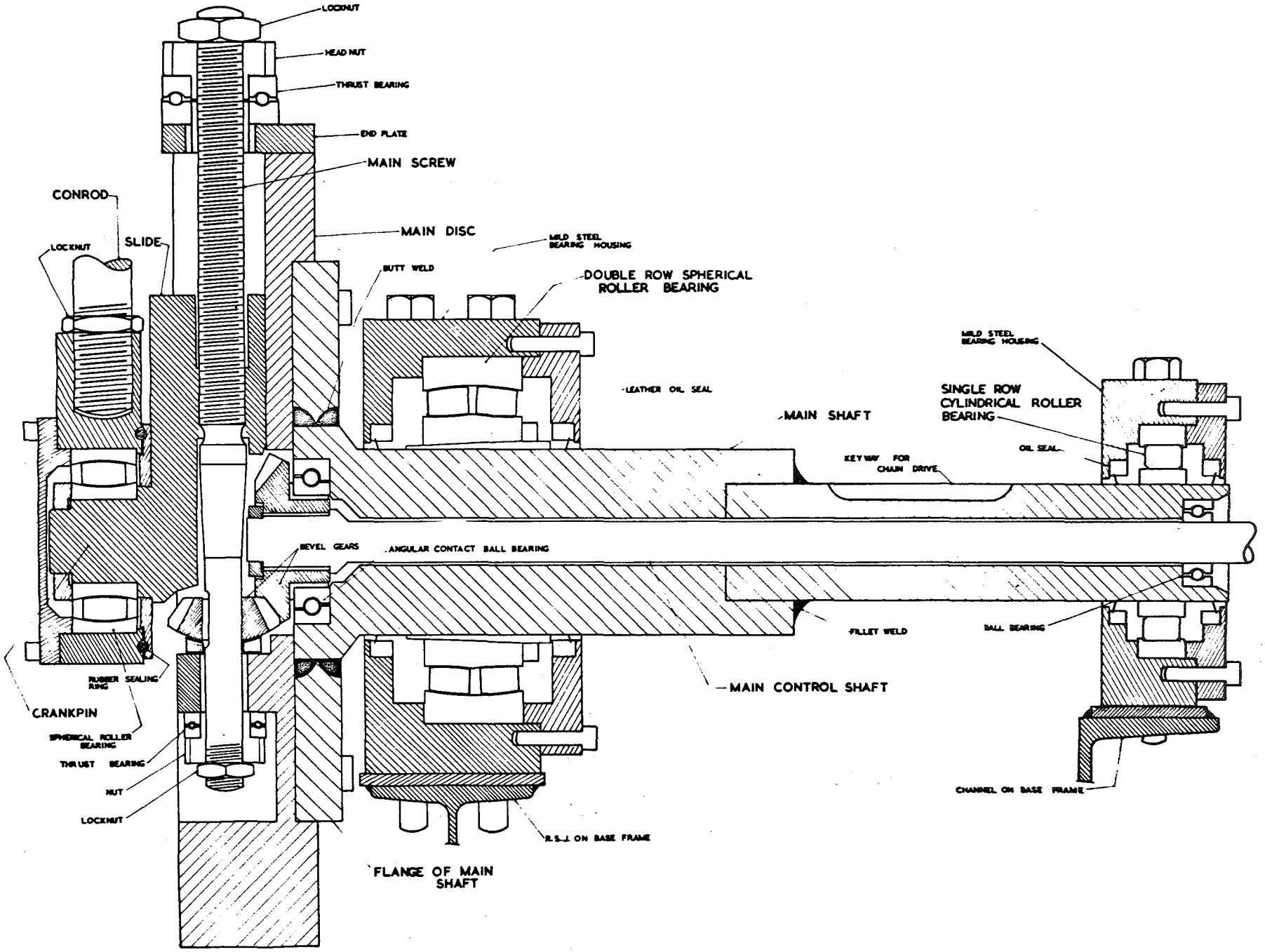

FIG. 3.2 MAIN ASSEMBLY

The ecentricity of the crankpin was controlled by the high tensile steel "Main Screw" which was connected through two bevel gears to the "Control Shaft" mounted concentric and within the main shaft. Thrust Bearings were mounted at each end of the main screw so that it could be rotated easily and precautions were taken at the ends of the screw threads to reduce the possibility of a fatigue failure. When the control and main shafts rotated at identical speeds there was no rotation of the main screw about its longitudinal axis and therefore there could be no change of throw of the crankpin. However when the two shafts rotated at different speeds the main screw rotated transversely and changed the throw of the crankpin. For each additional revolution of the control shaft relative to the main shaft the main screw turned through 1.6 revolutions as the bevel gear ratio was 1 : 1.6.

The main assembly was mounted in two bearings which were selected from the manufacturers design tables. The principle bearing was a double row Spherical Roller bearing while the second bearing was a cylindrical roller bearing. The bearing housings were machined from mild steel blocks to reduce their width so that the distance from the crankpin to the centre line of the main bearing could be reduced to a minimum and thereby reduce the maximum bending stresses in the main shaft. Both the bearings were oil lubricated and were sealed by sprung loaded, single lipped leather oil seals.

3.2.3. Differential Box.

The purpose of the differential box was to vary the

speed of the control shaft relative to that of the main shaft. The box consisted of an epicyclic train of bevel gears from a car differential mounted in a frame which formed part of the case of the box as shown in fig 3.3. The box was mounted so that the case and therefore the gear train could be turned by the worm and worm-wheel. The shaft leading into the differential box from the reduction box revolved at the same speed as the main shaft but in the opposite direction. However the epicyclic reversed the direction of rotation so that the control and main shafts rotated at identical speeds and in the same direction when the case of the differential box was stationary.

When the differential box was rotated the epicyclic gears caused the speed of the control shaft, i.e. the output shaft from the differential box, to change relative to that of the input shaft and for each revolution of the box the control shaft either made or lost two revolutions relative to the input shaft. Hence for each revolution of the box the control shaft turned through two revolutions relative to the main shaft of the Unit and the main screw turned transversely through 3.2 revolutions. The reduction of the worm and worm gear was 32 : 1 and therefore one revolution of the control handle, i.e. the worm, produced one tenth of a revolution of the main screw. As there were 12 threads per inch on the main screw the corresponding change of throw was .0083".

A revolution counter was attached to the end of the main control shaft and the throw of the crankpin was calibrated against the number of turns of the shaft.

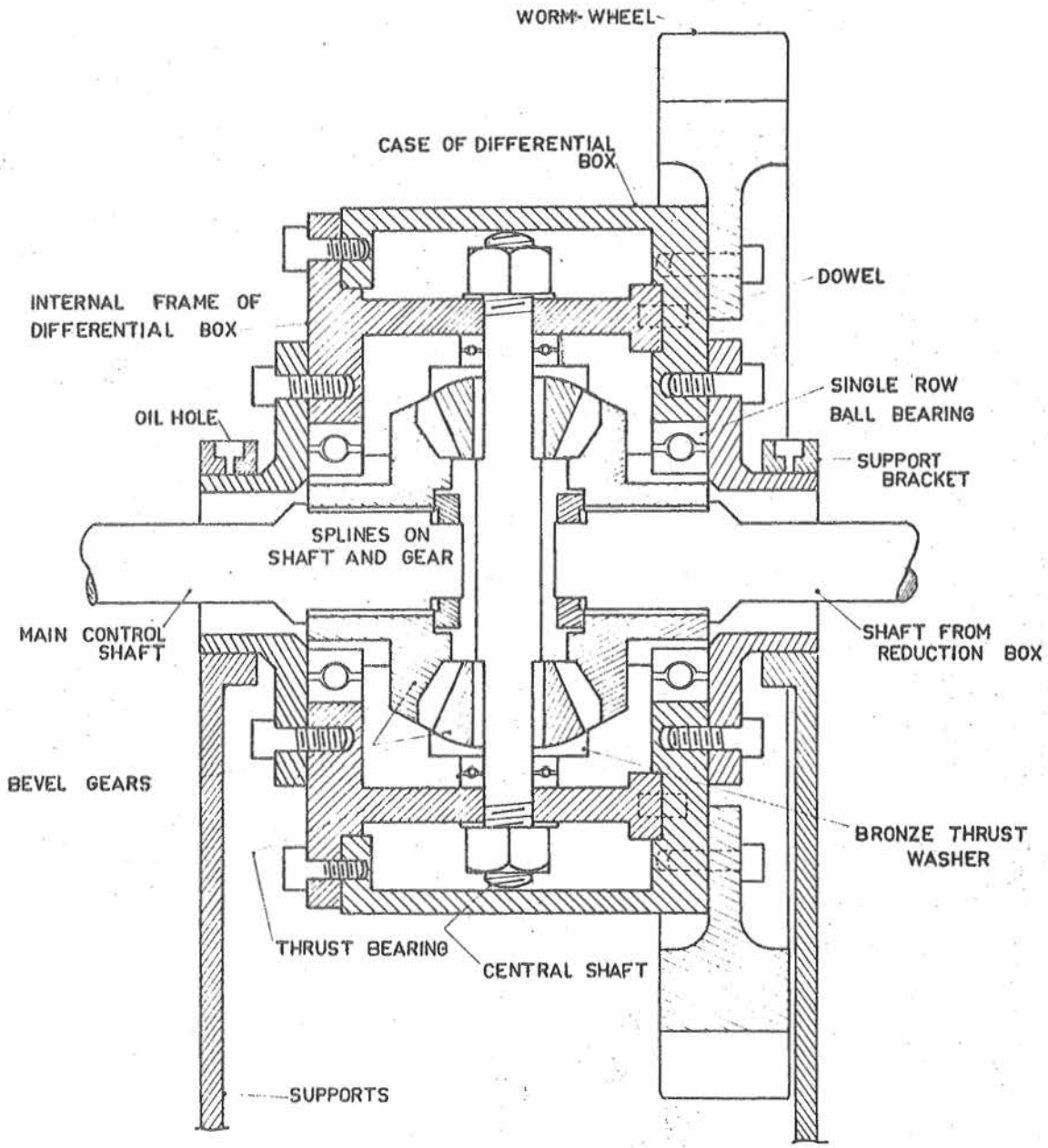

FIG. 3.3 CROSS-SECTION THROUGH THE DIFFERENTIAL BOX

3.2.4. Transmission System.

To ensure that the main shaft and control shaft rotated at identical speeds when the differential box was stationary it was essential that all the drives other than that from the motor to the flywheel shaft be positive, i.e. be either chains or gears.

The two principal drives were the motor-flywheel shaft drive and the flywheel shaft-main shaft drive. The former was a 4B Vee Belt Drive with a speed reduction of 2.67 while the latter was a $\frac{3}{4}$" triplex chain drive with a speed reduction of 5 giving an overall reduction of 13.3. The design charts showed that the vee belts could safely transmit 2 H.P. at 250 r.p.m. and 11 H.P. at 2500 r.p.m.; however the load-speed relationship was not linear.

The maximum safe torque which could be transmitted by the chain drive was 4.9 in-tons as the impulsive loading necessitated a load factor of 20 for the tension in the chain. The torque transmitted was a multiple of the load, the throw and the Beam Factor and as the Beam Factor was .758 for a load-deflection curve the shape of a cubic parabola the multiple of the load and throw could not safely exceed 6.5 in tons. The Beam Factors for a number of Load-Deflection curves are discussed in Appendix A.

3.2.5. Flywheels.

The flywheels were incorporated in the Dynamic Loading Unit to protect the motor from the large impulsive reversals of torque and load. The design was based on the torque angle

diagram for the main shaft shown in fig. A.1. Appendix A. Normally flywheels are designed to supply the fluctuations of energy in the machinery through changes in their Kinetic Energy due to small speed variations which are assumed to be not greater than 1% of the mean speed. The change of Kinetic Energy, as shown below, is proportional to the Moment of Inertia of the flywheel (I_f), the square of the angular velocity (w), and a speed variation factor ($\bar{C}$).

$$\text{Change of Energy} = I_f w^2 \bar{C}$$

The equation shows that the performance of the flywheels is improved by increasing the flywheel shaft-main shaft speed ratio. However, the energy capacity of the flywheels was insufficient to supply the total variations of energy at maximum load without relatively large variations of speed and hence the principal function of the flywheels was to reduce the peak impulsive load acting on the motor. An analysis of the energy capacity of the flywheels is presented in Appendix A.

3.2.6. Motor.

The motor used to drive the Unit was a constant torque Shraeger motor with an infinitely variable speed range of 250 - 2500 r.p.m. and with a rated capacity of 15 H.P. at 2500 r.p.m.

3.2.7. Base Frame and Supports.

The base frame of the Dynamic Loading Unit was made as rigid as possible and was bolted to a structural testing floor. The supporting frames were also designed for rigidity, especially the frame providing the lateral restraint for the reciprocating piston in the linkage system described in the following section.

3.2.8. Linkage System.

The linkage system, shown in fig 3.4, consisted of the conrod, reciprocating piston and guiding sleeve, load cell, distribution beam and beam stirrups. To reduce the lack of fit in the system all the connections were made with minimum tolerances. The conrod was a $1\frac{1}{4}$" dia. shaft with a spherical roller bearing within a mild steel bearing housing at the lower end to connect it to the crankpin, as shown in fig 3.2. The head of the conrod was connected by a silver steel gudgeon pin to the piston which was essentially a thick walled cylinder. The purpose of the piston was to convert the circular motion of the crankpin to vertical motion and to transfer the horizontal component of the force in the conrod through the sleeve to the frame of the Unit so that the load-cell and beams were subjected to vertical loading only. Experience showed that it was necessary that the internal surface of the steel sleeve be of a relatively soft material and that the area of contact between the sleeve and piston be well lubricated and clean. Hence a bronze liner was incorporated within the sleeve and the sliding surfaces were lubricated by the gravity feed oil system, shown in fig. 3.4. Double lipped sprung loaded, leather seals were found to be the only satisfactory means of sealing the ends of the sleeve.

The load cell was screwed into the piston and is described fully in section 3.4.

The distribution beam consisted of two channels welded $\frac{7}{8}$" apart and was connected to the beam by external stirrups.

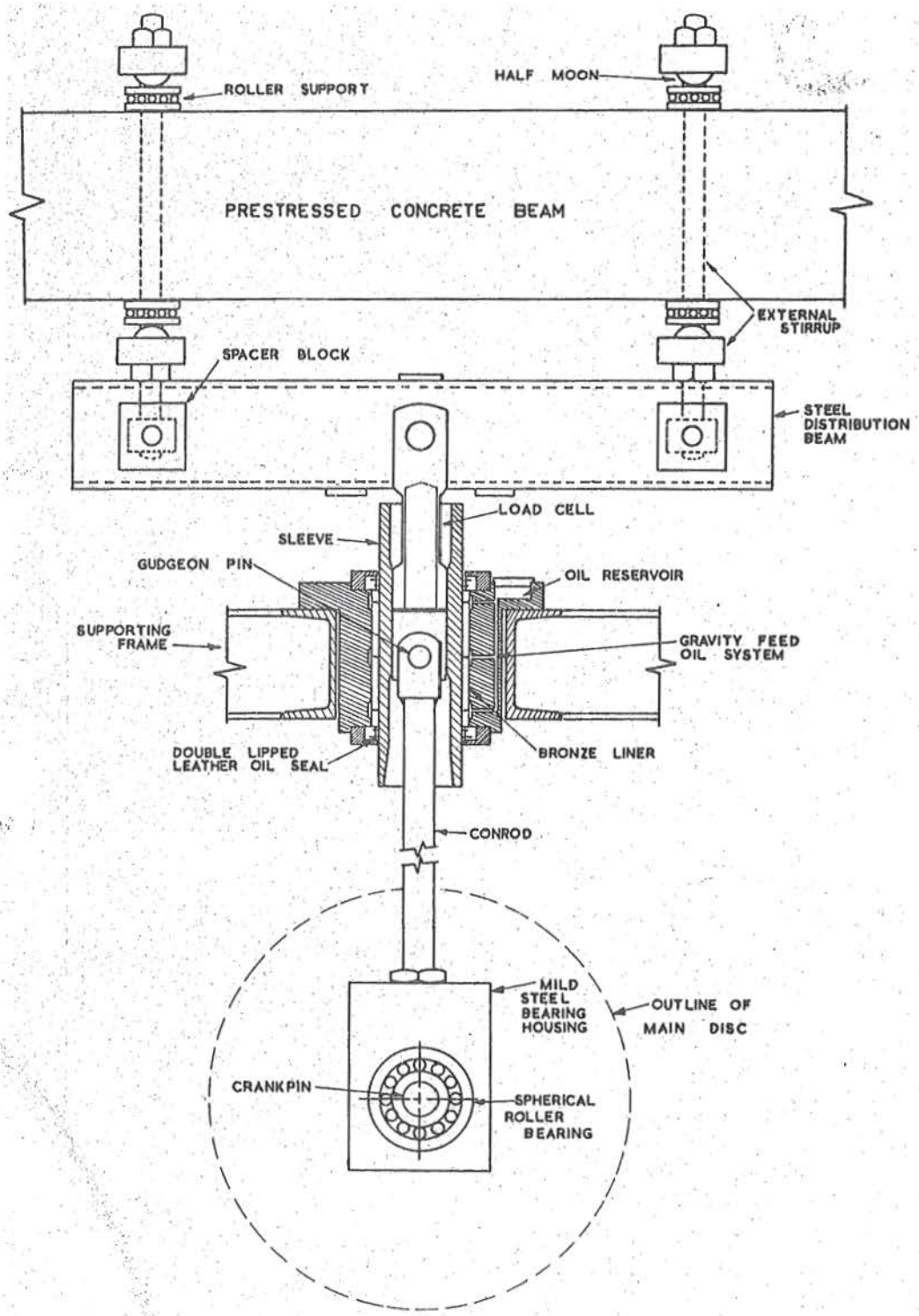

FIG 3.4 LINKAGE SYSTEM

Locknuts were used on the stirrups to clamp the beam rigidly to the linkage system and also to reduce the local compressive forces on the upper and lower faces of the beam before the load was applied.

3.2.9. End Collars.

The end collars, one of which is shown in Plate 4, formed the supports for the ends of the beams. The beam was supported between plates as shown in fig. 3.5 between which $\frac{1}{4}$" dia. rollers were placed if longitudinal movement of the beam was to be allowed. The plates were rigidly clamped to the beam by the two $\frac{3}{4}$" dia. bolts with the 5/16" dia. Allen screws keeping the plates stable. The Collars could rotate freely in the bearing blocks which were bolted

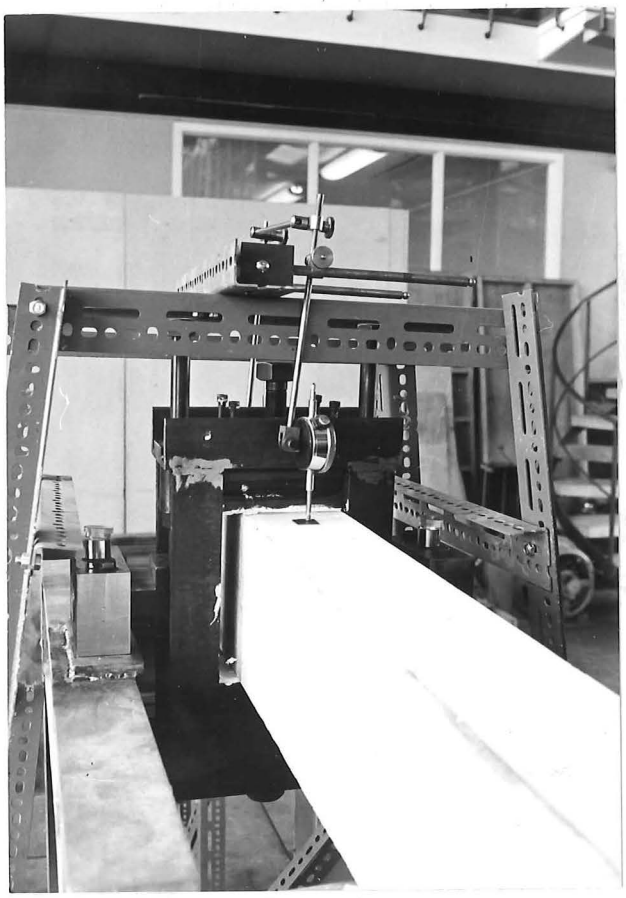

Plate 4. END COLLAR. Also shown is a dial gauge mounted in a dexion frame support.

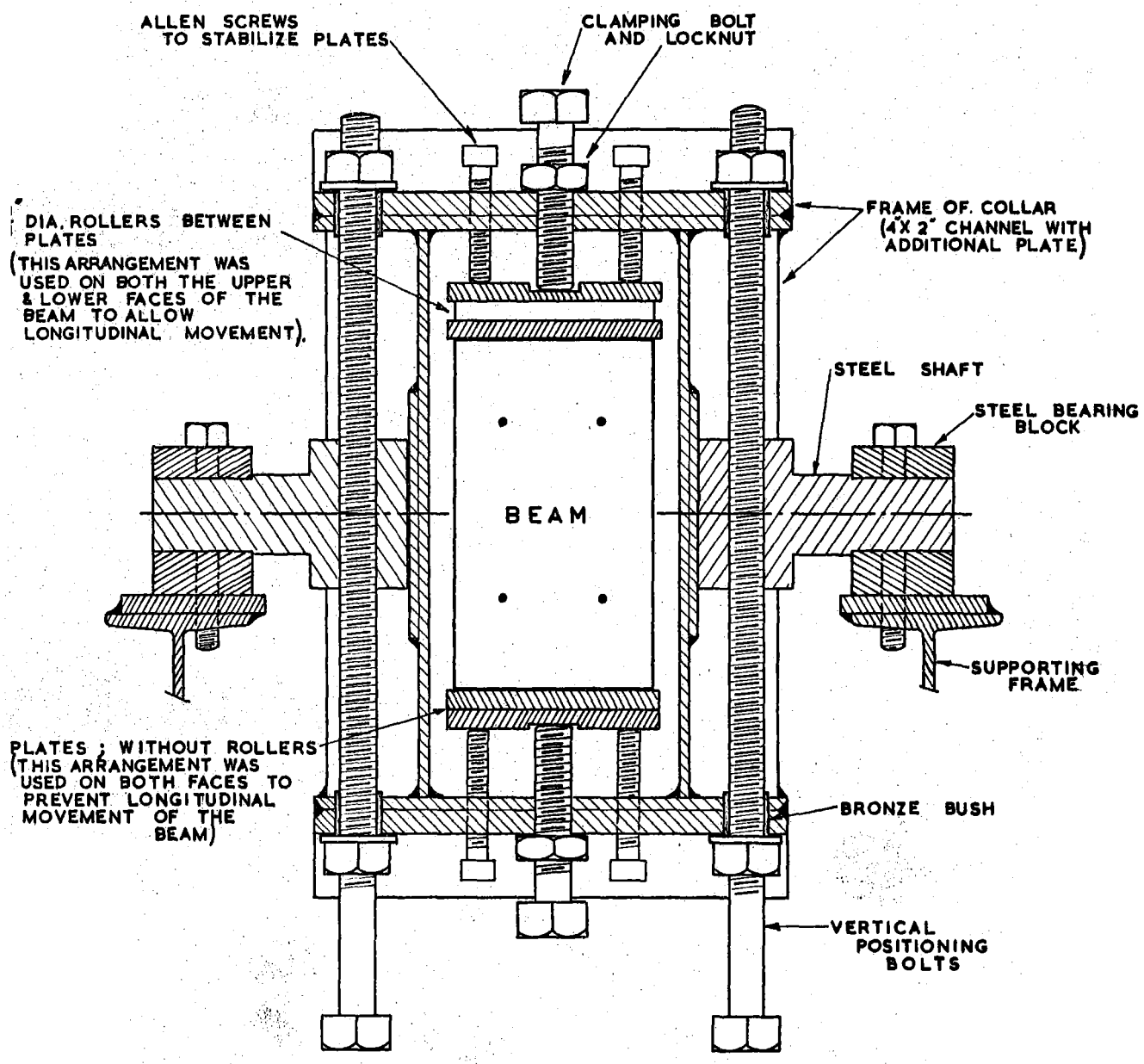

FIG 3.5 END COLLAR

to the supporting frames. Thus the ends of the beam could rotate and allow the beam to act as a simply supported beam.

Two dial gauges to check the nett vertical movement of the beam at the collars were mounted on dexion frames which may be seen in Plates 2 and 4. The dexion frames although built over the supporting frames for the beams were entirely independent of the Dynamic Loading Unit.

3.3. Load Cell.

The load cell, which is shown in fig. 3.6, was designed to register 1000 micro-strains at a load of 6000 lb assuming that the modulus of elasticity for the steel was 30.10^6 p.s.i. The external diameter of the load cell was 1.460" and the internal diameter was 1.370" which resulted in a wall thickness of .045".

3.3.1. Instrumentation.

Six 120 ohm PR Phillips strain gauges were glued to the external surface of the load cell. Three strain gauges were placed parallel to the longitudinal axis of the cell and connected in series to form one arm of the wheatstone bridge circuit while the remaining three were mounted transverse to the longitudinal axis and were also connected in series to form the second arm of the bridge circuit. The strain-gauges were water-proofed with Phillips water-proofing agent and the cell was wrapped in rubber splicing compound tape to protect the gauges. The output from the load cell due to a change in strain when a load was applied was amplified by a Phillips Direct Reading Strain Bridge, model PR 9300, and recorded on one channel of a four channel Phillips PT 2108 oscilloscript recorder. Three core shielded cable was used to connect the gauges to the amplifier while two core

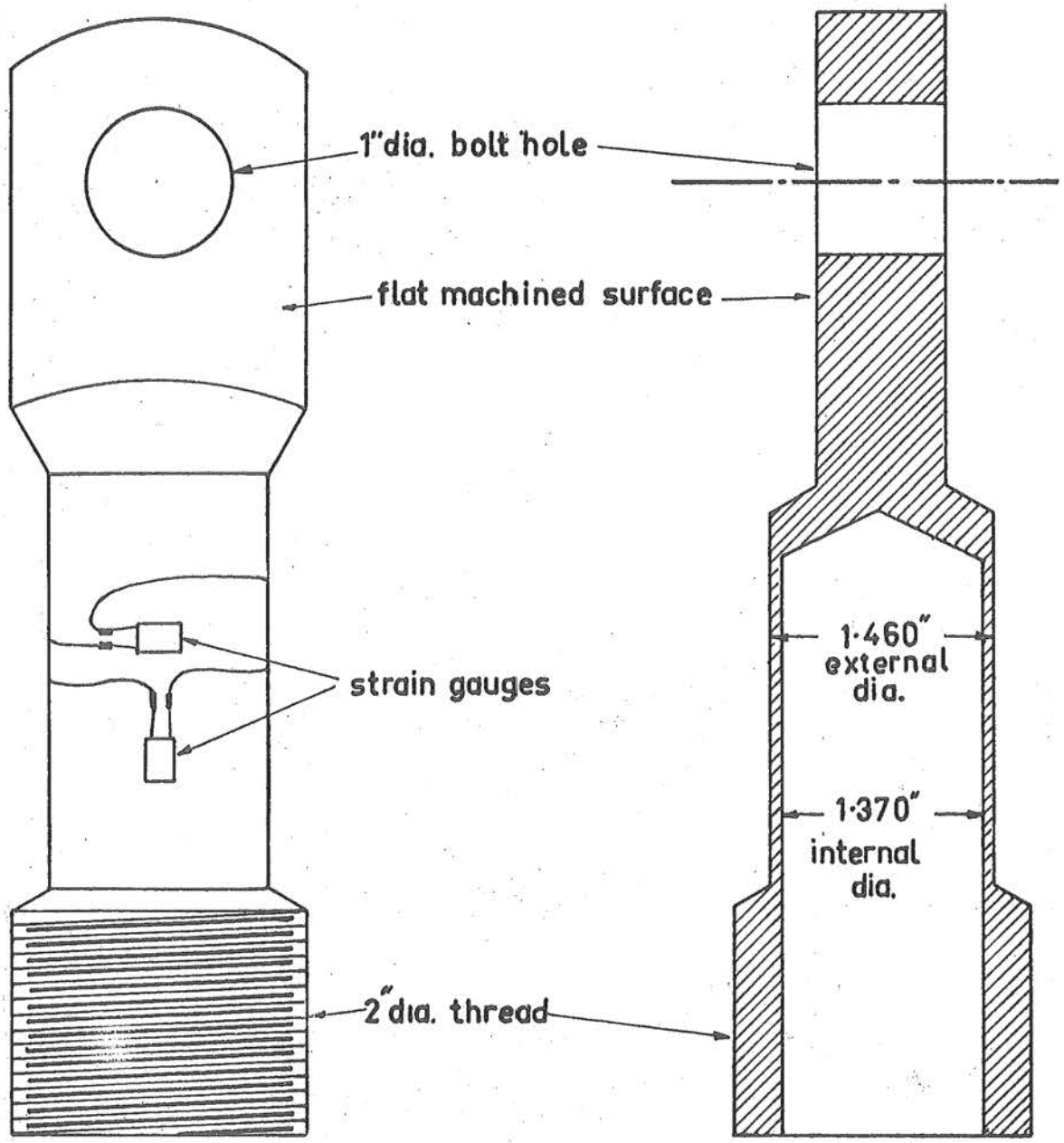

FIG 3.6 LOAD CELL

shielded cable was used between the amplifier and the oscilloscript. The Direct Reading Bridges, which were also used with the Dynamic Deflection Gauges, and the oscilloscript are shown in Plate 5.

3.3.2. Calibration.

The load cell was calibrated by applying a known load with a hydraulic testing machine and noting the resulting offset of the oscilloscript trace from the zero position. The cell was calibrated in separate operations for tension and compression and the overall range of calibration was 3600 lb tension to 3600 lb compression. The most sensitive range on the oscilloscript was used for the calibration although it was necessary to use three ranges of amplification on the bridge. The three ranges of load were 0-800 lb, 0-2200 lb, and 0-3600 lb and the corresponding trace widths were 1.46", 1.35" and .68". The width of the trace was measured to the nearest hundredth of an inch although the accuracy of the electronic equipment was probably on the order of ± .02". Therefore over the three ranges the maximum errors would have been ± 16 lb, ± 50 lb, ± 130 lb, which are 2.0%, 2.2% and 4.5% of the maximum calibrated loads for the respective ranges.

On the Direct Reading Bridge it was found that the load cell was linear over each of the tensile and compressive ranges although there was a very slight bi-linearity over the complete range from 3600 lb compression to 3600 lb tension. The change in the linearity occurred at the null point on the bridge and as the Budd Strain Indicator showed that the load

cell was linear over the entire range it is probable that the fault was within the Direct Reading Bridge. (Furthermore it is though that the weight of the meter needle on the bridge may have contributed partly or wholly to the bi-linearity.) This bi-linear effect could not be found on the trace of the oscilloscript as it lay within the reading error of the width of the trace. However the calibration of Load and the offset of the trace had a distinct bi-linear effect with the change of linearity occurring approximately one sixth of the width of the trace from one edge. It was found on the one side only and would have been caused by an unknown fault in the oscilloscript. The load-cell was calibrated with the meter on the bridge switched out and with the bridge at the null-point when the load was zero.

3.4. Dynamic Deflection Gauges.

Two sets of Dynamic Deflection gauges were required to measure the deflections as the normal dial gauges were unsuitable. The deflection gauges consisted of a metallic strip fixed in direction and position at one end and connected to the beam through a vertical arm attached to the "free" end. The gauges were designed to measure maximum deflections of .1" and 1" and the corresponding maximum strains measured were approximately 600 and 850 micro-strains. The two types of gauges are shown in fig. 3.7 (a) and (b) and a 1" gauge is shown in Plate 6. The vertical arm of the .1" gauge was pinned at both ends to prevent tensile strains developing in the metal strip as the vertical displacement of the free end of a cantilever is accompanied by a small lateral displacement. Universal joints

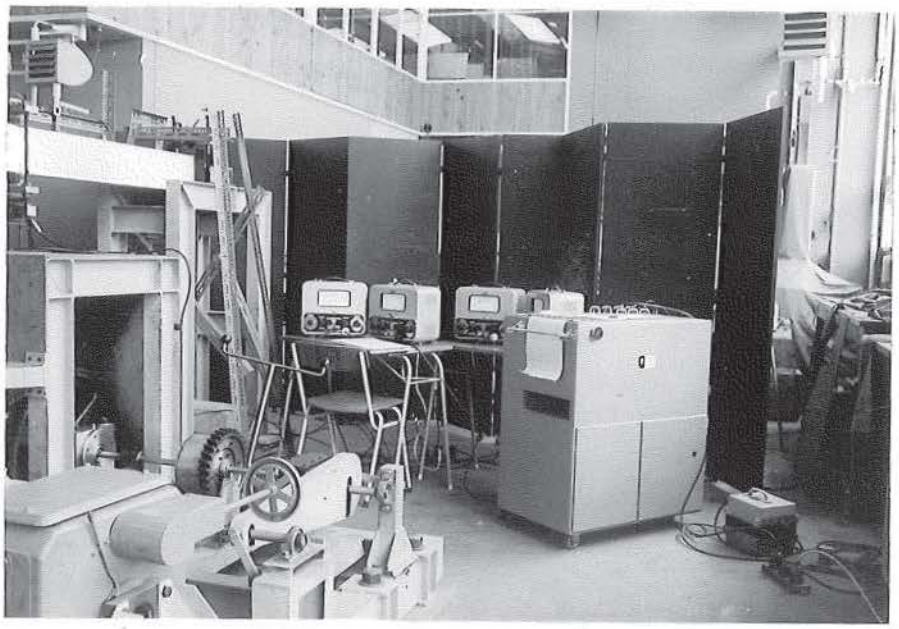

Plate 5. DIRECT READING STRAIN BRIDGES and OSCILLOSCRIPT.

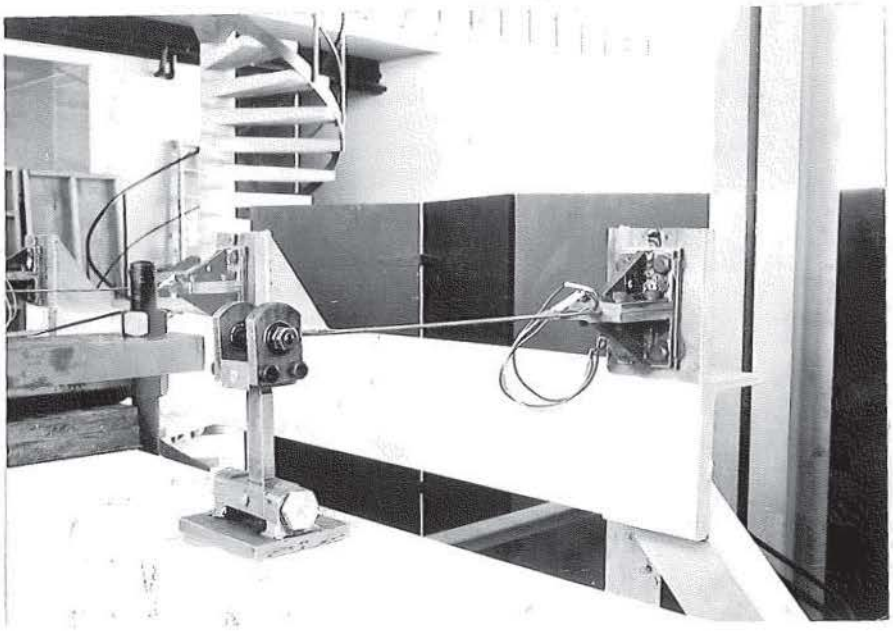

Plate 6. 1" DYNAMIC DEFLECTION GAUGE with universal joints at each end of the vertical arm.

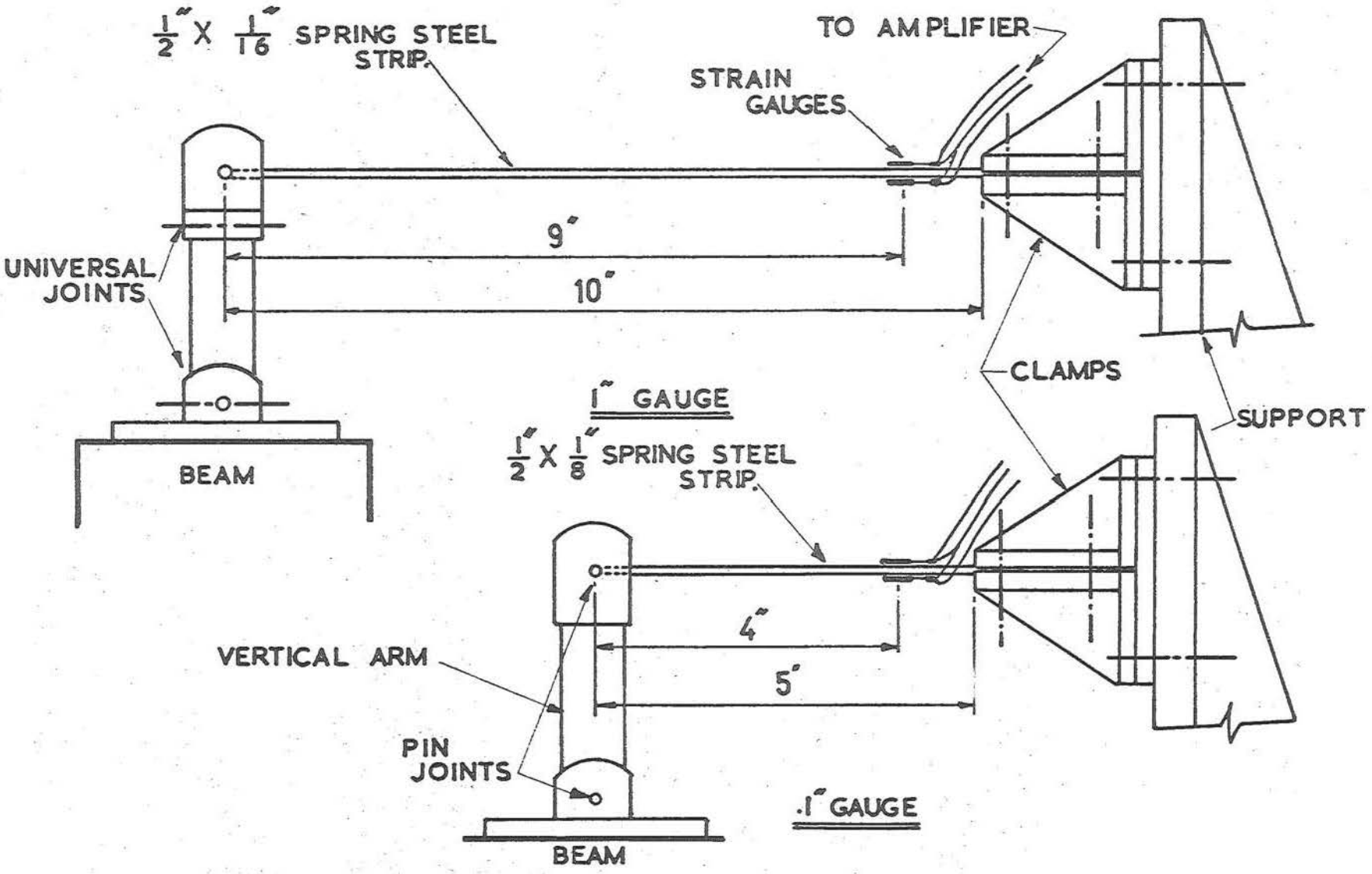

FIG. 3.7 DYNAMIC DEFLECTION GAUGES

were placed at both ends of the vertical arms of two of the 1" gauges to allow for the longitudinal movement of the beam as well as the lateral displacement of the end of the strip. The third 1" gauge was imilar to the .1" gauges since the longitudinal movement of the centre of the beams was small.

3.4.1. Instrumentation.

Two 120 ohm PR 9814 Phillips strain gauges were placed on each gauge as shown in fig. 3.7 (a) and (b) and each gauge formed one arm of adjacent arms on a wheatstone bridge circuit. Each deflection gauge was connected through a separate Direct Reading Strain Bridge (Model PR 9300), which acted as an amplifier, to a separate channel on the oscilloscript. As the oscilloscript was equipped with four channels one of which was used for the load cell only three gauges could be used at one time. Three core and two core shielded cables were used as for the load cell instrumentation.

3.4.2. Calibration.

The dynamic deflection gauges were clamped to an adapter plate on the top of the piston of the Dynamic Loading Unit and were calibrated at a speed of $\frac{1}{2}$ c.p.s. The stroke of the piston was measured by a dial gauge when the Unit was cycling slowly. The deflection, which was half the stroke, was calibrated against the overall width of the trace produced on the oscilloscript. Each gauge was calibrated separately with each pair of .1" and 1" gauge having its own set of cables, amplifying bridge and channel in the oscilloscript.

The .1" gauges required two ranges of amplification on the bridges to obtain the total range of deflection with maximum sensitivity. The ranges of deflection were 0 - .05" and 0 - .10" and the corresponding maximum widths of the traces were of the order of 1.6" and .9" respectively. The estimated errors due to both measuring the width of the trace and the accuracy of the equipment were ± .03", or 2% and 3% of the maximum values of deflection for the respective ranges.

The 1" gauges required three ranges of amplification on the bridges to obtain maximum sensitivity and, as for the load cell and the .1" gauges, the channels on the oscilloscript were operated on their most sensitive ranges. The ranges of deflection were 0 - .28", 0 - .89", 0 - 1.0" and the corresponding maximum widths of the trace were of the order of 1.4", 1.4", and .5" with estimated errors of 2%, 3% and 5½% of the maximum deflections for the respective ranges.

The graphs of deflection versus width were linear throughout and did not show any signs of the bi-linear effect found in the calibration of the load-cell. The speed of the Dynamic Loading Unit was found to have no effect on the calibration of the gauges.

The deflection of the gauges produced a reaction at the oscillating end of the metal strip which increased the load in the load cell. These reactions were calculated by the normal elastic theory methods and were allowed for in the dynamic tests.

4. DESIGN AND PROPERTIES OF BEAM

4.1 Introduction

Five similar 7" x 4" x 11'0" pretensioned concrete beams prestressed by four .200" dia. high strength steel wires stressed initially to 180,000 p.s.i. were cast. Positive end anchorages in the form of C.C.L. anchorages were attached to the wires and embedded in the concrete approximately an inch from each end of the beam. The position of the wires is shown in fig. 4.1. No shear reinforcement was used. The average cylinder crushing strength of the concrete in the five beams ranged from 6680 p.s.i. - 8340 p.s.i.

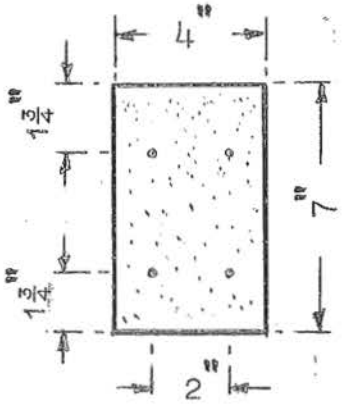

Fig. 4.1 CROSS-SECTION THROUGH BEAMS.

4.2. Steel Properties.

The prestressing wire was stress relieved high tensile strength steel. When the steel was delivered there was a heavy layer of rust on the surface of the wire and in a few areas the surface was badly pitted. The surface conditions for most of the wire ranged from the condition shown in Plate 7 to that shown in Plate 8, although there were a few small areas where the surface conditions were similar to that shown in Plate 9. Tests showed that the strength of the wire was adequate and as the strength of the steel - concrete bond has been found to be slightly improved by rusting the wire was accepted. Before the wire was used it was cleaned roughly with emery paper to

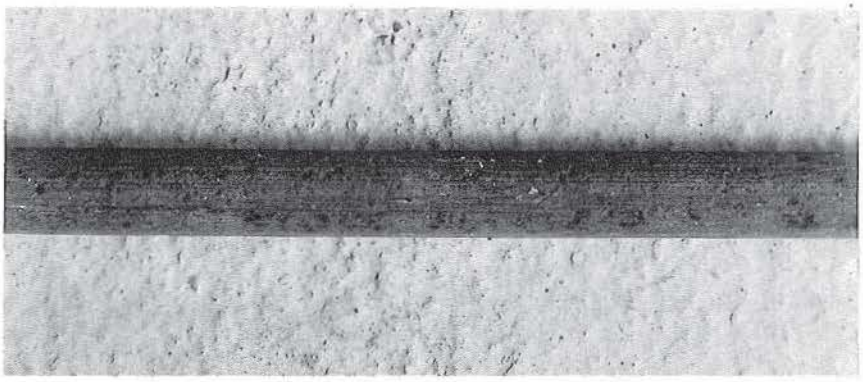

Plate 7. PRESTRESSING WIRE showing small pitholes due to corrosion

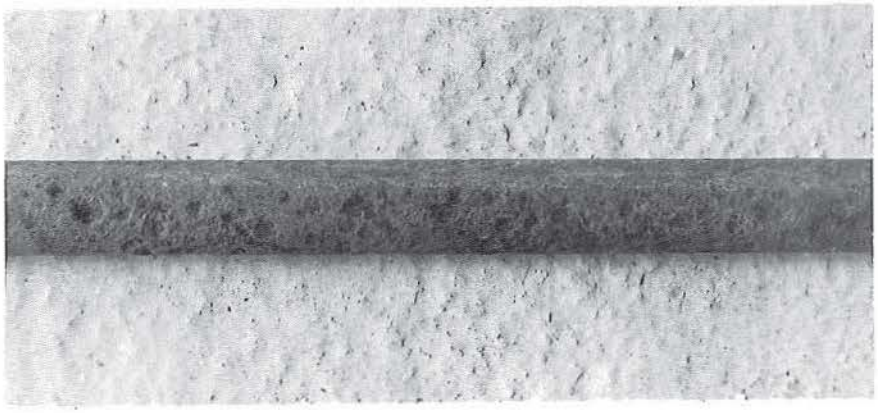

Plate 8. PRESTRESSING WIRE showing medium sized pitholes

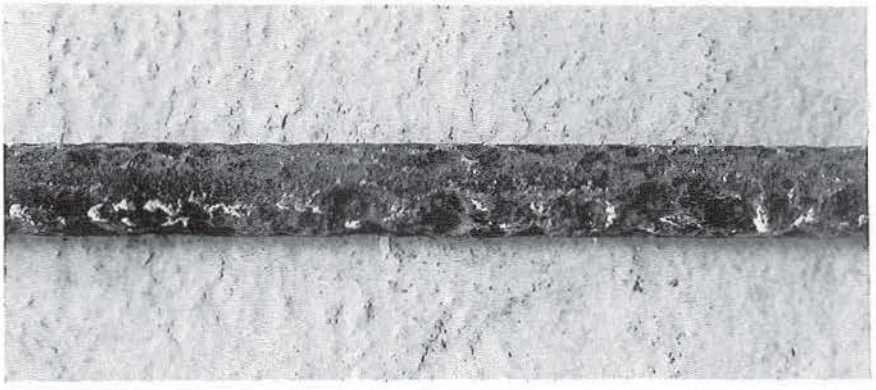

Plate 9. PRESTRESSING WIRE, badly corroded and pitted.

remove the excess rust and mill-scale. A stress-strain curve for the wire, obtained from tests on three specimens, is shown in fig. 4.2, and this curve has been used for all the analytical work.

4.3. Concrete.

The concrete was designed for a cylinder crushing strength of 7000 p.s.i. The grading of the concrete aggregates is shown in Table 4.1, the aggregate-cement ratio was 2.30 and

B.S. Seive Size	Percent retained
3/8 - 3/16	45
3/16 - 7	16
7 - 14	14
14 - 25	11
25 - 52	9
52 - 100	5

Table 4.1. Aggregate grading.

the water-cement ratio was .42. The conversion factor for obtaining the cylinder crushing strength from the crushing strength of cubes was found to be .89. This conversion factor was obtained by testing nine 6" dia. x 12" cylinders and nine 6" cubes at an age of 28 days in a hydraulic compression testing machine at equal rates of loading. The cylinders were filled in 3 layers and compacted by vibrating on a vibration table at a frequency of 3,200 c.p.m. for a total time of $2\frac{1}{2}$ mins. The cubes were also filled in 3 layers but were compacted by

a Kango Hammer applied to the sides of the mould for a total time of 2½ mins. The slump of the concrete was ¼" and the compaction factor was .91.

A stress-strain curve for the concrete was derived by placing Demec points for three 4" gauge lengths on the sides of 3 cylinders. As the cylinders were loaded by a hydraulic testing machine only the ascending portion of the curve was obtained directly. The peak and descending portions of the curve were derived from the results of previous research [28,29], on the complete stress-strain curve for concrete. The stress-strain curve adopted is shown in fig. 4.3, and has been used for all the analytical work. The coefficients for the concrete are shown in Table B.1, Appendix B.

4.4. Prestressing Bed.

A prestressing bed which had been designed and built for a current research project was used for stressing the wires. The bed, shown in Plate 10, consisted of a 25'6" - 20" x 6" U.B. with anchor blocks bolted to the top flange at each end and the steel beam mould was rigidly clamped to the top flange by G - clamps. Freyssinet anchorages were used at both ends of the wires and the load to the wires was applied by screwing out the head screws of the load cells attached to the anchor block shown in Plate 11. It was possible to apply any specific load to each wire as the load cells had been calibrated for the changes of the zero which occurred when loads were applied.

4.5. Casting and Curing Procedure.

All the beams were cast and cured in a fog room of

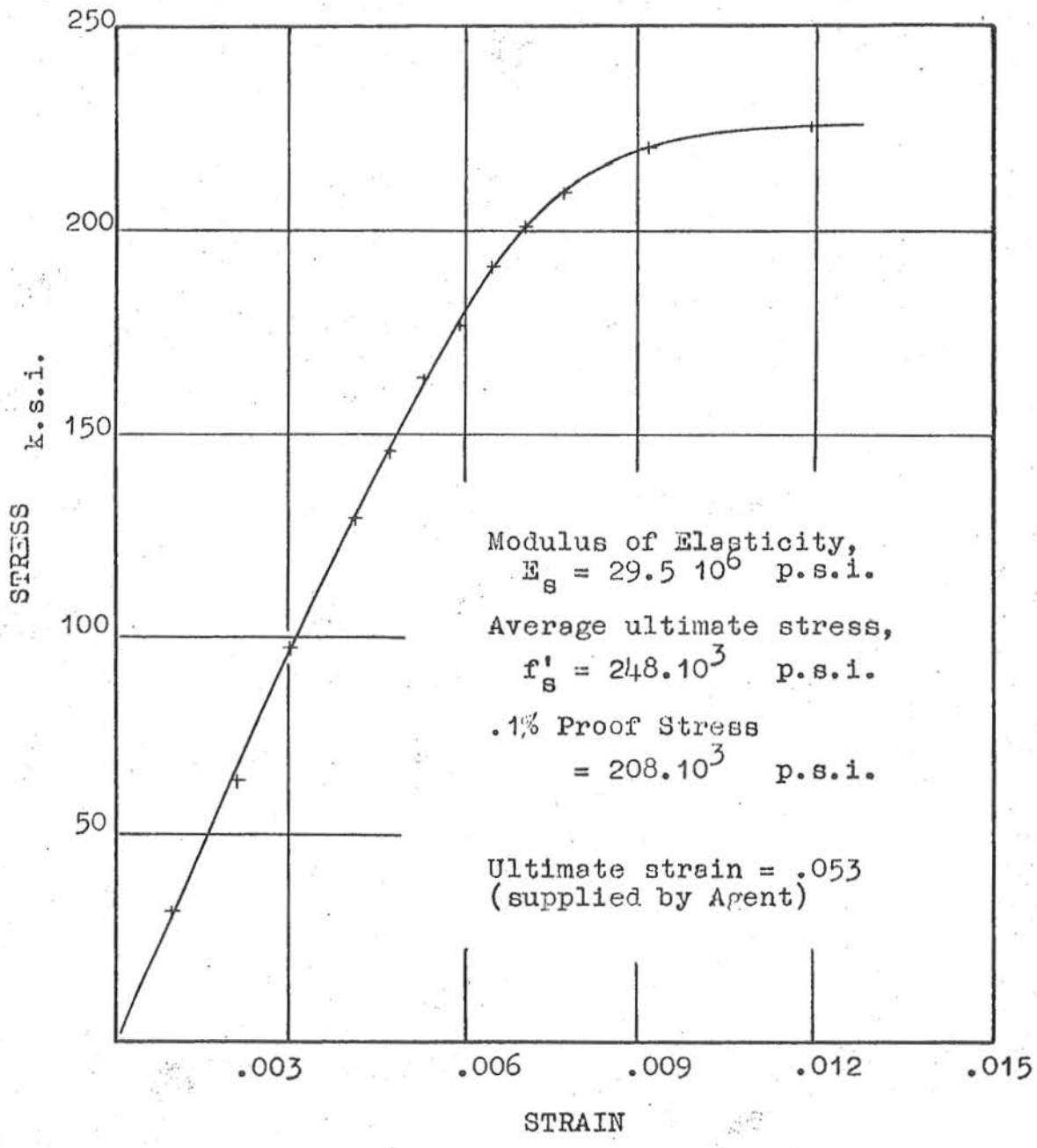

Fig. 4.2 STRESS-STRAIN CURVE FOR STEEL

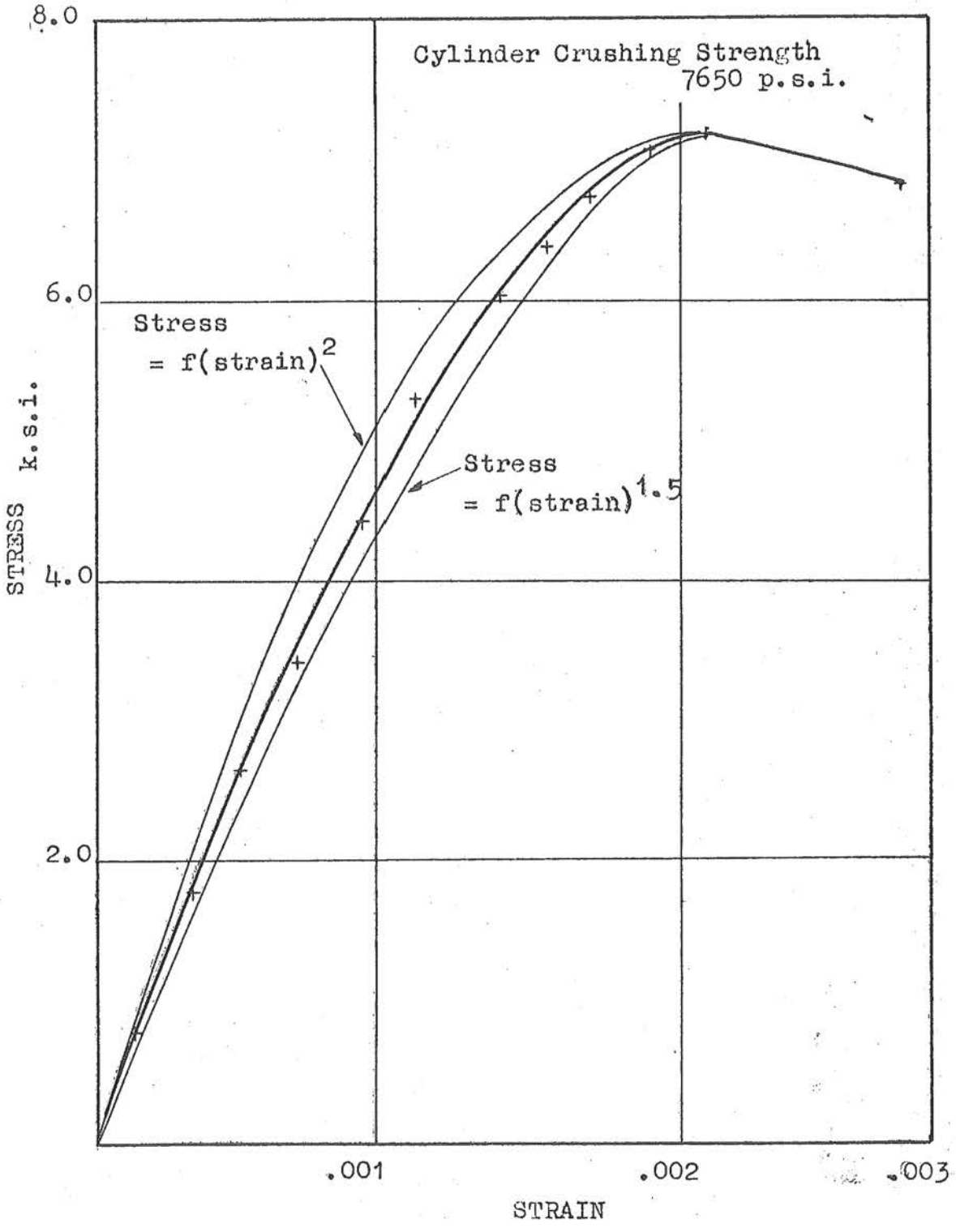

Fig. 4.3 STRESS- STRAIN CURVE FOR CONCRETE

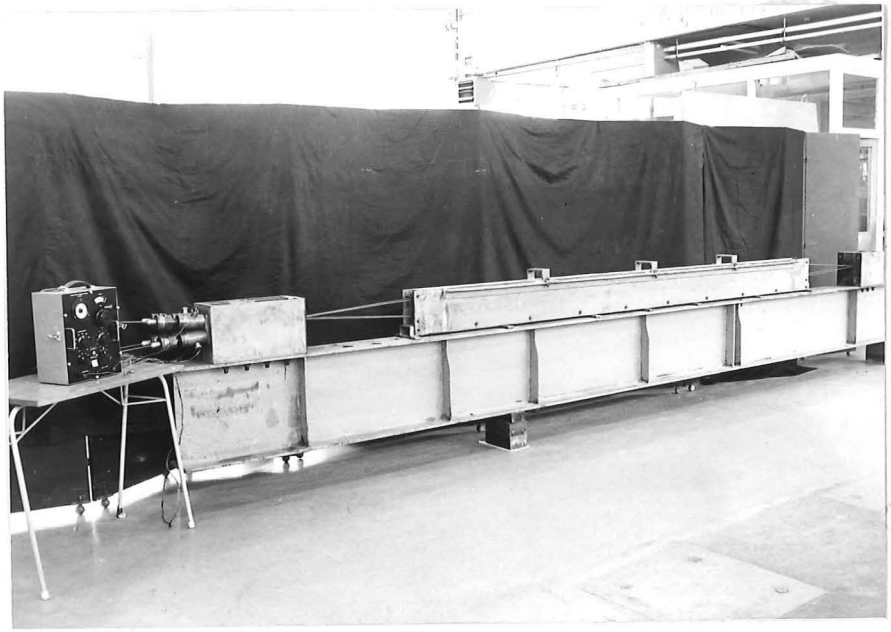

Plate 10 PRESTRESSING BED, with the Beam Mould and the Strain Bridge to measure the strain in the load cells.

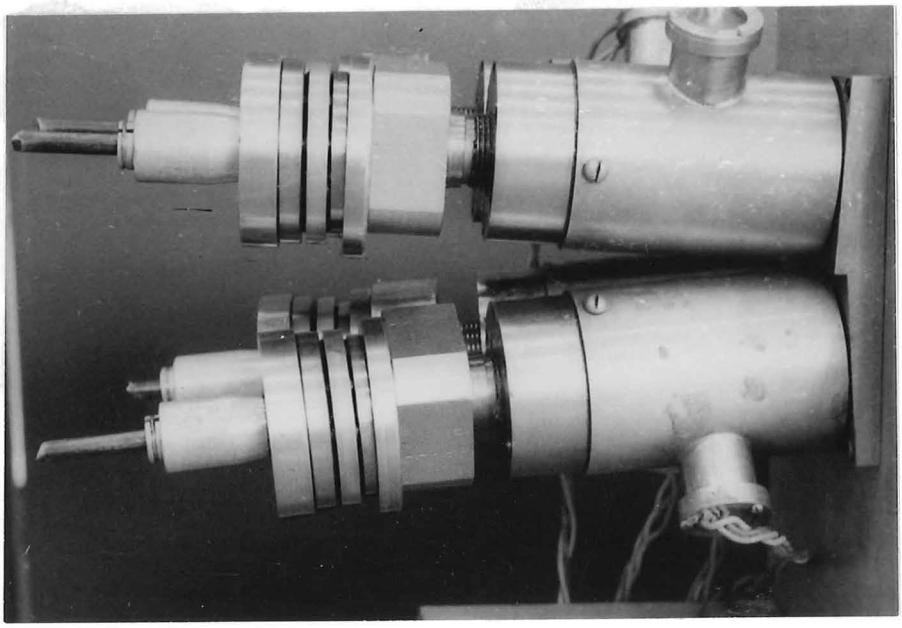

Plate 11 LOAD CELLS used to measure Prestress in wires. The head screws, thrust bearings and Freyssinet end anchorages are also shown.

constant temperature and 100% humidity. After the prestressing bed and beam mould had been set up and the wires stressed a bond breaker (Mobil Par B Oil) was applied to the varnished interior surfaces of the mould. Immediately prior to pouring the concrete, the surfaces of the prestressing wires were cleaned with acetone to remove any grease or oil. The concrete was mixed in two batches of 260 lbs. and 230 lbs. weight; the mixing time for each batch was 4 minutes. The concrete in the beams was compacted by applying a Kango Hammer to the sides of the beam mould while the concrete was being placed and the vibration of the concrete was continued until most of the air voids were removed. From each batch of concrete three 6" control cubes were cast and from the second batch a temperature control block was also cast. The cubes and control block were poured in the laboratory under normal atmospheric conditions and the cubes were filled in 3 layers and compacted by a Kango Hammer for $2\frac{1}{2}$ minutes. The cubes for the beams were placed in the fog room as soon as the beams had been poured and were subjected to the same curing conditions as the beams.

After two days the sides of the beam mould were removed and the cubes were also removed from their moulds. At 6 days the prestressing forces in the wires were transferred to the concrete and after 21 days Beams 1, 2, 4, and 5, together with their respective control cubes, were removed from the fog room in preparation for testing at 28 days.

4.6. Transfer of Prestress and Losses.

The stress was transferred from the steel to the concrete

by releasing each wire slowly so that the stresses in each wire were of the same order at any instant. To estimate the loss of stress in each wire due to creep of the steel over the 6 days while the concrete was curing, the load in each wire was found by taking the strain readings from its load cell before and after the transfer of stress. Demec points for 5 or 6 8" gauge lengths were placed on both sides of Beams 1, 2, 4, and 5, as shown in figs. 5.2, 5.5, 5.12, and 5.17 respectively to find the elastic strain in the concrete due to the pre-stressing force and also the combined shrinkage and creep strains over the period before testing. From the average of the measured strains it was possible to estimate the stresses in the concrete and steel before the testing began. The results are shown in Table 4.2. For Beam 3, one of the load cells was not functioning and it was necessary to estimate the number of turns required to produce the correct stress in the wire; also no Demec gauge readings were taken.

	Cylinder crushing strength p.s.i.	Initial steel stress k.s.i.	Stress in steel at transfer k.s.i.	Strains in Concrete			Loss of stress in steel k.s.i.	Final steel stress k.s.i.	Stress in concret p.s.i.
				Elastic shortening in/in	Creep and shrinkage in/in	Total in/in			
Beam 1	7840	180	168.7	.000173	.00325	.000498	14.7	154.0	690
Beam 2	8010	179	168.4	.000180	.000302	.000481	14.2	154.2	690
Beam 3	8340	180	163.7	-	-	-	-	-	-
Beam 4	7400	181	173.5	.000180	.000235	.000415	12.2	161.3	720
Beam 5	6680	181	172.5	.000180	.000283	.000463	13.7	158.8	710
Average	7650	180	169.1	.000178	.000286	.000464	13.7	155.4	700

Table 4.2. Estimated Prestress Losses for the Beams Cast.

5. EXPERIMENTAL PROCEDURE AND RESULTS.

5.1 Introduction

The five beams were all tested as simply supported beams over a span of 120" and equal transverse vertical loads were applied 10" on each side of the centre line of the beam t give a 20" zone of pure flexure as shown in fig. 5.1. The lar shear spans were necessary to reduce both the shear-bond stres and the possibility of a shear failure since no stirrups were used. Beams 1 and 2 were tested statically while Beams 3, 4, 5 were tested dynamically.

5.2. Beam 1.

5.2.1. Procedure.

Beam 1 was tested statically in the testing frame sho in Plate 12. The beam was loaded in approximately equal increm

Plate 12. TESTING FRAME for Static Tests.

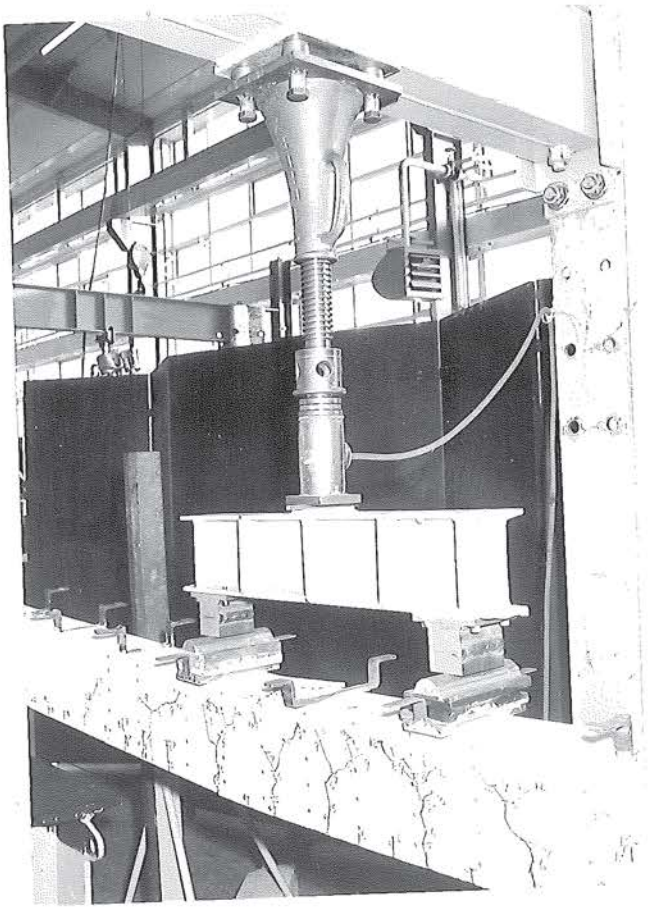

Plate 13. SCREW JACK LOAD-CELL LOADING SYSTEM. Also shows Beam 1 after failure.

of load until failure occurred. The load to the beam was applied by a screw jack, through a load cell and steel distribution beam as shown in Plate 13, and was measured by a Budd-Strain Indicator connected to the load cell. Deflection gauges were placed at 10" intervals along the beam in order that the load-deflection relationships and the deflected shape of the beam could be determined and to find the optimum positions for the three deflection gauges which were to be used in the dynamic tests. Demec points for strain readings were

placed on both sides of the beam as shown in fig. 5.2, and Demec points for 14 / 2" gauge lengths were also placed on the top face of the beam above the zone of pure flexure. Demec gauge lengths were placed on the temperature control block to enable corrections to be made for temperature changes during the test. The deflection gauges were read and the position and length of the cracks were marked at all increments of load but the Demec gauges were read at selected load increments only.

5.2.2. Results.

The results are shown in fig. 5.3 - 5.4 and Tables C.5.1 - C.5.3. The beam failed in flexure after large strains in the steel had caused a lift of the neutral axis leading to crushing of the concrete in the region above a crack. Although failure occurred within the zone of pure flexure there were a number of diagonal shear cracks, originating from tension cracks at the bottom face of the beam, which could have been critical if the flexural strength had been higher. The estimated ultimate moment, which is discussed in section 6.7, was 84.4 Kip-ins and the actual ultimate moment was 88.7 Kip-ins. The lower estimated failing moment could be attributed to the low assumed value for the maximum strain in the top compressive fibre as the results show that the actual maximum strain was larger.

5.3. Beam 2.

5.3.1. Procedure.

The beam was tested in the testing frame used for Beam 1, however there were a few minor additions to the apparatus

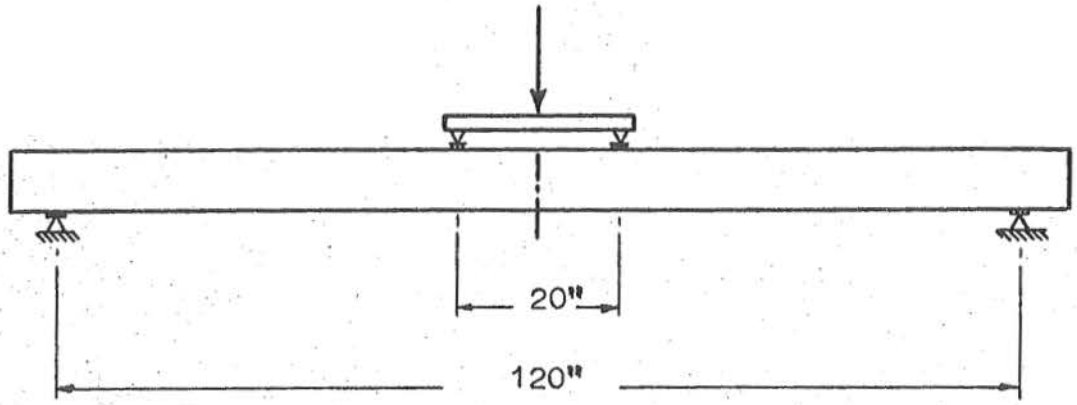

Fig. 5.1 TESTING CONDITION OF BEAM 1

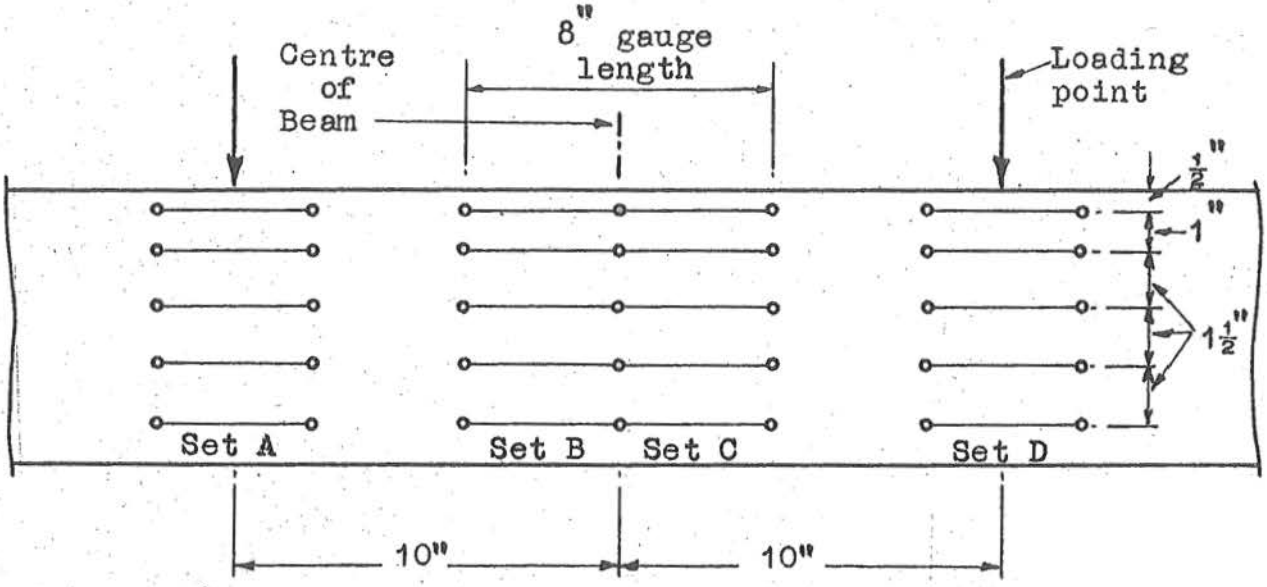

Fig. 5.2 4" DEMEC GAUGE POSITIONS ON BEAM 1

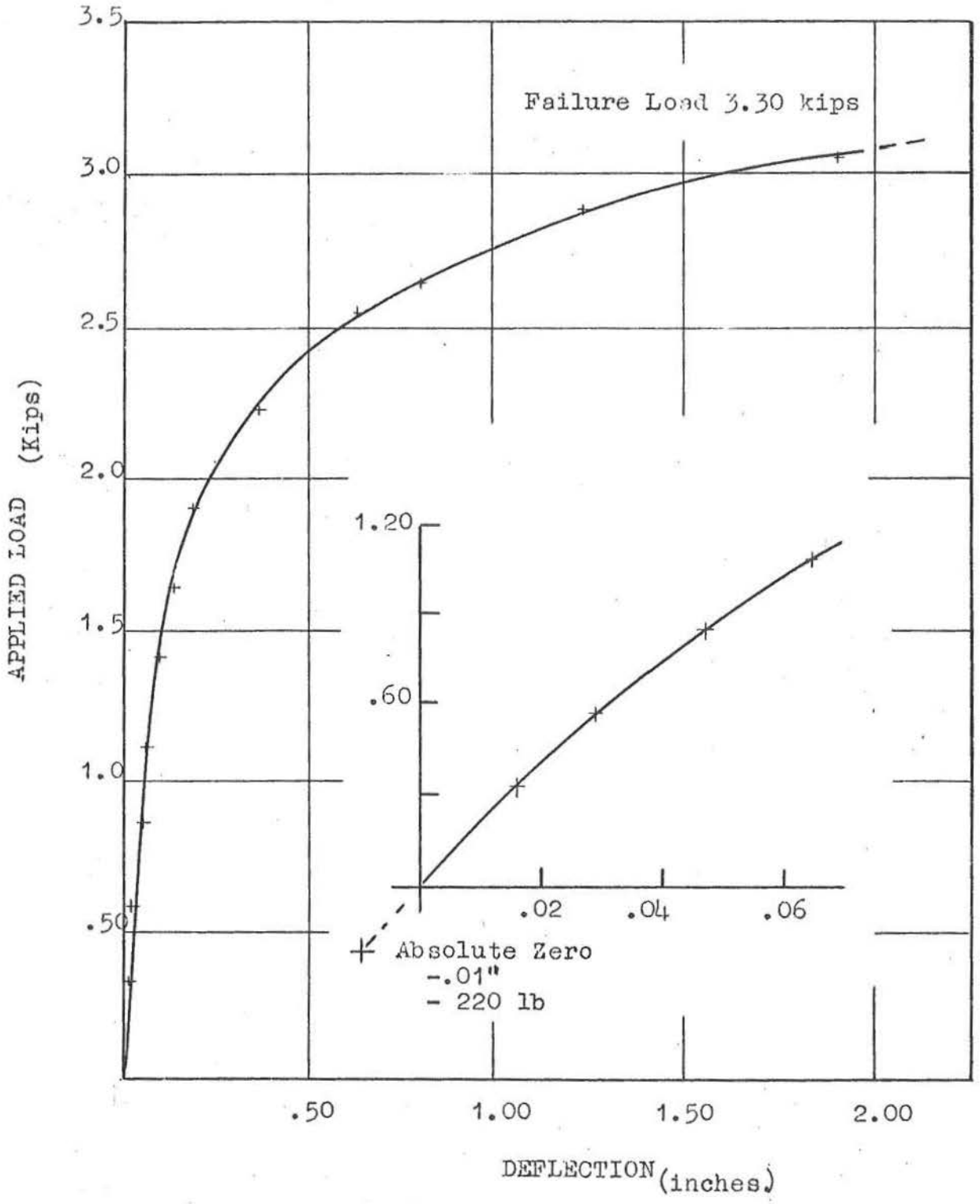

Fig. 5.3 LOAD-DEFLECTION CURVE FOR BEAM 1.

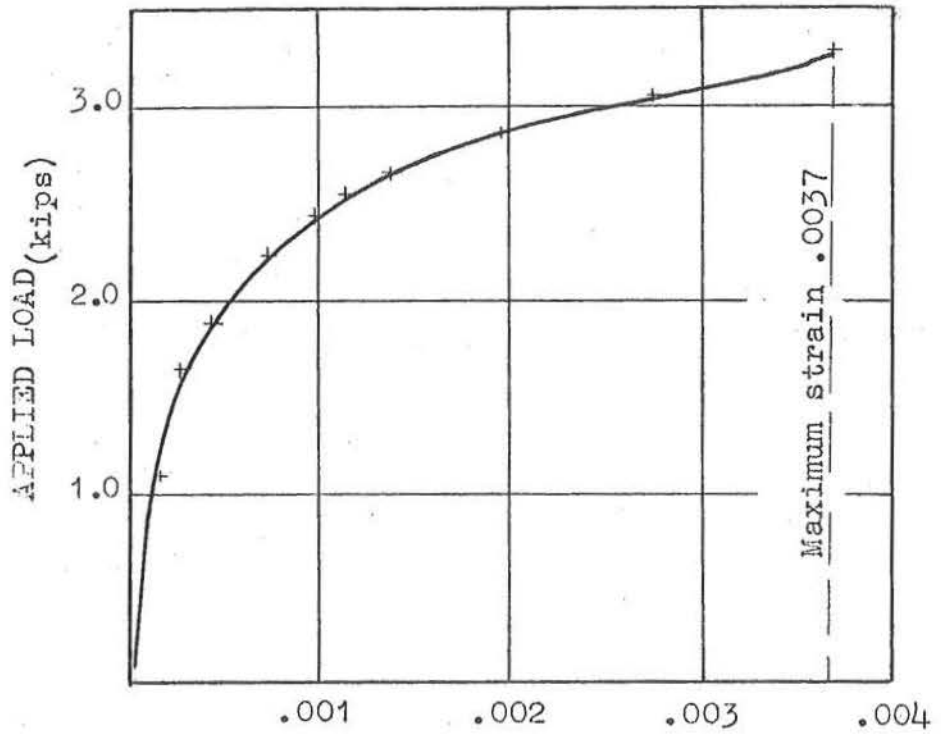

Fig. 5.4 STRAIN IN EXTREME COMPRESSIVE FIBRE OVER ZONE OF PURE FLEXURE ON BEAM 1.

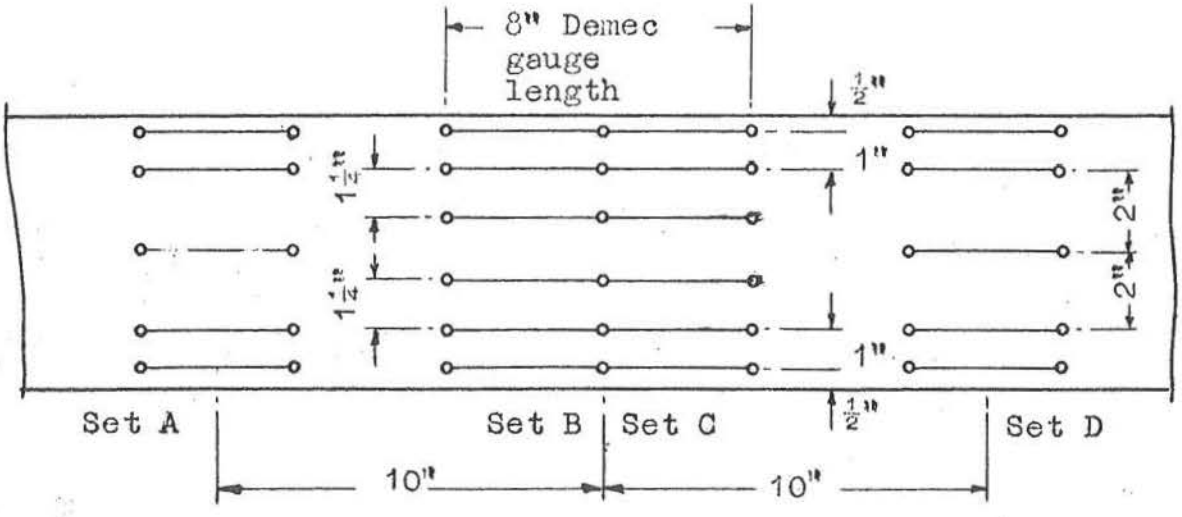

Fig. 5.5 4" DEMEC GAUGE POSITIONS ON BEAM 2

to enable the beam to be loaded in the reverse, i.e. upward, direction without turning the beam upside down and these are shown in Plates 14 and 15. The screw-jack - load cell system was used for applying the positive, i.e. downward, load while the hydraulic jack shown in Plate 14, which was operated by a Reihle hydraulic testing machine, was used to apply the negative, i.e. upward, load. Deflection gauges were mounted at 10" intervals over the central 80" of the beam and at the supports, the gauges at the ends were used to measure the vertical movement of the beam at the supports while it was being loaded upwards. Demec points for 22 / 4" gauge lengths were mounted on each side of the beam in the positions shown in fig. 5.5 and points for one gauge length were also mounted on the temperature control block. The beam took two days to test. The sequence of loading was as follows:

Load in increments to +1790 lbs Total moment 50.2 kip-ins (i.e. 59% of Mu)

release

Load in increments to -2100 lbs Total moment -47.0 kip-ins (55% of Mu)

release

Completion of first cycle

Load in increment to 2430 lbs Total moment 66.2 kip-ins (78% of Mu)

release

End of first day of testing

Load in increments to -2700 lbs Total moment -62.0 kip-ins (73% of Mu)

release

Completion of second cycle

Load in increments to failure

N.B. (1) The total moment shown above includes the effect of weight of the beam.

(2) Mu is the estimate ultimate moment.

At each increment of load the dial gauges were read and the position and length of the cracks were marked on the sides of the beam; however, the Demec gauges were read at selected load increments only. In all cases the load was released directly to zero without any intermediate readings being taken. A full set of dial gauge readings and Demec gauges readings were taken after each half cycle when there was no load on the beam.

5.3.2. Results.

The results are shown in fig. 5.6. and Tables C.5.4-C.5.5.

The beam failed in flexure in a similar manner to that of beam 1; diagonal tension cracks developed to the same extent and it would appear that the reversed loading and cracks across the compression zone had no significant effect on the ultimate load properties of the beam. The bending moment at failure was 87.2 Kip-ins which was slightly lower than the ultimate moment for Beam 1 but this is within the range of the experimental error for the beams. The estimated ultimate moment was 87.3 Kip-ins.

Plate 14. HYDRAULIC JACK for applying negative load to Beam 2.

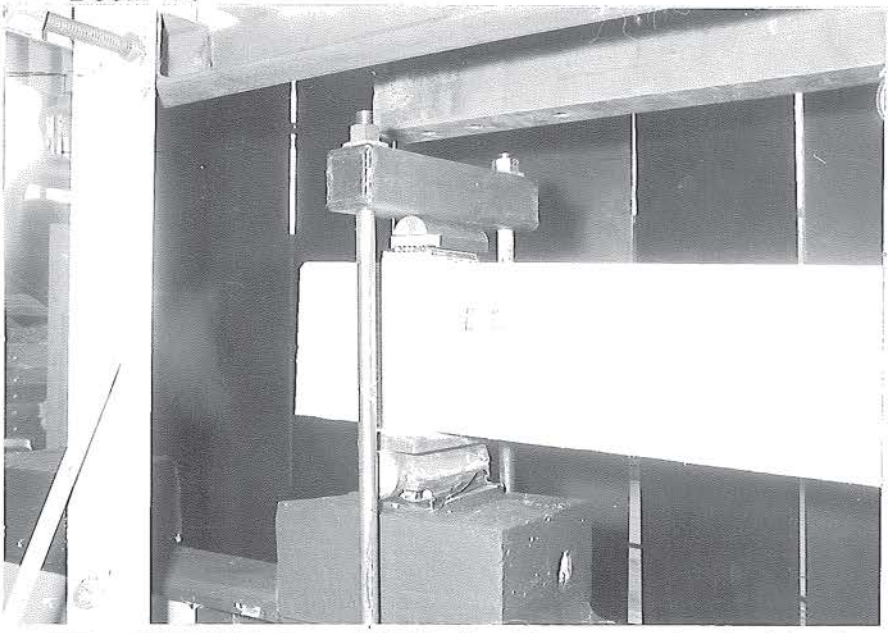

Plate 15. END SUPPORT FOR BEAM 2. The vertical tie bars and bearing plates and rollers were added for the test on Beam 2.

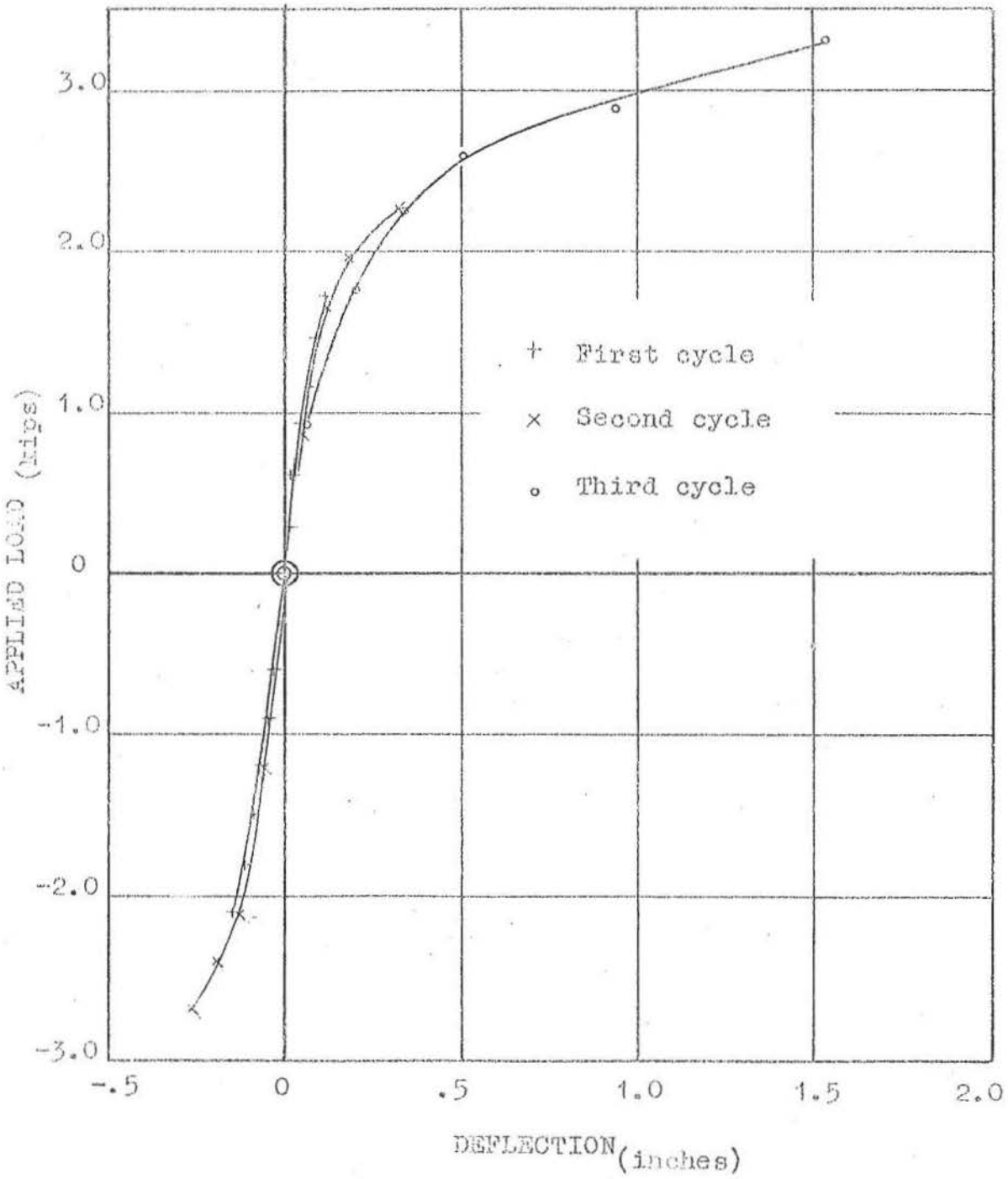

Fig. 5.6 LOAD-DEFLECTION CURVE FOR BEAM 2

5.4. Beam 3.

5.4.1. Procedure.

Beam 3 was the first beam to be tested dynamically and one of the primary purposes of the beam was to test the dynamic testing equipment. The beam was removed from the fog room after 67 days and the first dynamic tests were made after 92 days. The fatigue test was made at 98 days and the beam was tested to failure statically 102 days after it was poured. The beam was supported in the Dynamic Loading Unit as shown in fig. 5.7 and the deflection gauges were mounted on the centre of the width of the top face in the positions shown. No Demec gauges were used. When the concrete beam was being connected to the distribution beam of the Loading Unit care was taken to ensure that no additional loads were applied to the beam. During all the dynamic tests a continuous record of the range of load and the deflections was made by the oscilloscript.

The elastic range tests were made at the three frequencies of $\frac{1}{2}$, 1, $1\frac{1}{2}$ c.p.s. respectively and the magnitude of the maximum applied load during each test was increased from zero to the order of 1000 lbs in five approximately equal increments. During a test the number of cycles of load at each increment was the same although the number was varied for the different tests. Dial gauges mounted on frames constructed from dexion angle were placed at the ends of the beam as shown in Plate 4 to measure the vertical movement of the beam in the supports.

The magnitude of the mean maximum load in the fatigue test was 2360 lbs and the resulting moment was 59.0 Kip-ins

which was 70% of the estimated static ultimate moment. The applied load was increased to the maximum load for the test in five increments and was maintained constant for the remainder of the test. The testing frequency was 1 c.p.s. and the test was stopped after 9460 cycles. During the test there was a power failure which forced a rest period of 75 minutes. It was also necessary to stop the test at predetermined intervals to allow the position and length of the cracks to be marked on the faces of the beam; stops were made at 910 cycles, 1380 cycles, 2890 cycles and 6670 cycles. The first stop i.e. at 910 cycles, was made approximately 50 cycles after the maximum load for the test was first applied and the last stop was that caused by the power failure.

After the dynamic tests the beam was loaded to failure statically. For the static test the beam was left in the supports of the Dynamic Loading Unit while the distribution beam and load cell were disconnected and removed from the Loading Unit. The deflection gauges were also removed and replaced by dial gauges for the static test. A testing frame which was sufficiently wide to span the Dynamic Loading Unit was used to provide the support for the hydraulic jack used to load the beam as shown in Plate 16. The hydraulic jack was connected to the Reihle testing machine and in the test the concrete beam was loaded, through a steel distribution beam, in 300 lb increments until failure occurred. At each increment of load dial gauge readings were taken and the length and position of any new crack, or extension of any existing crack, was marked on the face of the beam.

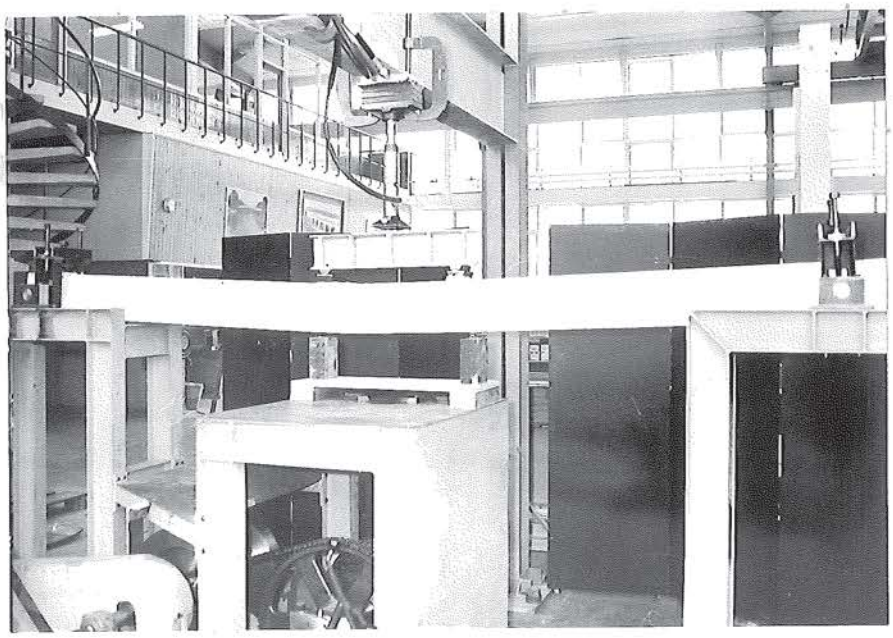

Plate 16 BEAM 3 after failure in the Static Test. The dial gauges for measuring the Deflection have been removed but otherwise the plate shows the conditions for the Static Test.

5.4.2. Results.

The results are shown in fig. 5.8 - 5.10 and Tables C.5.6 - C.5.8.

The Load-Deflection envelope for the beam shown in fig. 5.8 shows the relationship between the average maximum load acting on the beam and the central deflection and does

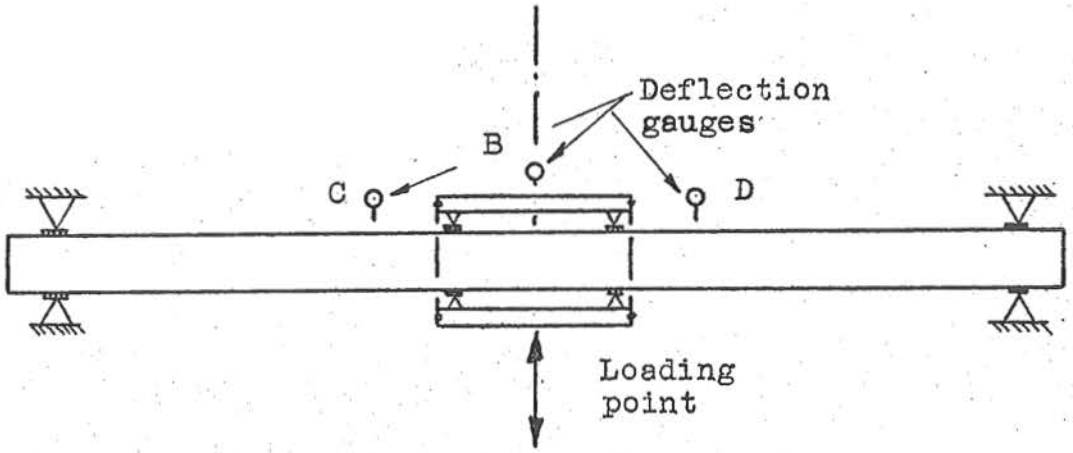

Fig. 5.7 TEST CONDITION OF BEAM 3

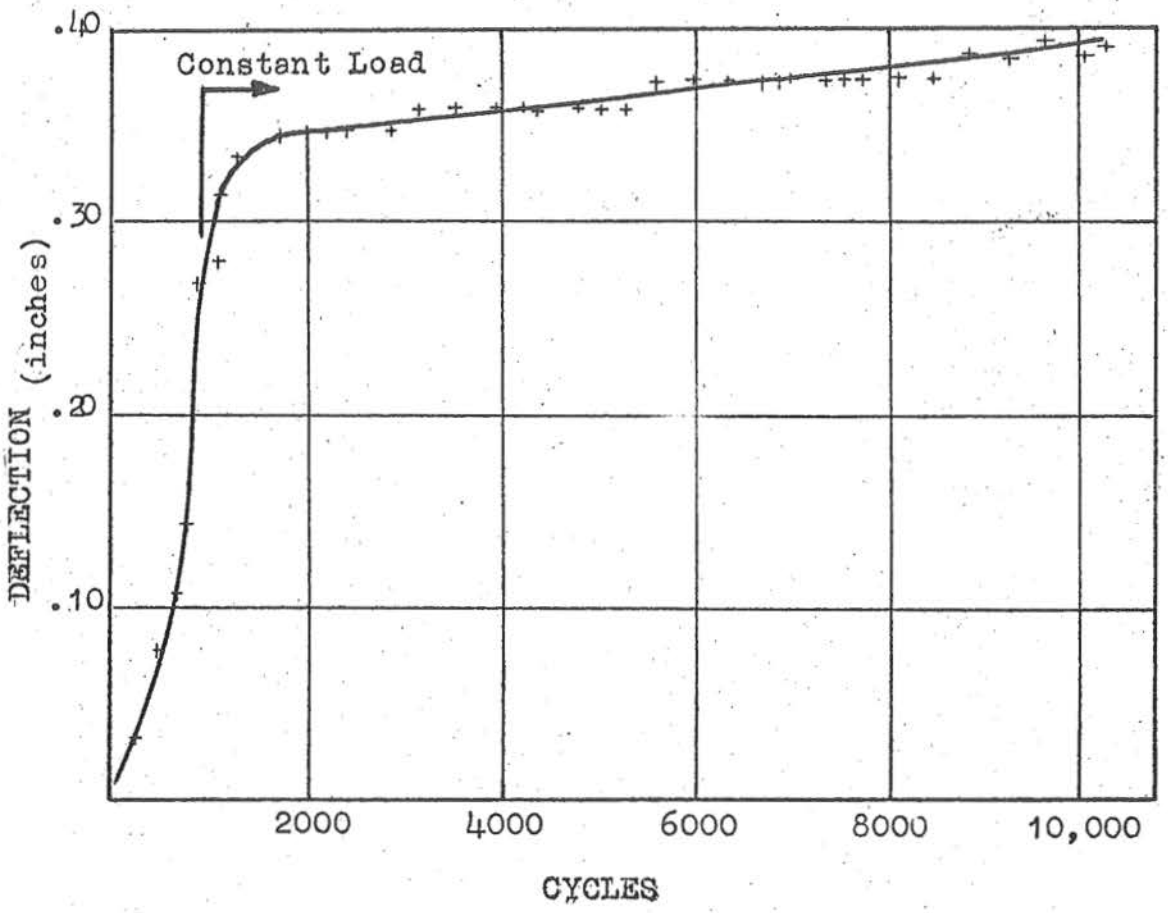

Fig.5.8 DEFLECTION-CYCLE GRAPH FOR BEAM 3

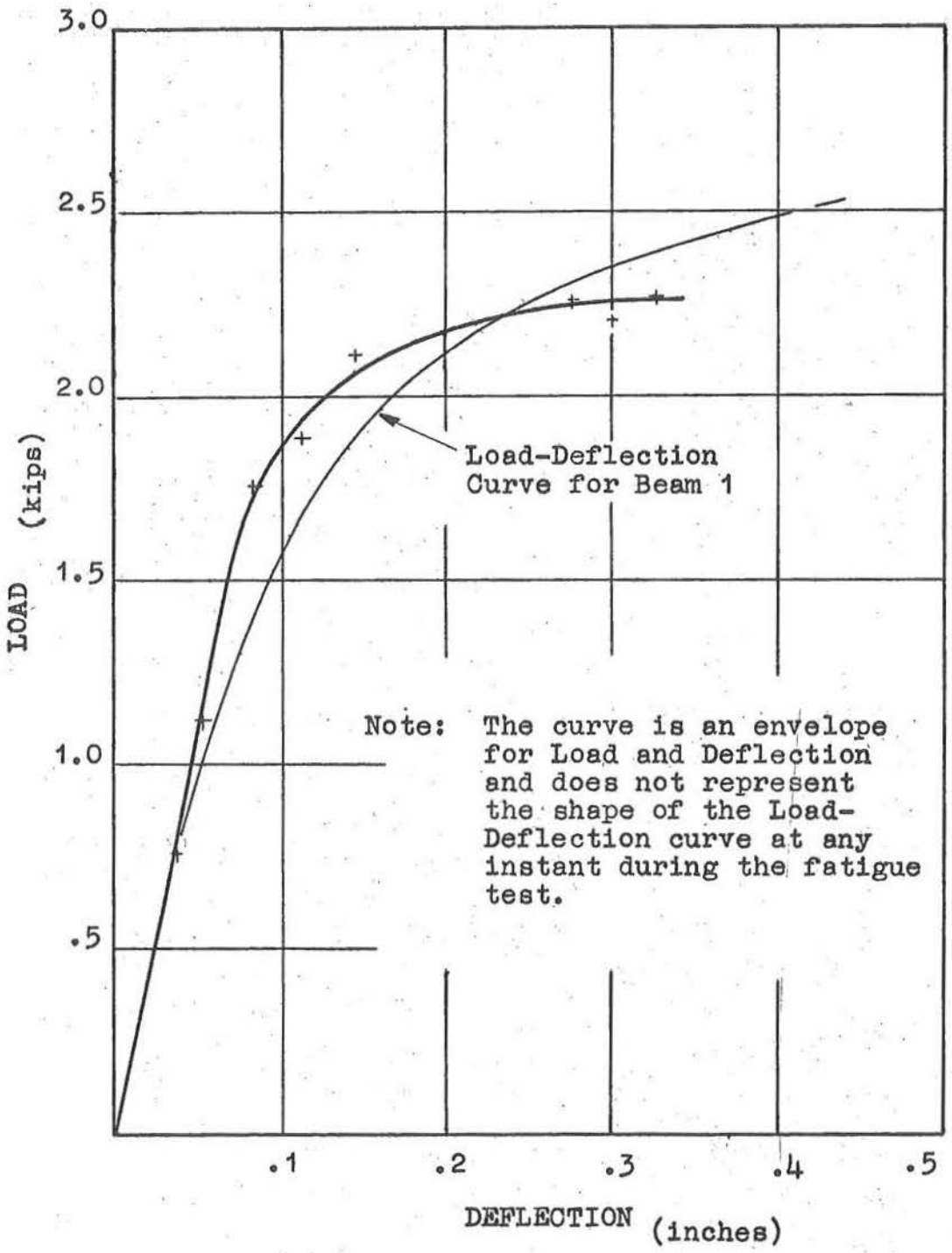

Fig. 5.9 LOAD-DEFLECTION ENVELOPE FOR BEAM 3.

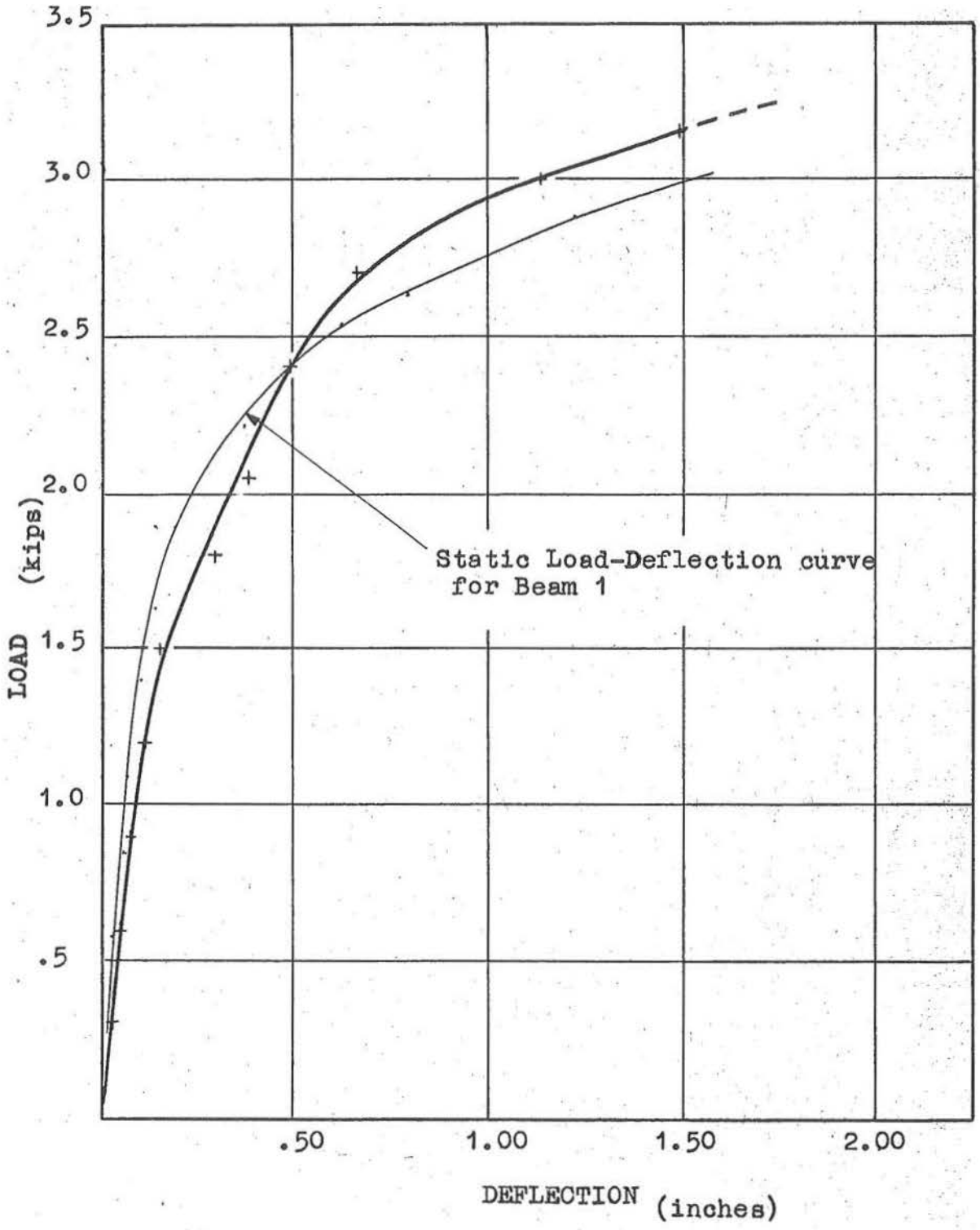

Fig. 5.10 STATIC LOAD-DEFLECTION CURVE FOR BEAM 3.

not give any indication of the shape of the Load-Deflection curves for the beam under the action of cyclic loading. The value of the average load includes the effect of the weight of the beam and the deflection is half the total range of deflection.

The beam failed due to crushing of the concrete in the compression zone but the primary cause of the failure was due to a combination of excessive elongation of the steel and a local breakdown of the steel-concrete bond, adjacent to the critical crack. As failure was approached it could be seen that the crack above which failure subsequently occurred was much wider than the critical cracks in the two statically tested beams.

5.5. Beam 4.

5.5.1. Procedure.

Beam 4 was tested dynamically and statically by similar procedures to those used for Beam 3. The dynamic testing was started on the 28th day after the beam was cast and completed the following day; the static test to failure was made on the 31st day after the beam was cast. The setting up procedure for the dynamic tests was similar to that for Beam 3, although there was a small change in the support condition which is shown in fig. 5.11. Demec points for 15 / 4" gauge lengths on each side of the beam, positioned as shown in fig. 5.12, were used and the zeros were taken before the dynamic testing was started. Demec points were also placed on the temperature control block, and readings from this gauge length allowed corrections to be made for temperature changes during the test and also for any shrinkage which occurred over the four days of the test.

The frequencies of the elastic range tests were 1, 1½, and ½ c.p.s. respectively but otherwise the tests were as for Beam 3.

The magnitude of the mean maximum applied load in the fatigue test was 2670 lb. resulting in a moment of 66.7 Kip-ins, which was 80% of the estimated ultimate moment. The testing frequency was 1 c.p.s. and the load was increased to the maximum for the test in five increments of approximately 190 cycles. Stops to mark the length and position of the cracks was made after 1200 cycles, 1800 cycles, and 7680 cycles; the first stop being 170 cycles after the maximum load for the test was first applied. The test was stopped after 9900 cycles of load and at this stage it appeared that the beam was approaching failure; the top face of the beam at this stage is shown in Plate 17.

For the static test the beam was left in the Dynamic Loading Unit supports while the distribution beam and load cell were uncoupled and removed as for Beam 3. The deflection gauges were also removed and replaced by dial gauges. The load to the beam was applied by a screw jack acting through a load cell and distribution beam and the support conditions were the same as for the dynamic tests. The load cell was connected to the Budd strain indicator from which the load could be obtained and the beam was loaded in approximately equal increments until failure occurred. At each increment of load the dial gauges were read and the length and position of any new cracks, or extension of the existing cracks, were marked. However, the Demec gauge

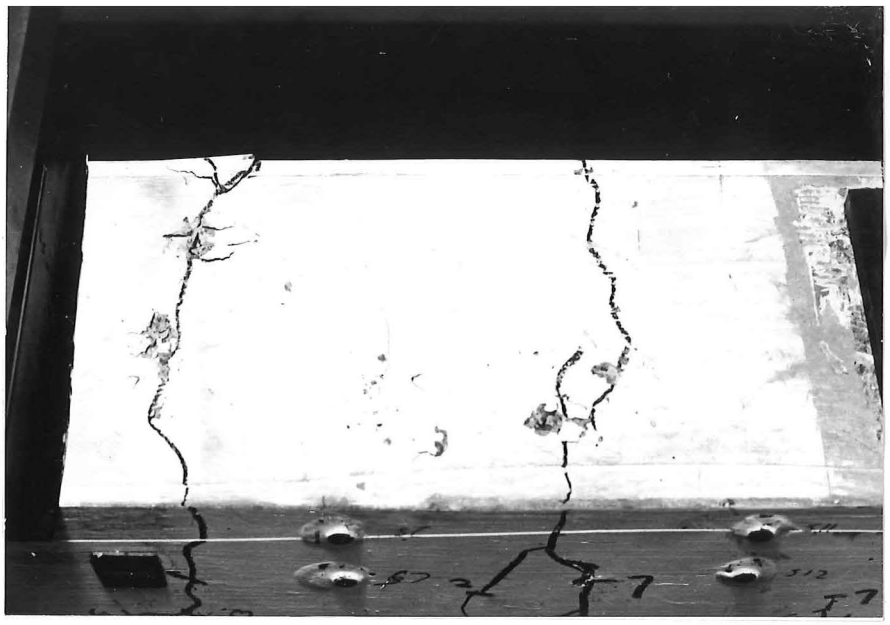

Plate 17. CRUSHING ON TOP FACE OF BEAM 4 following fatigue test.

readings were only taken at selected increments of load.

5.5.2. Results.

The results are shown in fig. 5.13 - 5.16 and Tables C.5.9 - C.5.12.

Failure of the beam in the static test was caused by the fracture of one of the lower wires. As there were no stirrups it was possible to check for the fracture of a wire with a high resistance meter and when the beam was broken up the position of the fracture was found to be at the widest crack. Very large 'apparent' strains were obtained from the Demec gauge readings for the gauge lengths across the critical crack which indicated a break down of the steel-concrete bond in the region adjacent to the crack. It was also found that

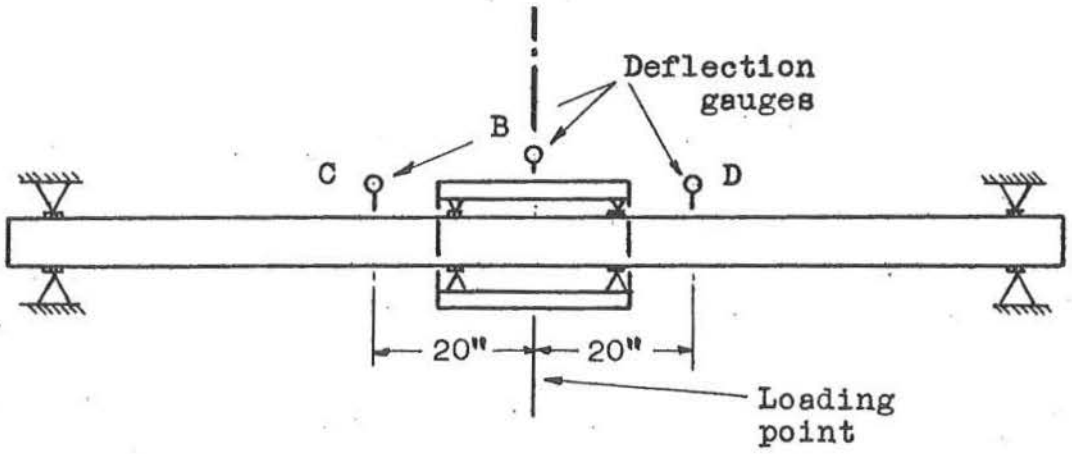

Fig. 5.11 TEST CONDITION OF BEAM 4

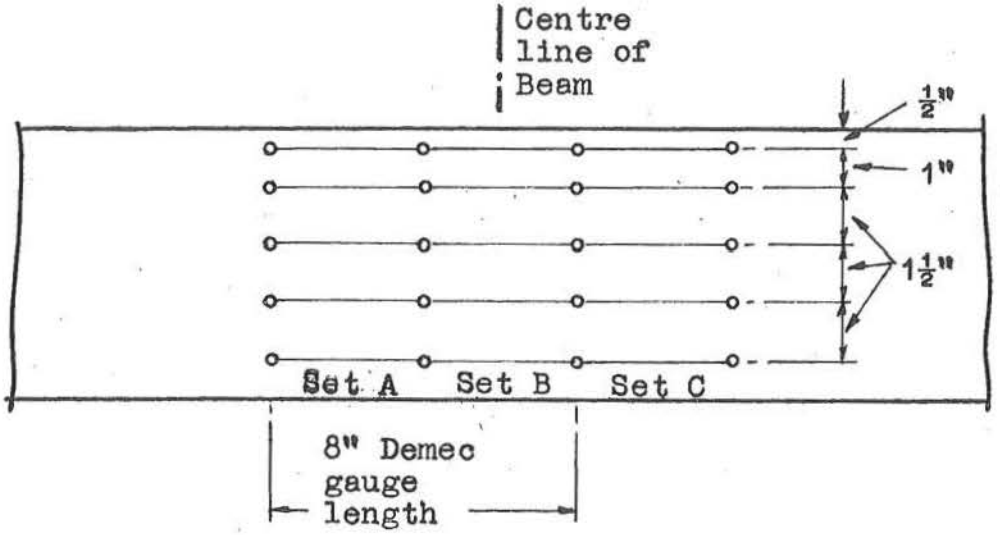

Fig. 5.12 4" DEMEC GAUGE POSITIONS ON BEAM 4

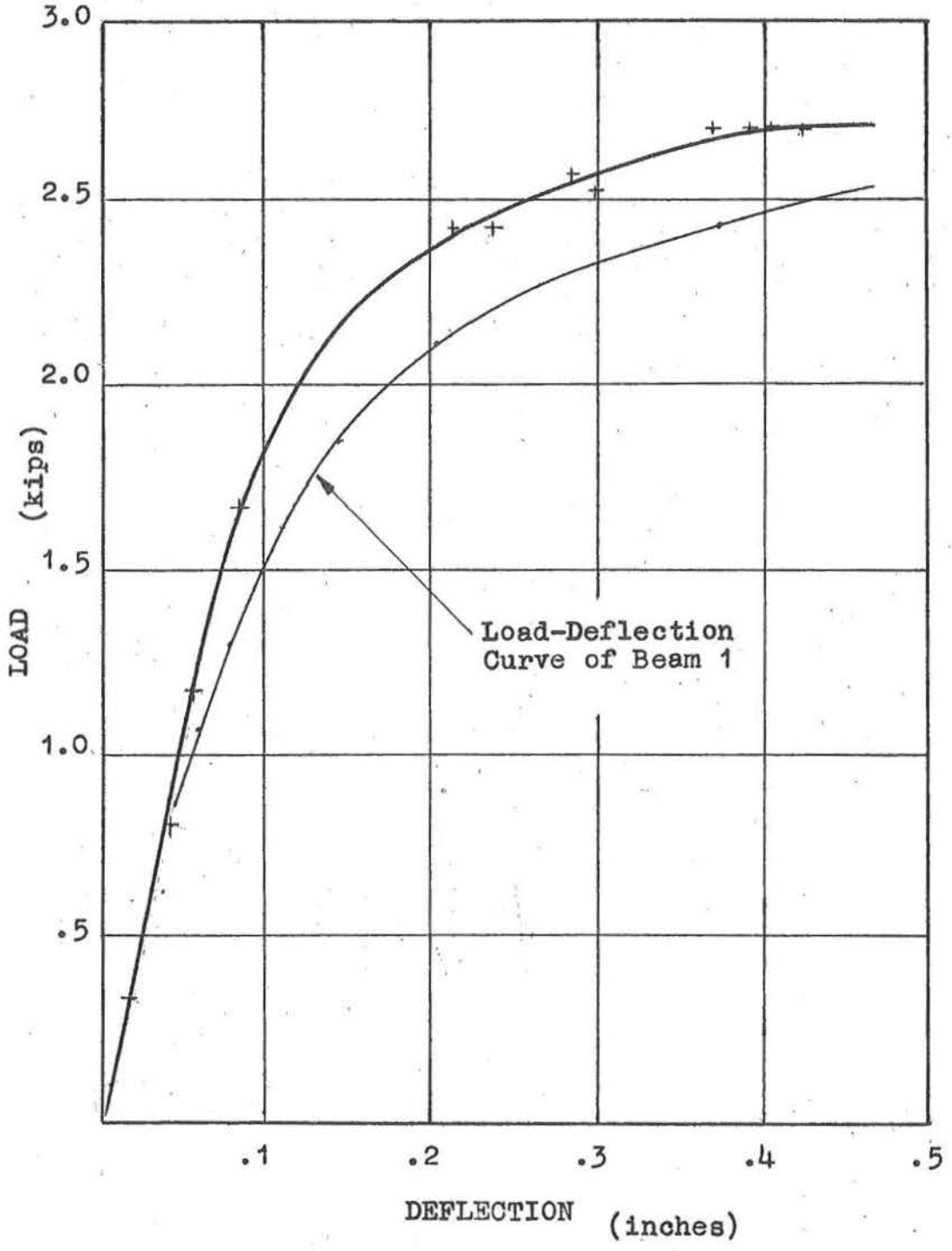

Fig. 5.13 LOAD-DEFLECTION ENVELOPE FOR BEAM 4

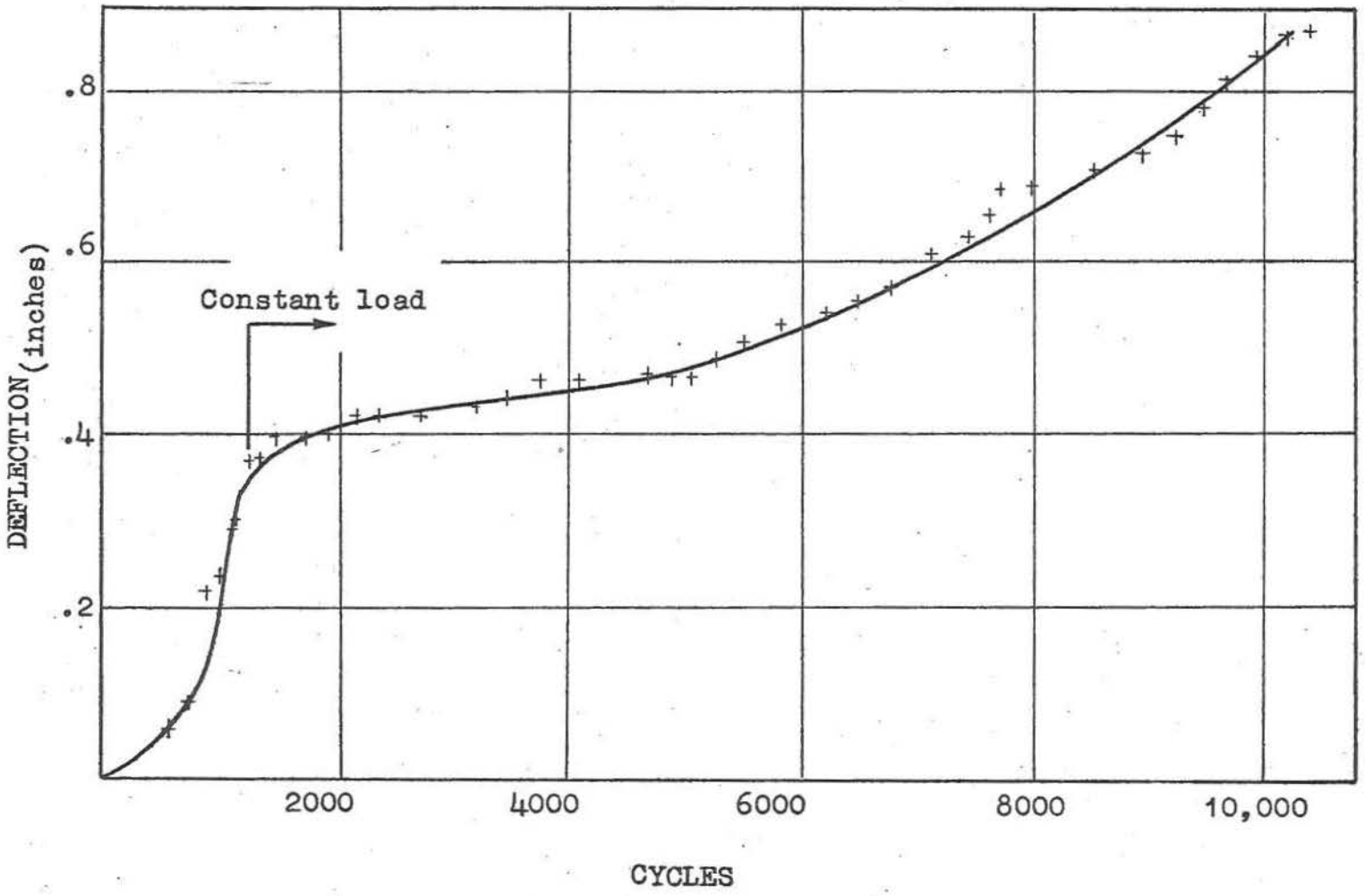

Fig. 5.14 DEFLECTION-CYCLES CURVE FOR FATIGUE TEST ON BEAM 4

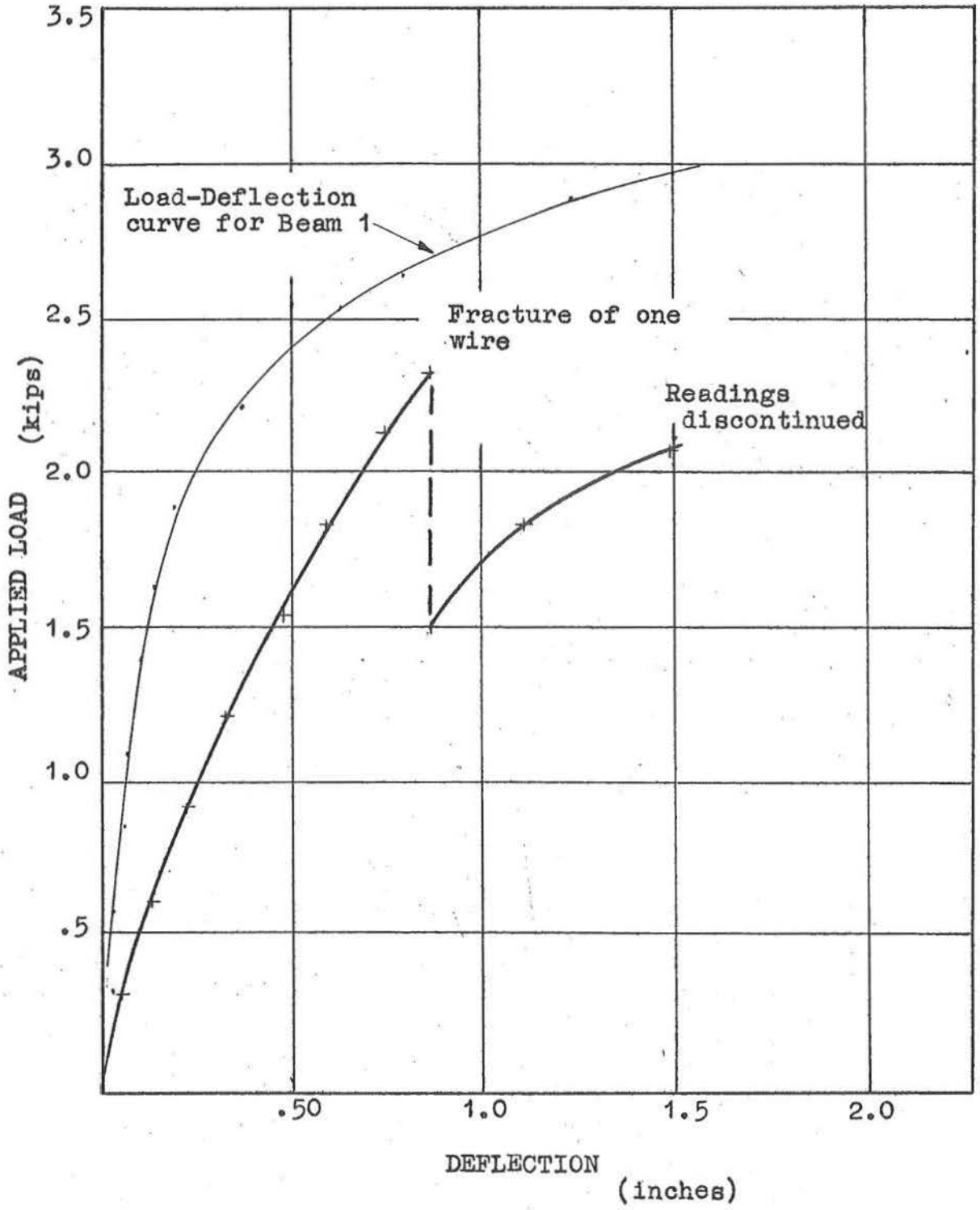

Fig. 5.15 STATIC LOAD DEFLECTION CURVE FOR BEAM 4

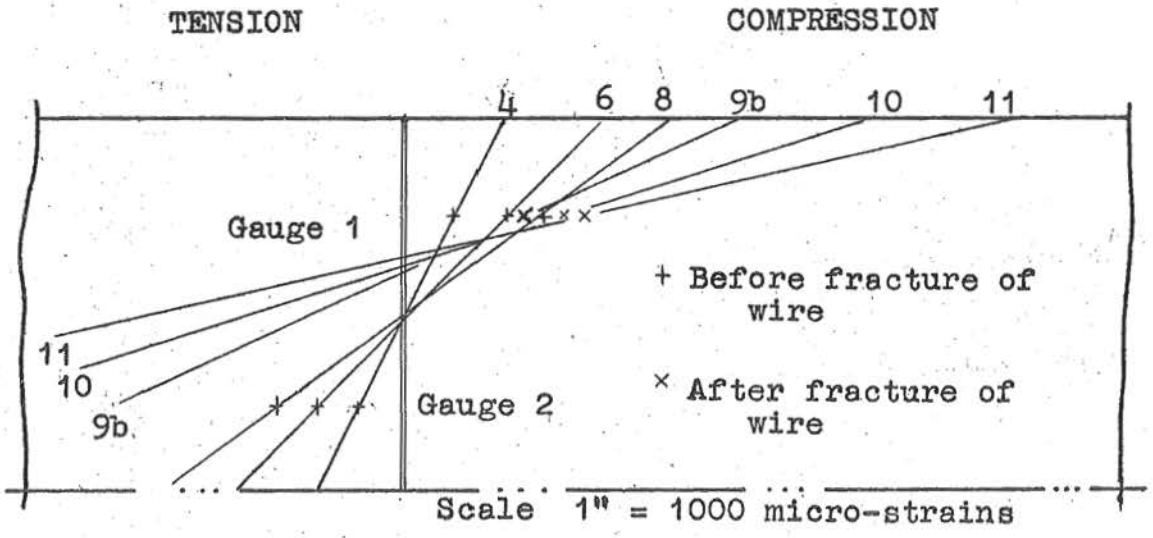

Fig. 5.16 MEAN STRAINS OVER COMPRESSION ZONE OF REGION OF PURE FLEXURE ON BEAM 4.

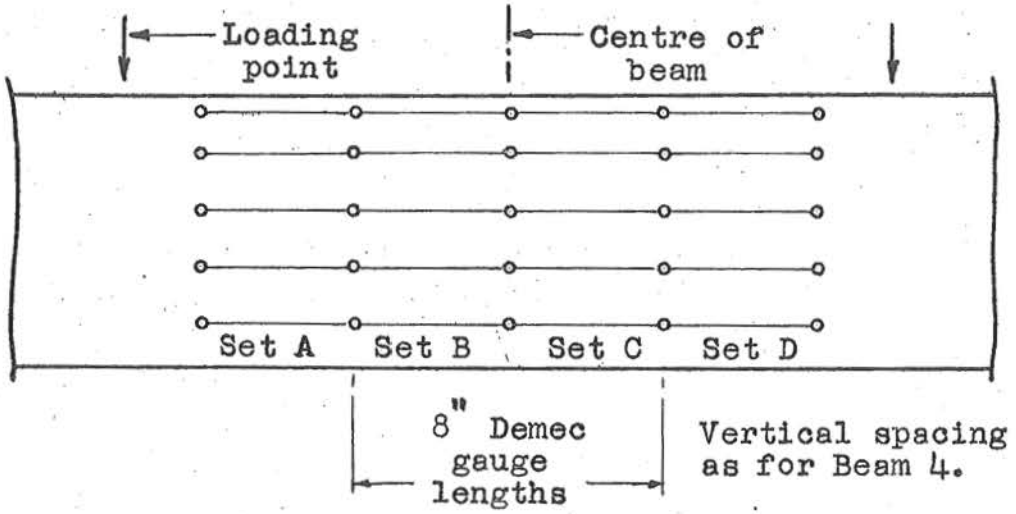

Fig. 5.17 4" DEMEC GAUGE POSITIONS ON BEAM 5

the surface of the fractured wire over the region where the fracture occurred was badly rusted and pitted. The total moment at failure was slightly less than the moment applied in the dynamic test, but the deflection of the beam was slightly greater and this could possibly be due to creep and the loss of bond. The moment at failure was 59.2 Kip-ins and the estimated ultimate moment was 83.5 Kip-ins.

5.6. Beam 5.

5.6.1. Procedure.

The procedure for testing Beam 5 was the same as for Beam 4 with the exception of the changes recorded below. Four sets of 4" Demec gauge lengths placed on both sides of the beam as shown in fig. 5.17 and on the temperature control block were used; the zeros were taken before the start of the dynamic testing.

In the elastic range tests the speeds were $1\frac{1}{2}$, $\frac{1}{2}$, 1 and 2 c.p.s. respectively and for the fatigue test the mean maximum applied load was 2870 lb. with a range of 2690 lb - 2990 lb. The mean resulting moment was 89% of the estimated ultimate moment which was 81.0 Kip-ins. Stops to mark the cracks were made at 1680 cycles, which was 70 cycles before the application of full load, and at 2280 cycles. The test was stopped after 2440 cycles when failure was imminent.

The static test procedure was as for Beam 4.

5.6.2. Results.

The results are shown in figs. 5.18 - 5.21 and Tables C.5.13 - C.5.16.

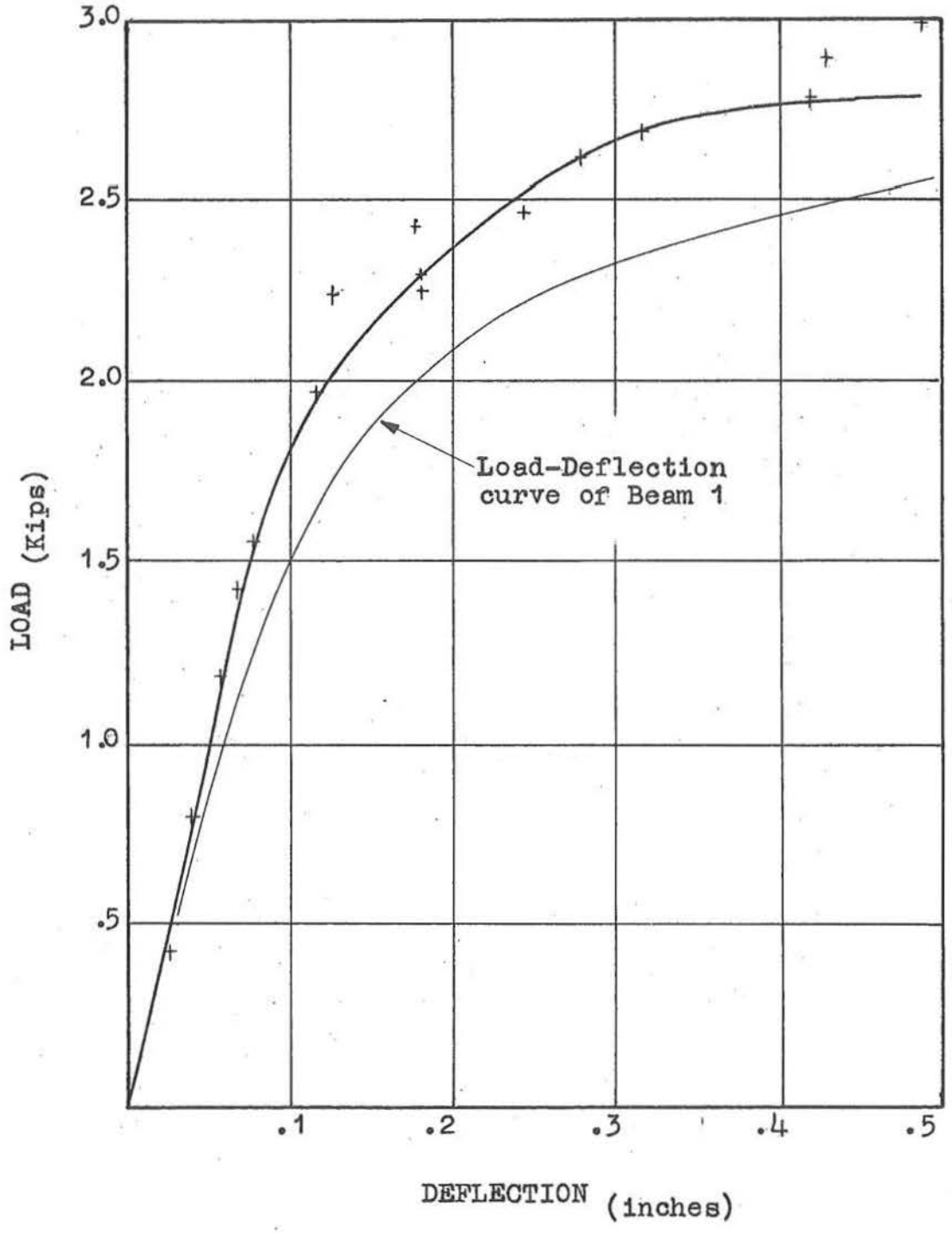

Fig. 5.18 LOAD-DEFLECTION ENVELOPE FOR BEAM 5.

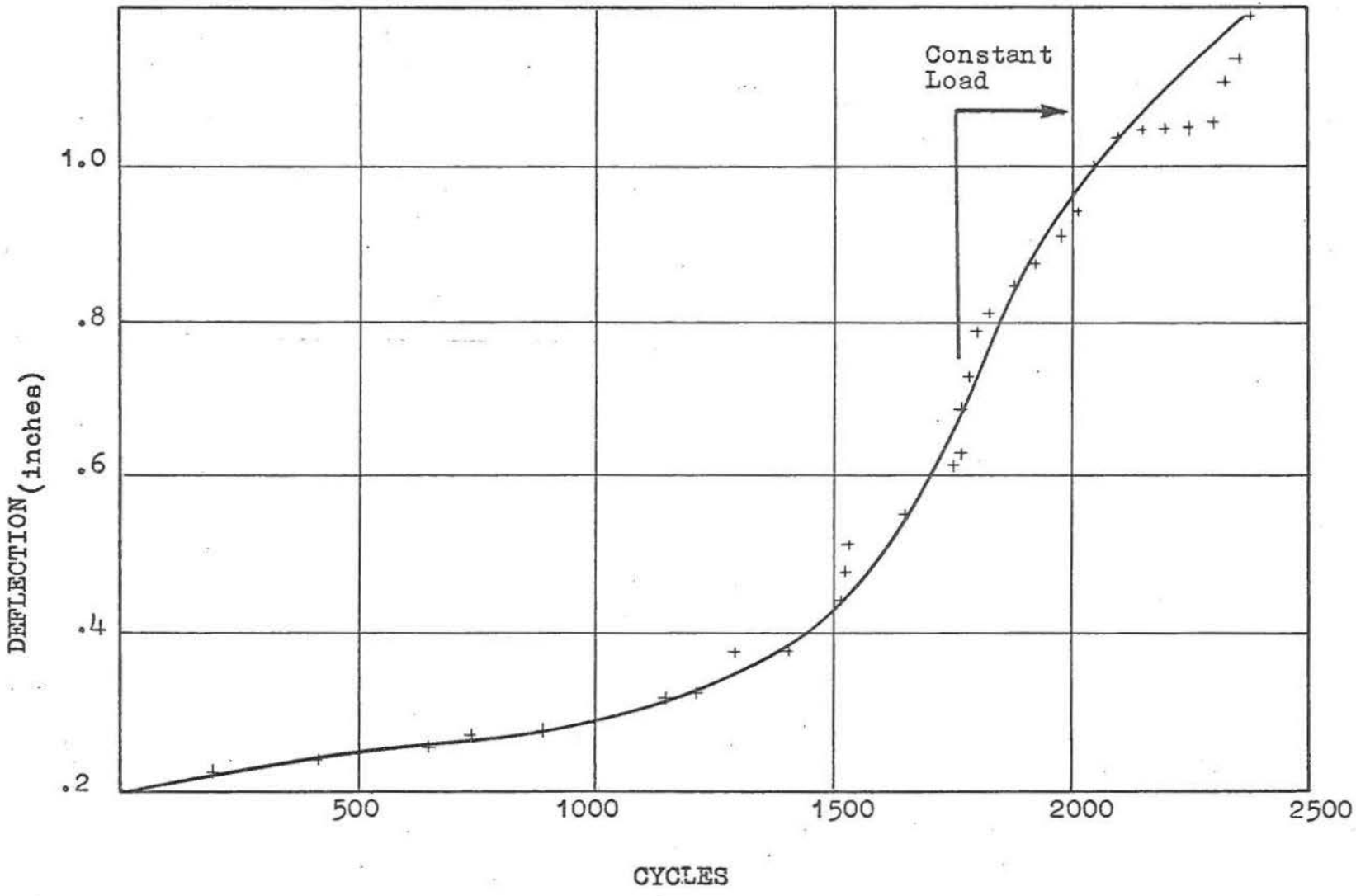

Fig. 5.19 DEFLECTION CYCLES ENVELOPE FOR FATIGUE TEST ON BEAM 5

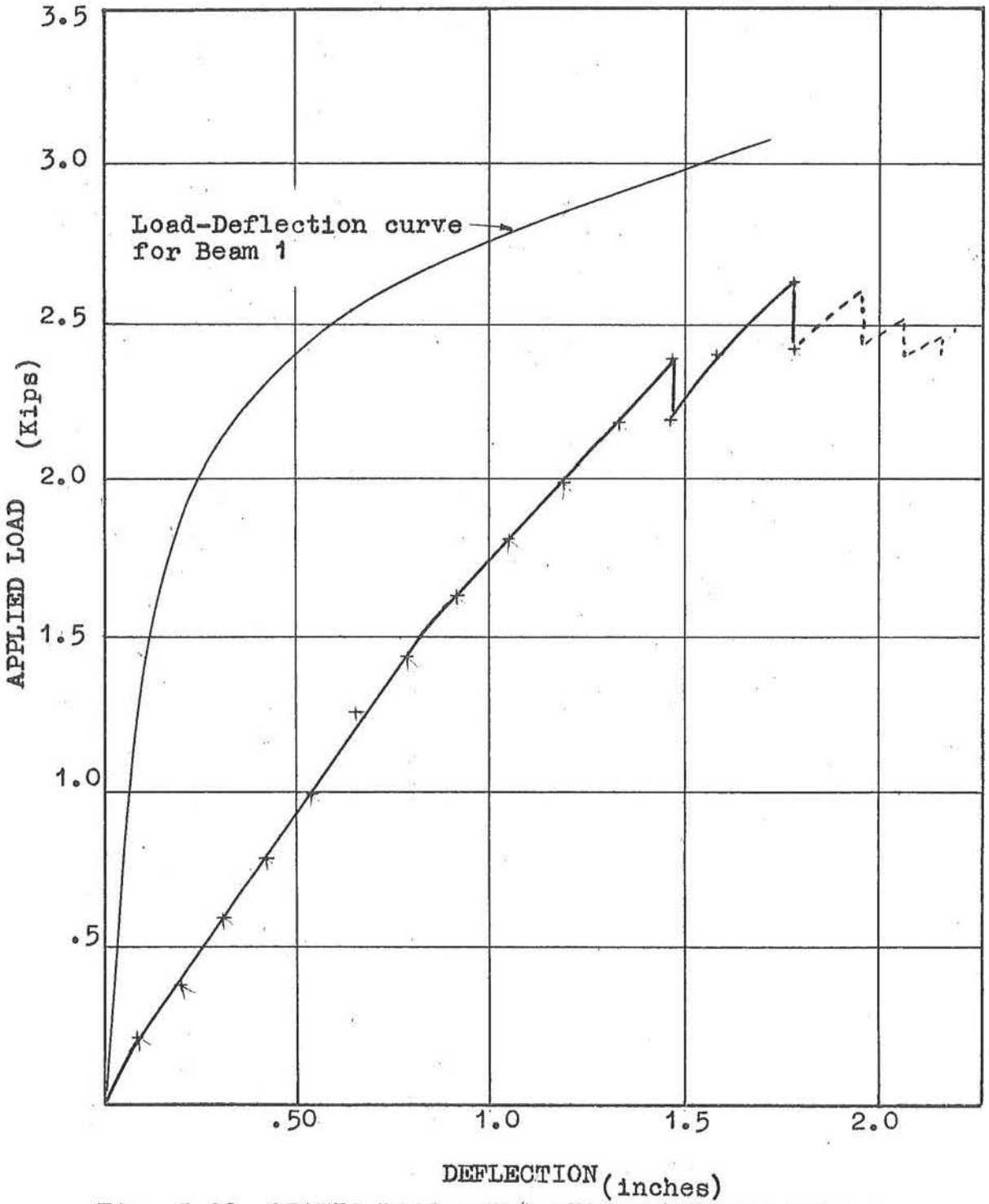

Fig. 5.20 STATIC LOAD-DEFLECTION CURVE FOR BEAM 5

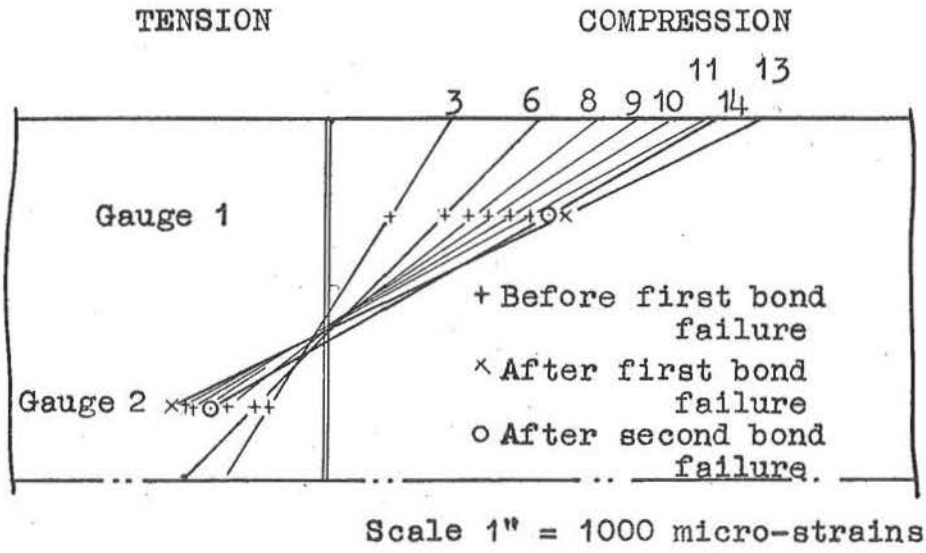

Fig. 5.21 MEAN STRAINS OVER COMPRESSION ZONE IN REGION OF PURE FLEXURE ON BEAM 5.

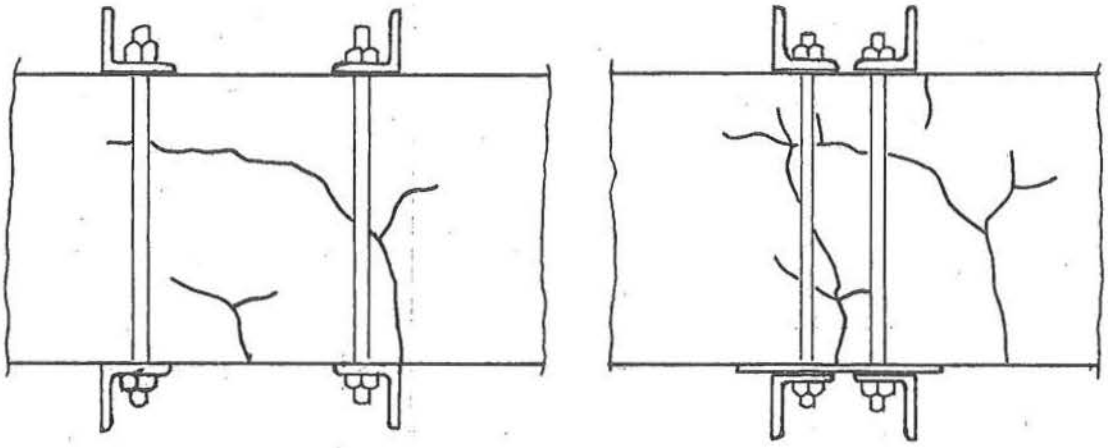

Fig. 5.22 DEVELOPMENT OF SHEAR CRACKS IN MIDDLE OF SHEAR SPAN OF BEAM

During the fatigue test before the first stop a large shear crack, shown in fig. 5.22 (a), developed at the centre of the shear span and threatened to cause a premature failure. When the test was stopped, at 1680 cycles, two external stirrups were placed around the beam as shown in fig. 5.22 (a). When the test was restarted the cracks developed as shown in fig. 5.22 (b) and at the second stop the stirrups were shifted to the position shown in fig. 5.22 (b). A short length of 2" x $\frac{1}{4}$" flat bar was also placed on the bottom face of the beam to act as additional reinforcement and to prevent the cracks from opening. The second arrangement proved to be satisfactory and no further difficulties were experienced from these cracks during the remainder of the fatigue test and during the static rest. The reason for the development of the 'shear' cracks is unknown.

The fatigue test was stopped when a horizontal crack appeared approximately $\frac{1}{2}$" below the top surface of the beam, as shown in Plate 18, and tending to lift a wedge of concrete out of the top surface of the beam. At this stage the beam could not have sustained many more cycles of load without failing.

In the Static Test the beam failed when a section of the compression zone of the concrete lifted out. It is likely that the primary cause of failure was due to large strains in the steel which, during the fatigue test, caused a loss of flexural bond close to the cracks and an overall reduction of the flexural bond strength over the remaining length of the wire within the zone of pure flexure. Hence during the static

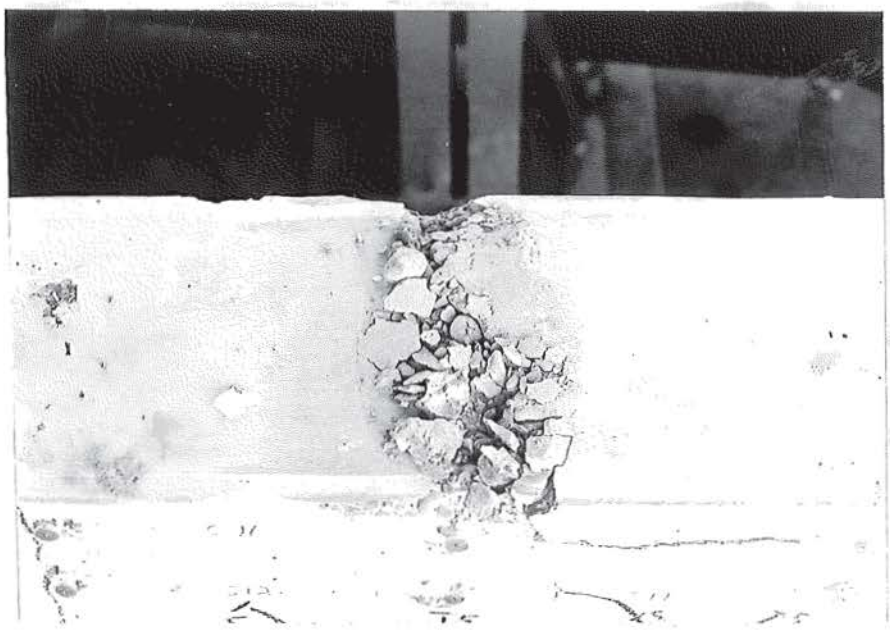

Plate 18. CRUSHING ON TOP FACE OF BEAM 5 following fatigue test.

test the large strains in the wire and the loss of bond would have caused an uplift of the neutral axis which led to the lifting out of the wedge of concrete. The maximum moment in the static test was 63.3 Kip-ins.

6. ANALYSIS OF RESULTS.

6.1. Modulus of Elasticity.

Within the elastic range of prestressed concrete beams the properties of the concrete will almost completely control the behaviour of the beams with the properties of the steel having practically no influence. Consequently the elastic flexural stiffness of a beam is proportional to the modulus of elasticity of the concrete (E) and the second moment of area (I) of the transformed section. Therefore the stiffness of a series of beams which have equal second moments of area will be proportional to the modulus of elasticity of the concrete.

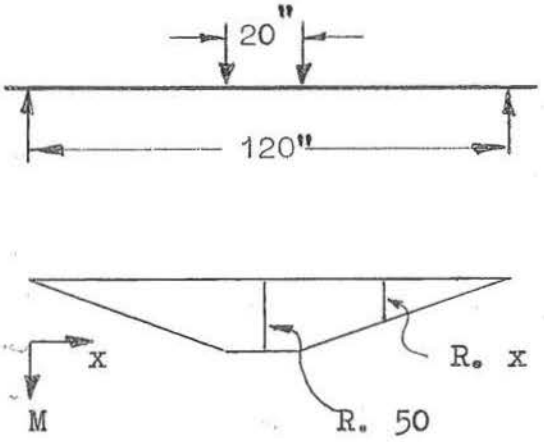

Fig. 6.1. Bending Moment Diagram.

To calculate the modulus of elasticity of the concrete in the beams tested it was assumed that the beams were slender elastic members. The analysis which is presented below was based on the shape of the Bending Moment Diagram produced by the applied loads and shown in fig. 6.1.

$$M = R. x - [R (x - 50)] \qquad \ldots. \quad 6.1$$

as $$\frac{d^2y}{dx^2} = - \frac{M}{E I}$$

equation 6.1 becomes

$$M = \frac{1}{E\,I} \left(R.x - [R\,(x - 50)] \right) \quad \ldots\ldots \quad 6.2$$

integrating 6.2 twice and as $\frac{dy}{dx} = 0$ when $x = 60$

and $y = 0$ when $x = 0$

$$y = \frac{R}{E\,I} \left(1750.x + \left[\frac{(x - 50)^3}{6}\right] - \frac{x^3}{6} \right) \quad \ldots\ 6.3$$

Considering increments of deflection and load and also transposing equation 6.3 becomes

$$E = \frac{dR}{dy} \frac{1}{I} \left(1750.x + \left[\frac{(x - 50)^3}{6}\right] - \frac{x^3}{6} \right) \quad \ldots\ 6.4$$

where dR = increment of reaction at the support

dy = increment of deflection at any position

x = distance from the position considered to the nearest support

by putting $f(x) = 1750.x + \left[\frac{(x - 50)^3}{6}\right] - \frac{x^3}{6}$

equation 6.4 becomes

$$E = \frac{dR}{dy} \cdot \frac{f(x)}{I} \quad \ldots\ 6.5$$

For the beams tested the value of I for the transformed section was 116 and assumes a modular ratio of 5.5 for the steel and concrete.

The values of $\frac{dR}{dy}$ for the positions along the beam were found by drawing graphs of Load versus Deflection for the elastic range of behaviour as shown in fig. 5.3 (b).

The calculations for the values of the modulus of elasticity are shown in Tables D.6.1 - D.6.5 and are summarized in Table 6.1.

Beam Number	Testing Frequency c.p.s.	Cylinder crushing strength of concrete p.s.i.	Modulus of Elasticity x 10^{-6} p.s.i.	Standard Deviation	$\frac{E}{E_{static}}$
1	static	7930	5.01		.96
2	static	8010	5.43	.13	1.04
3	$\frac{1}{2}$ 1 $1\frac{1}{2}$	8340	5.84 6.19 6.16	.13 .23 .23	1.12 1.19 1.18
4	$\frac{1}{2}$ 1 $1\frac{1}{2}$	7400	5.84 5.94 5.81	.14 .21 .23	1.12 1.14 1.11
5	$\frac{1}{2}$ 1 $1\frac{1}{2}$ 2	6680	6.01 6.28 6.16 5.96	.18 .10 .14 .33	1.15 1.20 1.18 1.14
Average Values	static $\frac{1}{2}$ 1 $1\frac{1}{2}$ 2	7970 7440 7440 7440 7440	5.22 5.90 6.14 6.02 5.96	 .17 .24 .26 .33	1.00 1.13 1.17 1.15 1.14

Table 6.1. Values of the Elastic Modulus for Concrete.

6.2. Moment - Curvature Relationships.

The curvatures of the beams at each increment of load where Demec gauge readings were taken, were found from the average of the strains on the two faces of the beams shown in Tables C.5.2, C.5.5, C.5.12 and C.5.16. Graphs of the

distribution of strain across the face of the beam were drawn to find the depth to the Neutral Axis, $k_u.d$, and the strain in the top compressive fibre, e_c, as shown in fig. 6.2 (and also figs. 5.16 and 5.21). Over the compression zone it was assumed that plane sections remained plane. The curvature at a section is ϕ where

$$\phi = \frac{e_c}{k_u.d} \qquad \ldots 6.6$$

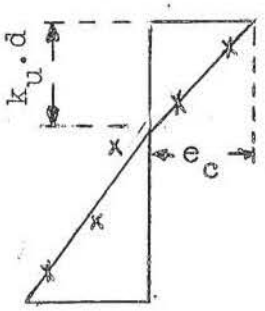

Fig. 6.2.

The results are shown in Tables D.6.6. - D.6.9 and in figs. 6.3 - 6.7.

6.3. Ductility.

The ductility of a beam is a measure of its plasticity and the ductility of prestressed concrete beams may be defined as "the ratio of the deflection of the beam at a particular load to the deflection, under similar loading conditions, at the flexural cracking load; the flexural cracking load being the load at which the beam will start to crack if the modulus of rupture of the concrete is 10% of the cylinder crushing strength." The ductility of a beam at the failure load is normally referred to as the "ductility factor". The ductility of the beams tested is shown in Table 6.2.

The maximum ductility of Beams 4 and 5 were 11 and 12 respectively and since both these beams were close to failure when the fatigue tests were stopped it is probable that the ductility factors would have been only slightly greater and thus would have been of the same order as the ductility factors of the two statically tested beams.

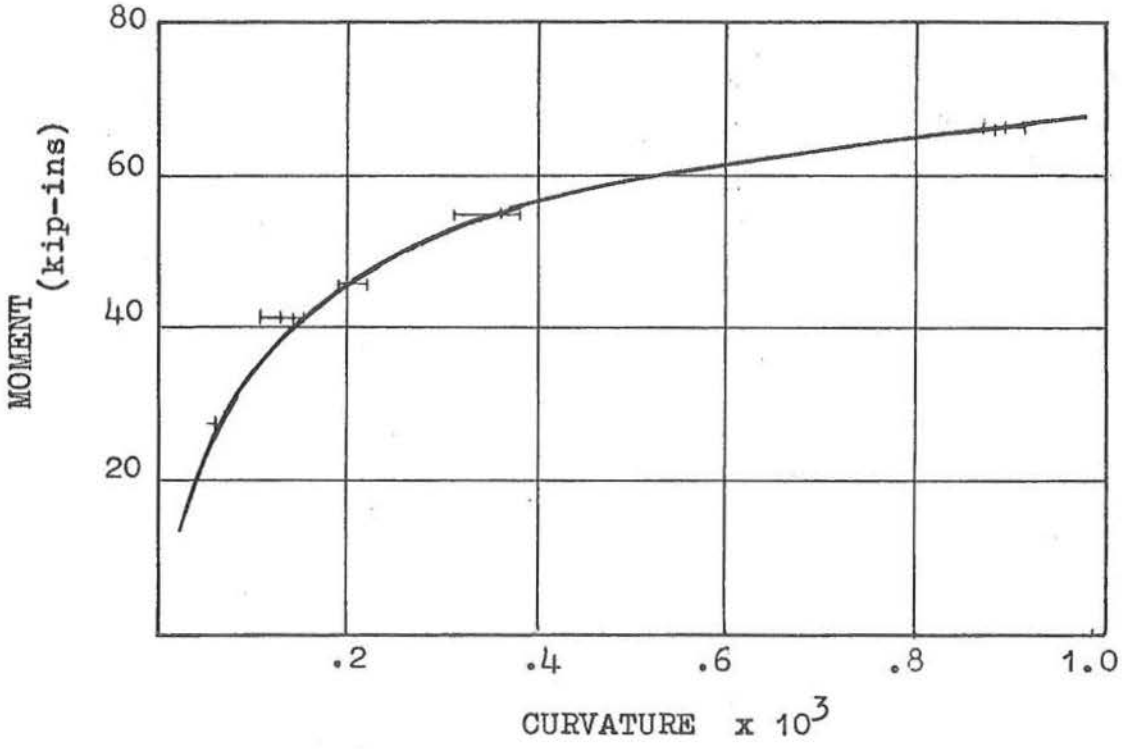

Fig. 6.3 MOMENT CURVATURE RELATIONSHIP FOR BEAM 1

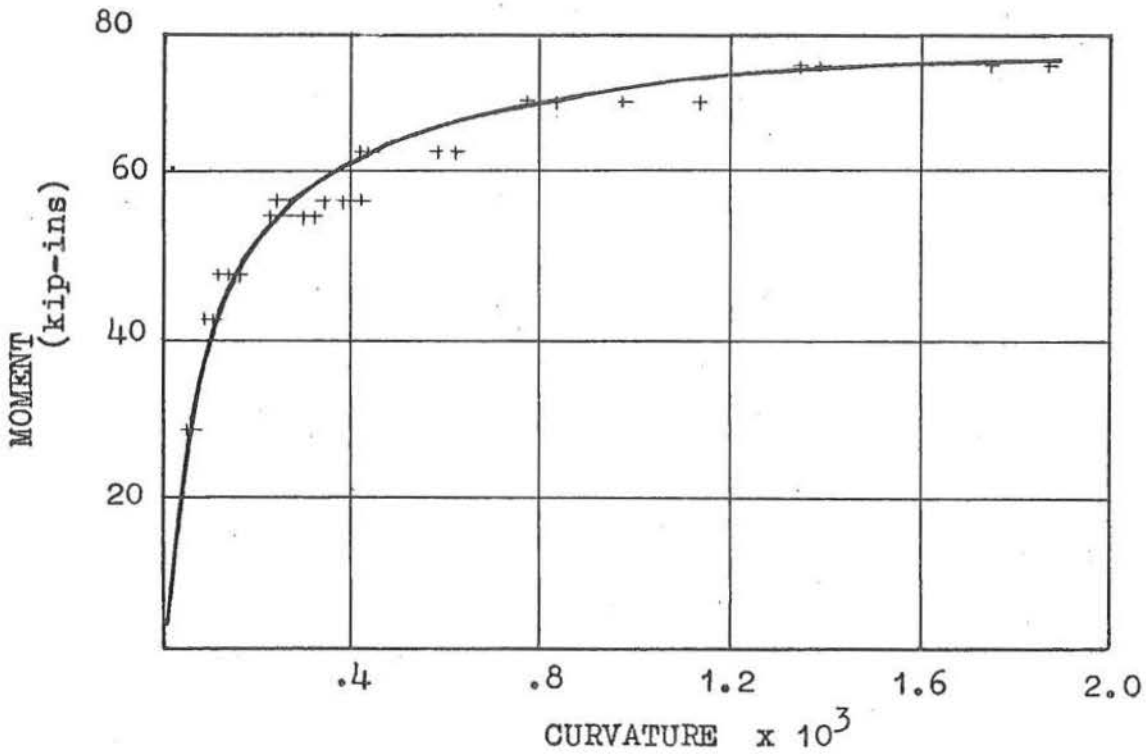

Fig. 6.4 MOMENT CURVATURE RELATIONSHIP FOR BEAM 2

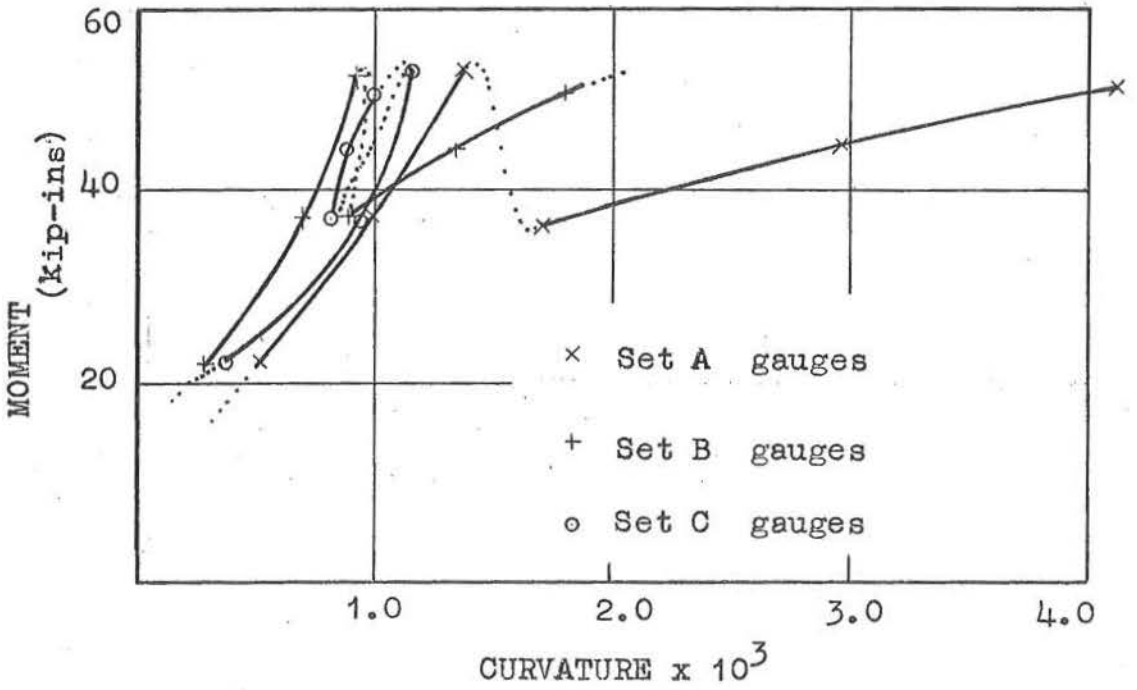

Fig. 6.5 MOMENT CURVATURE RELATIONSHIPS FOR BEAM 4

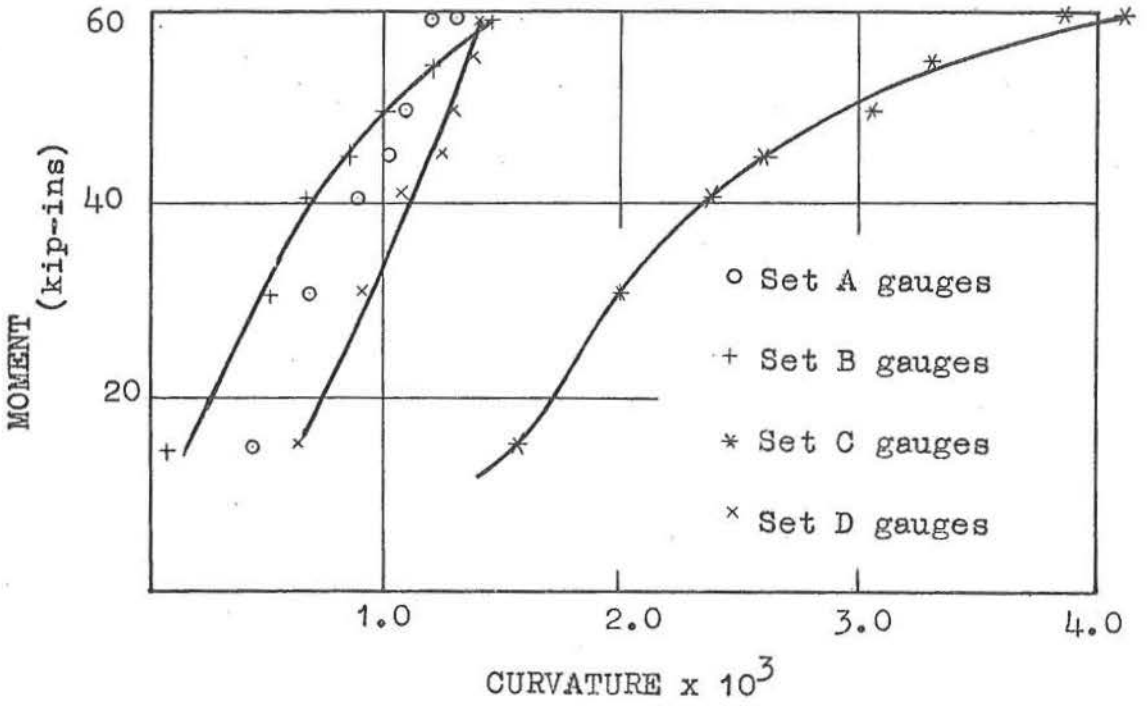

Fig. 6.6 MOMENT CURVATURE RELATIONSHIPS FOR BEAM 5

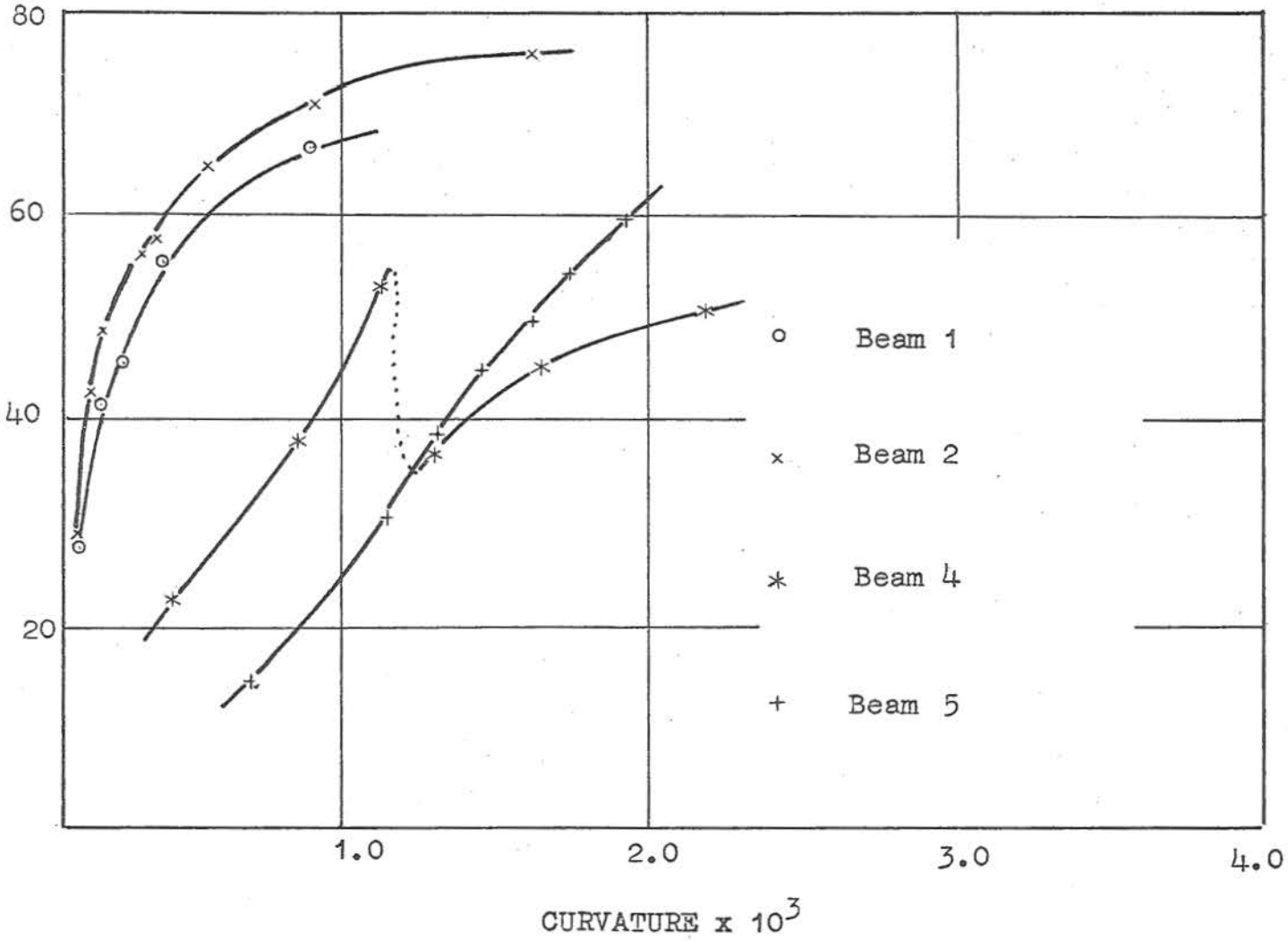

Fig. 6.7 AVERAGE MOMENT CURVATURE RELATIONSHIPS FOR BEAMS 1, 2, 4 AND 5.

Beam Number	1	2	3	4	5
Flexural cracking load (lbs)	1700	1730	1750	1690	1600
Deflection at cracking (inches)	.16	.13	.095	.090	.073
Maximum Deflection (inches)	2.3	1.9	2.2	.91	1.79
Ductility Factor	14	15	-	-	-
Maximum Dynamic Load (lbs)	-	-	2360	2670	2870
Maximum Dynamic Deflection (inches)	-	-	.39	1.02	.87
Maximum Ductility	-	-	4	11	12

Table 6.2 Ductility of Beams.

6.4. Resonant Frequency

For a slender elastic beam the nodal frequencies are given by

$$f_n = C' \sqrt{\frac{E I}{m L^4}} \qquad \ldots\ldots \quad 6.7$$

reference 30

where f_n - frequency of the n^{th} mode of vibration(c.p.s.)

I - second moment of area of the transformed cross-section (in^4)

E - modulus of elasticity for concrete (p.s.i.)

m - mass of the beam per unit length ($lb\text{-}sec/in^2$)

L - length of the beam between supports (in)

C' - a constant which is a function of the support conditions and the mode of vibration

The formula assumes the normal assumptions associated with the elastic analysis of beams and also that the horizontal inertia forces due to the shortening and lengthing of the longitudinal fibres of the beam are negligible. For the beams tested the frequency of the first mode of vibration was calculated to be 34 c.p.s. assuming: $C' = 1.57$, (see fig. 5.8 of reference 30) $I = 116$, $E = 5{,}300{,}000$ p.s.i. As the greatest testing frequency was 2 c.p.s. it may be shown that the dynamic response of the beams to the forced motion was negligible even when the damping was assumed to be zero.

6.5. Inertia.

When a beam is subjected to cyclic loading a portion of the applied force is required to accelerate the mass of the beam while the remainder is absorbed by the normal "static" resistance to deformation. The portion of the load absorbed by the acceleration of the beam is referred to as the inertia of the beam.

Consider the small element of a beam shown in fig. 6.8, length dx, weight w', which is subjected to a forced sinusoidal

motion of frequency F and maximum displacement y.

The maximum acceleration is $\ddot{y}$

where $\ddot{y} = -n^2 y$

and n is the circular frequency

therefore $\ddot{y} = -4 \pi F^2 y$ 6.8

Since Force = mass x acceleration

the maximum inertial force for the element is P'

where $P' = m (- 4 \pi F^2 y)$ ... 6.9

now $m = \frac{w' . dx}{g}$

$= \frac{\bar{w} . A . dx}{g}$

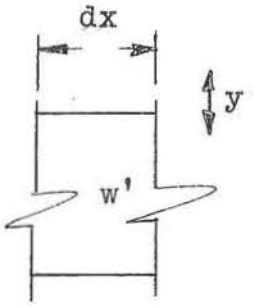

Fig. 6.8 Element of a beam.

where $\bar{w}$ is the weight per unit volume of the beam.

A is the cross-sectional area of the beam.

and therefore $P' = - \frac{\bar{w} . A . dx}{g} 4 F^2 y$ 6.10

For the complete beam the inertial load is P_i

where $P_i = -4 \pi F^2 \frac{\bar{w} . A}{g} \int y . dx$ 6.11

For the beams tested

$P_i = - .25 F^2 \int y . dx$ 6.12

assuming $\bar{w} = 152$ lb / ft^3

Therefore the inertial load on a beam is proportional to the mass of the beam, the square of the testing frequency and the deflected shape of the beam. The distribution of the inertial load along the beam will be identical to the deflected shape of

the beam.

If only the inertial load is considered to act on the beams tested, as shown in fig 6.9 (a), it may be seen that the beam effectively becomes a three span beam with the two points at which the load is applied becoming the additional two supports. Therefore the inertial load will be resisted at four points and the overall effect will cause an increase of the load applied by the Dynamic Loading Unit and a decrease of the reactions at the external supports.

From the results of the test on Beam 1 it may be seen in fig 6.9 (b) that a linear distribution of load in the shear spans and a uniform distribution of load in the zone of pure flexure is a reasonable approximation to the actual deflected shape. The reactions at the four points at which the inertial load was resisted were calculated from the assumed load distribution by moment distribution methods and it was found that 76% of the inertial load would have been applied through the load-cell while 24% was resisted by the end supports. As the distribution beam on the Dynamic Loading Unit oscillated with the concrete beam a portion of the total force registered by the load-cell would have been absorbed by the inertia of the distribution beam which weighed 65 lbs.

To estimate the inertial forces applied through the load-cell the deflected shapes of the beam for the elastic and fatigue tests were assumed as indicated in Table 6.3. The value of $\int y.dx$ was calculated and substituted into equation 6.12 to give the total inertial load due to the prestressed

beam only which was distributed to the central loading points and the external supports in the ratio shown in fig. 6.9 (b). The inertial load of the distribution beam was found using equation 6.9 and was added to the inertial load of the concrete beam applied by the load-cell to give the total increase of the applied load due to inertia. The results are shown in Table 6.3.

Fatigue Test			Elastic Range Tests			Test
$y = f(y)^{1.5}$			$y = f(y)^{2}$			Assumed Deflected Shape.
$\frac{1}{2}$	$\frac{3}{4}$	1	.05	.05	.05	Maximum Deflection (ins)
1	1	1	1	$1\frac{1}{2}$	2	Testing Frequency (c.p.s.)
9	14	18	1.1	2.5	4.5	Total Beam Inertial Load (lbs.)
7	11	14	.8	1.9	3.5	Beam Inertial Load resisted by Load Cell (lbs.)
5	7	10	.5	1.2	2.0	Inertial force absorbed by Distribution Beam (lbs.)
12	18	24	1.3	3.1	5.5	Total Inertial Load resisted by Load cell (lbs.)

Table 6.3. Inertial Loads on Beams.

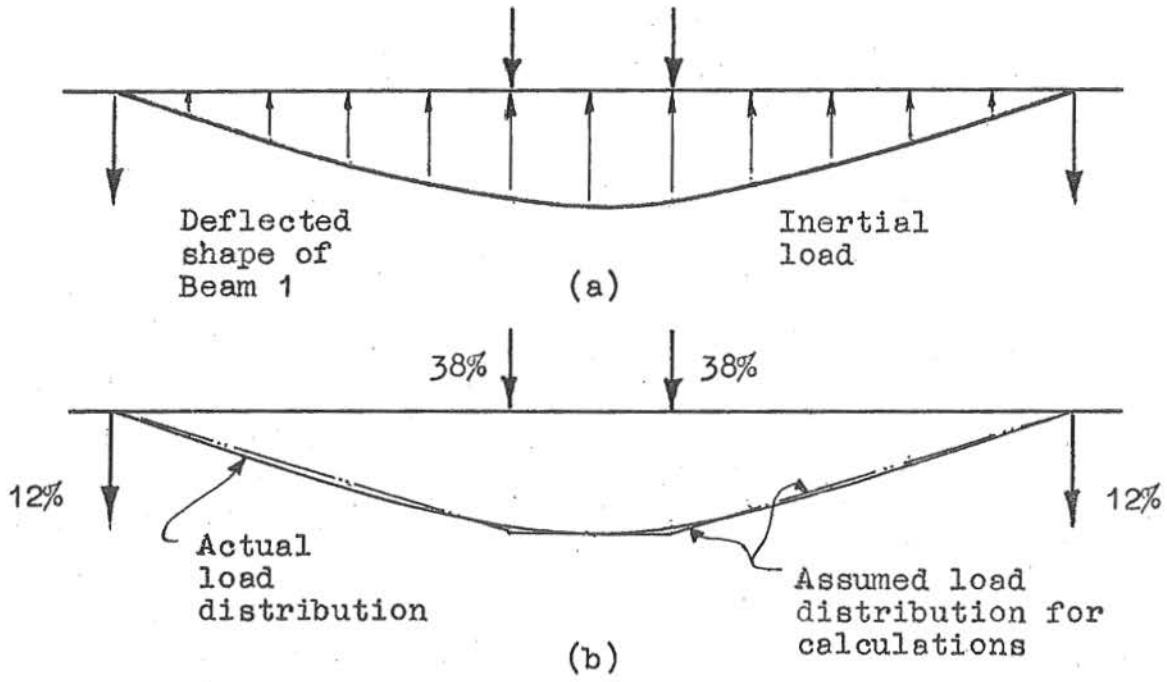

Fig. 6.9 DISTRIBUTION OF INERTIAL LOAD

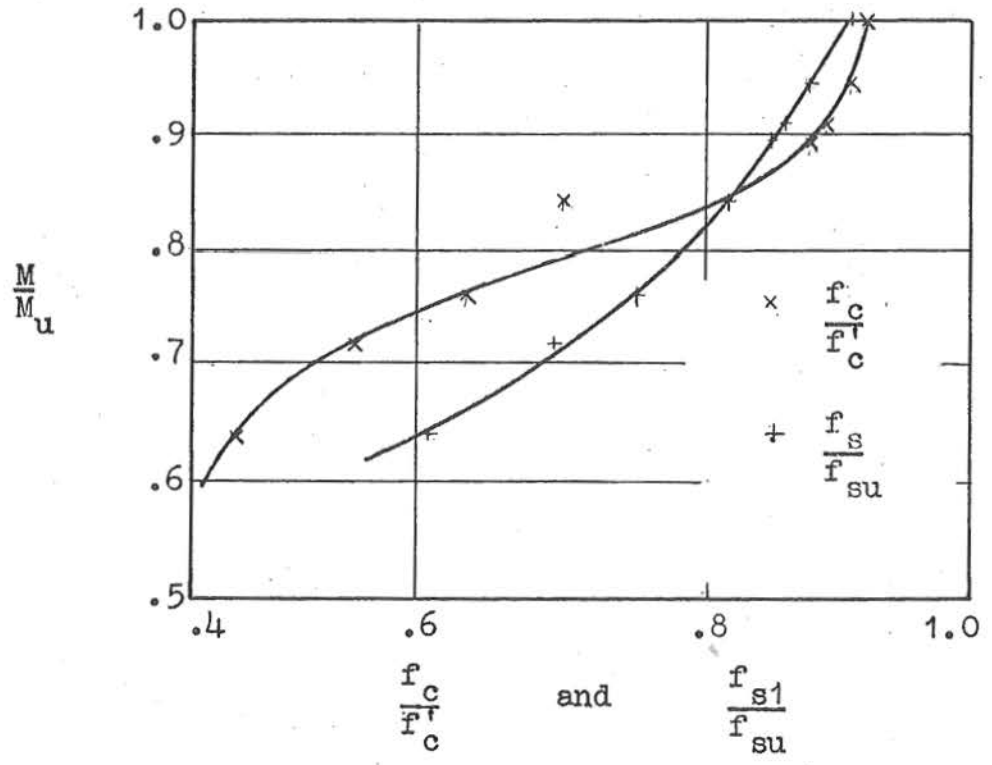

Fig. 6.10 RATIO OF STEEL AND CONCRETE STRESSES IN BEAMS TO ULTIMATE STRESSES OF STEEL AND CONCRETE RESPECTIVELY

6.6. Analysis of Stresses in Beams.

After the stress losses in the five beams had been evaluated an average beam was derived and is shown in Table 4.2. This average beam has been analysed to determine the order of the steel stresses and the maximum compressive stresses in the concrete. The results are shown in fig. 6.10 and Table D.6.10.

The analysis was based on the stress-strain properties of the concrete and steel shown in figs. 4.2 and 4.3 and the following assumptions were made:

1. Plane sections remain plane.
2. The concrete carries no tension after the cracks have developed.
3. Full bond is achieved at all times.

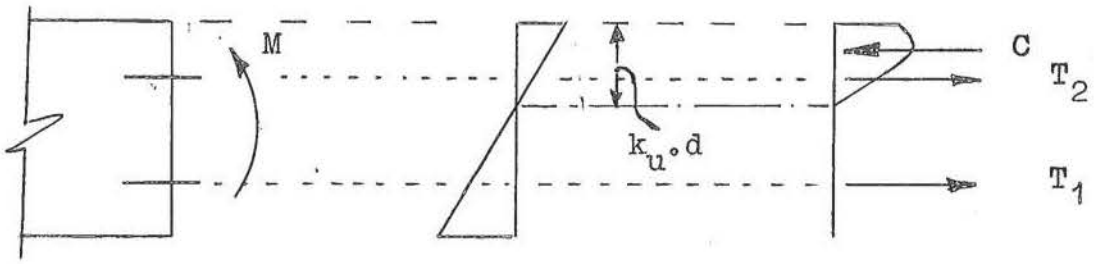

$$C = k_1.k_3.f_c.k_u d.b \quad \ldots\ldots 6.13$$

$$T_1 = f_{s1} A_s \text{ and } T_2 = f_{s2} A_s \quad \ldots\ldots 6.14$$

$$T = T_1 + T_2 \quad \ldots\ldots 6.15$$

$$M = T_1 (5.25 - k_u d) + T_2 (1.75 - k_u d) \quad \ldots 6.16$$

Fig. 6.11 Moments and Forces acting over a section of a beam.

The trial and error method adopted to analyze the beam is outlined below using the notation shown above in fig. 6.11.

1. Assume a value for the strain in the extreme compression fibre of the concrete (e_c) due to the unknown load.
2. Assume a depth of the compression zone ($k_u.d$).
3. Calculate the compressive force (C) acting on the section using equation 6.13; the value of the coefficients k_1, k_3, which are shown and explained in Appendix B, were derived from the stress-strain curve for the concrete shown in fig. 4.3.
4. From compatibility considerations estimate the imposed strains in the steel due to the applied load and add to the strain due to the prestressing forces.
5. From the total steel strains and using the stress-strain curve for the steel shown in fig. 4.2 find the individual stresses in the wires. Using equations 6.14 and 6.15 find the total tensile force T acting on the section.

6.(a) If the tensile and compressive forces are unequal, i.e. $C \neq T$, adjust the depth of the compression zone and repeat steps (2) - (5).

(b) If the tensile and compressive forces are equal i.e. $C = T$, calculate the moment acting on the section using equation 6.16. Finally calculate the applied load from the known loading conditions.

7. Assume a new value for the compressive strain in the extreme concrete fibre, e_c, and repeat steps 2 - 6.

6.7. Ultimate Strength of Beams.

The calculation of the ultimate moments for each of the beams was based on the stress-strain relationships for the steel and concrete and on the three assumptions outlined for the analysis of the stresses in the average beam and stated in section 6.5. To calculate the ultimate moment the maximum compressive strain in the extreme compressive concrete fibre was assumed to be .0029; this assumption being based on the results of Hognestad, Hanson and McHenry[28]. The procedure for calculating the ultimate moment followed steps (2) - (6) for analyzing the stresses in the beam. The ultimate moments of the beams are shown in Table 6.4.

Number of Beam	Concrete Strength p.s.i.	Steel Prestress k.s.i.	Estimated Ultimate Moment Kip-ins.
1	7840	154	84.4
2	8010	154	84.9
3	8340	-	84.8
4	7400	161	83.5
5	6680	159	81.0

Table 6.4 Ultimate Moments of Beams.

7. DISCUSSION.

7.1. Introduction.

Previous research has shown that there will be a wide range of results from fatigue tests on concrete specimens and that the range is likely to be greater than the range produced in normal static tests. Concrete is not unique in this as the results of fatigue tests on steel and other materials indicate a similar trend. Recent research on the properties of plain concrete, reinforced concrete and prestressed concrete has therefore tended towards testing a large number of specimens and subjecting the results to a rigorous statistical analysis to obtain reliable quantitative results. However, as only three beams were tested dynamically it was possible to study only the general qualitative flexural properties and behaviour of prestressed concrete beams when subjected to reversed cyclic loading within the elastic range and at high intensities of loading.

7.2. Primary Static Tests. Beams 1 and 2.

The load deflection curves for prestressed concrete beams normally exhibit three stages of behaviour. The first stage is practically linear with the upper limit being at the load when flexural cracks begin to form at the tension face. The second stage continues until the steel begins to yield and is characterized by the rapidly changing slope of the load - deflection curve. The third stage continues from the yielding of the steel until failure occurs and is the portion of the load - deflection curve where there is a decreasing rate of change of slope with the curve becoming almost linear as failure is

approached.

Beam 1 of the test series exhibited all three stages of behaviour with the limits for the three regions being close to those predicted analytically. The limit for the end of the second stage was taken as being when the steel in the lower portion of the beam reached the limit of proportionality. The load deflection curves for Beam 2 showed similar characteristics. Both beams had relatively long elastic, i.e. linear, and plastic.

For both Beams 1 and 2 small cracks became visible under magnifying glasses (Magnification 20 X, 10 X,) at considerably lower loads than those predicted by a modulus of rupture of 10% of the cylinder crushing strength of the concrete. It is thought that large shrinkage strains developed in the concrete during the 6 day period before the beam was stressed and caused sufficiently large stresses which led to the development of small hairline cracks. Furthermore it is likely that these cracks were relatively shallow and did not penetrate to the depth of the prestressing steel. When the beam was stressed the cracks closed but reopened when the beams were tested and became visible at loads slightly greater than the loads corresponding to zero stress in the bottom fibre. At higher loads some of these cracks developed into normal flexural cracks, some closed and in one case a flexural crack started within an inch of the shrinkage crack which reclosed. Similar shrinkage cracks also occurred in the beams tested dynamically.

The presence of cracks across the compression zone of Beam 2 did not appear to cause any changes in either the mode

of failure, which was primary tension for both Beams 1 and 2, or in the ultimate load. The estimated ultimate load was lower than the actual ultimate load for both beams because the assumed value of the strain in the extreme compressive fibre was less than the actual strain at failure. Hence for the beams tested the depth of the compression zone was less than predicted and although the change of the compression and tension forces on the section would have been negligible a small increase of the internal lever arms would have led to the slightly larger ultimate moments.

7.3. Dynamic Elastic Range Tests. Beams 3, 4 and 5.

7.3.1. General.

The calculated modulus of elasticity for the concrete in the beams tested dynamically over frequencies of $\frac{1}{2}$ - 2 c.p.s. was an average of 15% greater than the average modulus for the two statically tested beams. Since the stiffness of prestressed concrete beams is proportional to the elastic modulus of the concrete, as discussed in section 6.1, it follows that the stiffness of the dynamically tested beams was an average of 15% greater than the stiffness of the beams tested statically. Bate [26] found a similar increase of stiffness, as shown by the range of deflection, for prestressed concrete beams subjected to cyclic loading within the working range; however the beams tested by Bate were not subjected to reversals of load.

The increase of stiffness for the dynamically tested beams may be attributed to:

1. friction at the supports of the beams which produced a small degree of end restraint; however, it is unlikely

that this accounts for more than a very small portion of the increase;

2. an increase of the modulus of elasticity for the concrete due to the faster rates of loading; combined with
3. a change of the stress-strain curve for concrete due to the cyclic loading which eliminated the effect of the permanent strains,
4. the inertia of the beam which was shown in section 6.5 to be small during the elastic range tests.

7.3.2. Concrete Stress-Strain Curves for Dynamic Loading.

McHenry and Shideler[31] in their review of the effect of the rate of loading on the properties of concrete found that the modulus of elasticity increased as the rate of loading increased and that the increase in the elastic modulus became greater as the maximum stress level rose. However, the results of the numerous investigations reviewed varied over a wide range and the effect of repeated loads was not considered.

Leonhardt[32] produced the stress-strain curves shown in fig. 7.1 which shows that the stress-strain curve for concrete after the first cycle of load becomes practically linear and parallel to the initial tangent modulus for the first cycle. The figure also shows that the maximum strain increases under the action of cyclic loading and it was stated that the cyclic loading increased the rate of creep. As the maximum concrete stresses in the beams during the elastic range tests were relatively low and since only a small number of cycles of load were applied the creep in the beams would have been negligible

and it is possible that the maximum strains in the dynamic case would have been less than those in the static case. From the results of Leonhardt and the review by McHenry and Shideler it is probable that the stress-strain curves shown in fig. 7.2 are typical for the concrete in the statically and dynamically tested beams.

The rates of loading in the extreme concrete fibres of the beams for maximum applied loads of ± 1000 lb at testing frequencies of $\frac{1}{2}$, 1, $1\frac{1}{2}$, and 2 c.p.s. were calculated to be 1530, 3060, 4590, and 6120 p.s.i. per sec and the corresponding mean rates of loading, because of the stress gradient, were 1020, 2040, 3060, and 4080 p.s.i. per sec. The mean rate of loading for the static test was of the order .25 p.s.i. per sec. and from the graphs produced by McHenry and Shideler the increase of the elastic modulus for the concrete from the static to the dynamic case would have been 5-7%. The increase in the elastic modulus for an increase of rate of stressing from 1530 - 6120 p.s.i. per sec. was small and would have been approximately 2%. Hence it is possible to present one stress-strain curve for the concrete in the beams tested dynamically which has an elastic modulus for the first cycle 5-7% greater than that for the static curve. For the subsequent cycles the curve will be approximately parallel to the initial tangent modulus of the dynamic curve although the permanent strains will tend to increase the maximum strain as shown in fig. 7.2.

7.3.3. Increase of stiffness due to Dynamic Loading.

By considering the stresses and strains in the top and bottom fibres of a beam, as shown in fig. 7.3 and assuming that

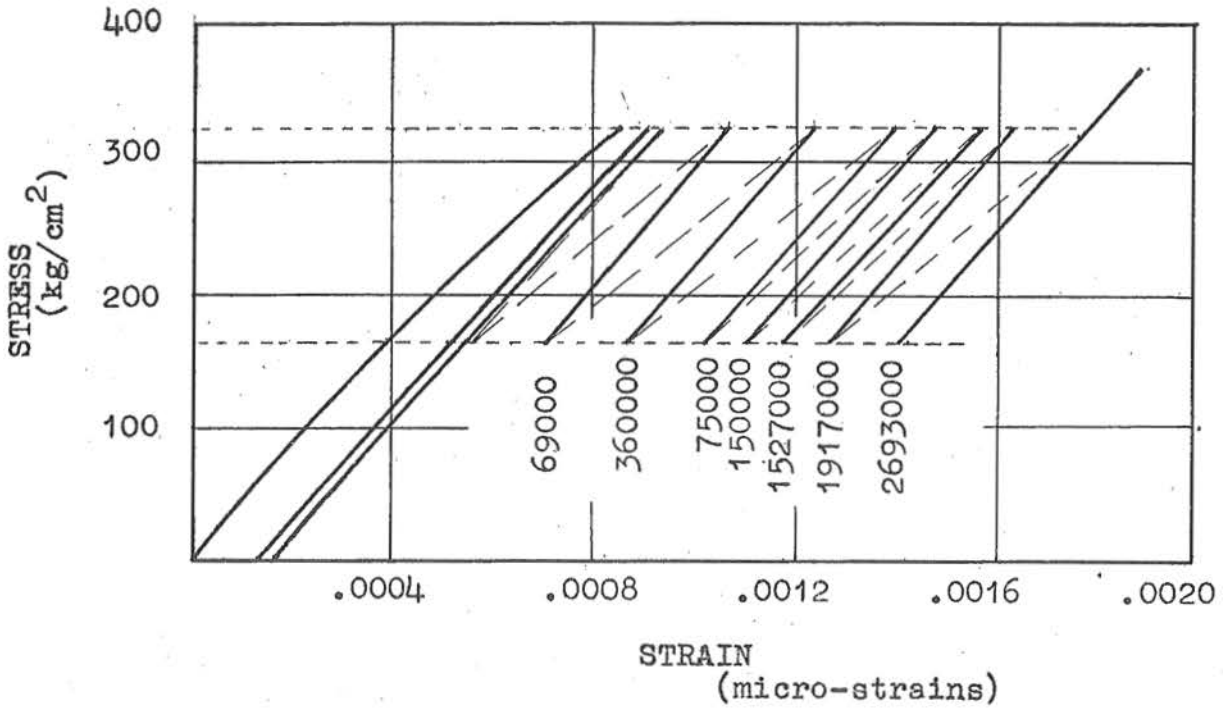

Fig. 7.1 STRESS-STRAIN CURVES FOR CONCRETE PRISM SUBJECTED TO CYCLIC LOADING (Leonhardt[33])

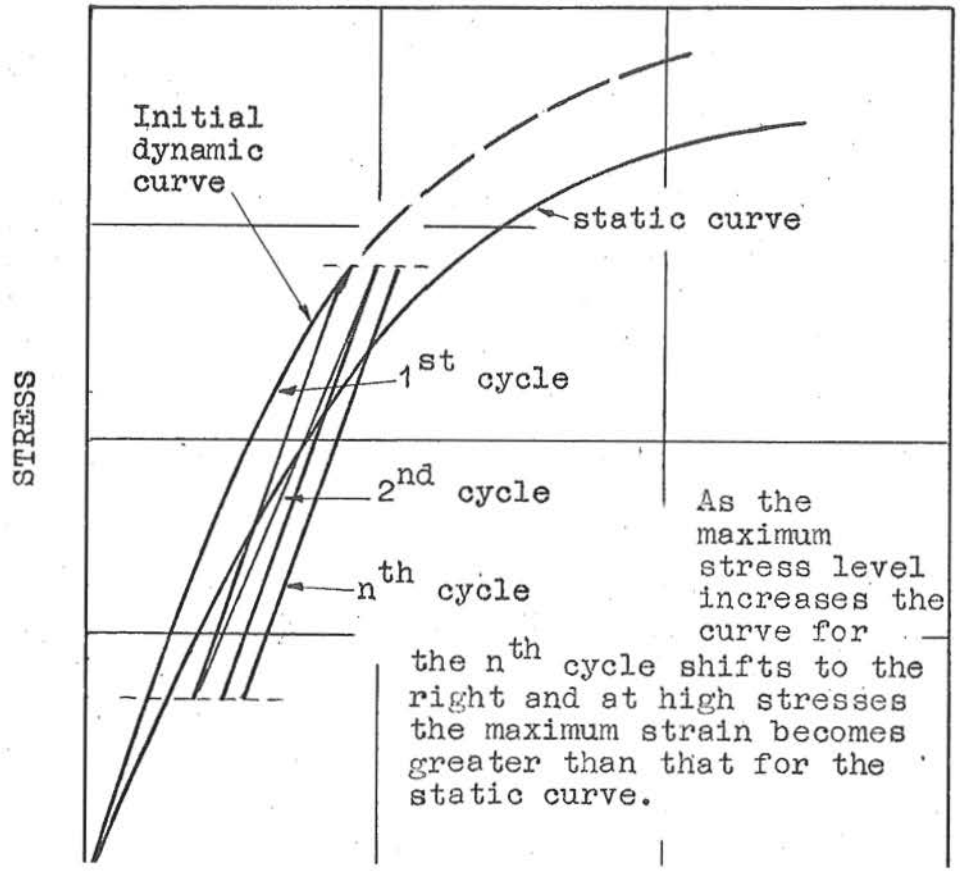

plane sections remain plane, it will be shown below that the range of curvature when the load is applied statically is greater than half the total range of curvature in the n^{th} cycle. The notation used refers to fig. 7.3.

For a statically applied load the change of curvature is ϕ_s

$$\text{where} \quad \phi_s = \frac{e_{s1} + e'_{s1}}{D} \qquad \ldots\ldots \quad 7.1$$

and for the first $\frac{1}{4}$ cycle of a dynamic test the range of curvature is ϕ_{d1}

$$\text{where} \quad \phi_{d1} = \frac{e_{d1} + e'_{d1}}{D} \qquad \ldots\ldots \quad 7.2$$

$$\text{Therefore} \quad \frac{\phi_s}{\phi_{d1}} = \frac{e_{s1} + e'_{s1}}{e_{d1} + e'_{d1}} \qquad \ldots\ldots \quad 7.3$$

since $e_{s1} > e_{d1}$ and $e'_{s1} > e'_{d1}$ as shown in figs. 7.3 (e) and (f).

$$\frac{\phi_s}{\phi_{d1}} > 1 \qquad \ldots\ldots \quad 7.4$$

For the n^{th} cycle of the dynamic test the total range of curvature is ϕ_{dt}

$$\text{where} \quad \phi_{dt} = \frac{e_{d2} + e_{d3} + e'_{d3} + e'_{d4}}{D} \qquad \ldots\ldots \quad 7.5$$

In equation 7.5 it is assumed that the load-deflection curves for the 2^{nd} cycle and the n^{th} cycle are parallel as discussed in section 7.3.2.

If in the n^{th} cycle the change of curvature from zero load to the maximum positive and negative loads is ϕ_{dn}

$$\text{then} \qquad \phi_{dn} = \frac{\phi_{dt}}{2} \qquad \ldots\ldots \quad 7.6$$

since $e_{d3} = e_{d2}$ and $e'_{d3} = e'_{d4}$ as shown by fig. 7.3

$$\text{then} \qquad \phi_{dn} = \frac{e_{d3} - e'_{d3}}{D} \qquad \ldots\ldots \quad 7.7$$

$$\text{therefore} \quad \frac{\phi_{d1}}{\phi_{dn}} = \frac{e_{d1} + e'_{d1}}{e_{d3} + e'_{d3}} \qquad \ldots\ldots \quad 7.8$$

as $e_{d1} > e_{d3}$ and $e'_{d1} > e'_{d3}$

$$\frac{\phi_{d1}}{\phi_{dn}} > 1 \qquad \ldots\ldots \quad 7.9$$

Equation 7.4 shows that the change of curvature of a statically tested beam is greater than the change of curvature for the same range of load during the first cycle of a dynamically tested beam because of the greater modulus of elasticity of the concrete in the dynamically tested beam. Equation 7.9 shows that the range of curvature from zero load to the maximum load in the n^{th} cycle is lower than that in the first cycle because of the absence of the effects of the permanent strains.

The curvature of an elastic beam is inversely proportional to the stiffness and therefore if the range of curvature of a

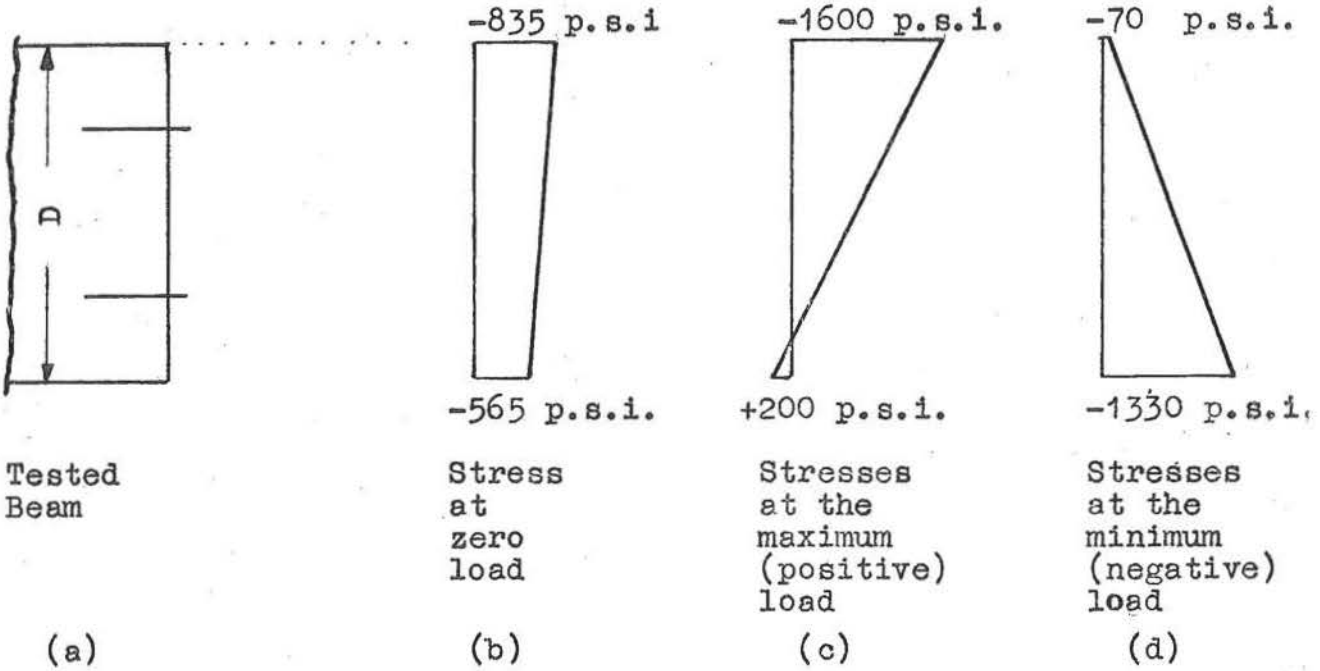

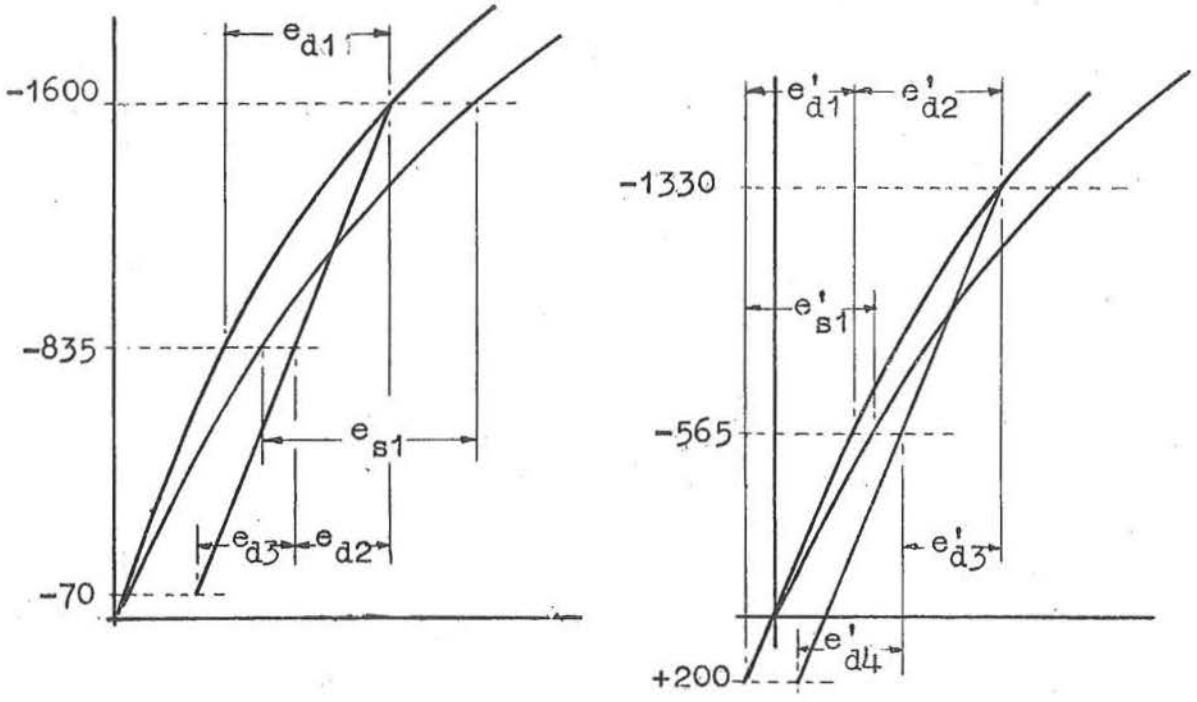

Fig. 7.3 STRESS-STRAIN CONDITIONS WITHIN THE AVERAGE BEAM OF THE SERIES OF BEAMS TESTED. THE MAGNITUDE OF THE MAXIMUM AND MINIMUM LOADS WERE 1000 LBS.

beam is reduced the stiffness of the beam is increased. For the beams tested dynamically the increase of stiffness was approximately 15% and the review by McHenry and Shideler indicates that 5-7% of this increase was due to the greater modulus of elasticity of the concrete when loaded dynamically while the remainder was principally due to the removal of the effect of the permanent strains in the concrete by the cyclic loading.

The increase in the stiffness of the beam due to the inertia of the weight of the beam is small, as shown in Table 6.3, and for the elastic range tests its effect may be neglected.

7.4. Fatigue Tests.

The results of the tests on the five prestressed concrete beams showed that the stiffness of the dynamically tested beams as shown by the range of deflection was greater than that of the statically tested beams. The increase of stiffness increased as the load increased but there was a limit above which the stiffness of the dynamically tested beams began to decrease. This limit was a function of the maximum loads and the number of cycles of load. It is interesting to note that Aladapo[33] found that the stiffness of prestressed concrete beams tested to failure in .05 seconds by a rapidly applied load, as distinct from an impulsive load, was greater over the entire range of loading than that of similar beams tested to failure over a period of 10 minutes. However, because of the different techniques of testing there is very little basis on which to compare the results.

The deflection-cycle curves from the fatigue tests on the dynamically tested beams show that the rate of increase of deflection increased as the maximum loads increased. These results indicate that the apparent modulus of elasticity of the concrete in the dynamically tested beams, as shown by the range of deflection, was initially greater than that of the statically tested beams. The effect of the cyclic loading at the higher load levels caused the stiffness of the beams to decrease. Since the relationship between the modulus of elasticity of concrete and the stiffness of a cracked prestressed concrete beam is complex and practically inderterminate it is not possible to determine the effect of the cyclic loading on the elastic modulus of the concrete in the beams. Therefore the effect of cyclic loading on the stiffness of prestressed concrete beams will be discussed rather than the effect of the cyclic loading on the modulus of elasticity of the concrete in the beams.

The load - deflection characteristics of cracked prestressed concrete beams reflects the moment - curvature properties of the beams over the zone of pure flexure and the area of the shear span over which flexural cracking occurs. Over the post-elastic ranges the properties of the steel influences the behaviour of prestressed concrete beams and as the load increases the influence of the steel properties on the stiffness also increases. Therefore the change in the stiffness of dynamically loaded beams would have been caused by a change of the stress-strain relationships of both the

concrete and steel. Nevertheless the reasons for the changes in the stiffness of the prestressed concrete beams subjected to cyclic loading were complex and are difficult to determine precisely.

In the beams tested dynamically the breakdown of the steel - concrete bond after the cracks had formed was greater than that in the statically tested beams. Also it is probable that the permanent strains in the concrete and steel, due to creep, were greater within both the concrete and steel of the dynamically tested beams. Hence there would have been a loss of prestress and a reduction of the stiffness of the beams.

Unfortunately little is known of the properties of the stress-strain curves for either concrete or steel under cyclic loading of similar nature to that produced in the beams tested dynamically. Therefore it has been necessary to assess typical stress-strain curves and apply them to the beams to obtain an indication of the reasons for the changes in the stiffness. The mechanisms of the initial increase of stiffness, the loss of prestress and the breakdown of the steel - concrete bond are discussed in the following sections.

7.5. Stiffness Under Reversed Cyclic Loading.

7.5.1 Stress-Strain Curve for Steel under Cyclic Loading.

Clark and Woodhead[34] have shown that there is a substantial increase in the yield stress of mild steel when it is rapidly loaded. For stronger steels with no specific yield point the increase in the limit of proportionality appeared to decrease as the strength of the steel increased but the increase varied greatly and tests would be necessary to find the limit of

proportionality for a particular steel at higher rates of loading.

It is also known that strain age hardening and work-hardening will raise the limit of proportionality of steels with the increase, in general, being greatest for the lower strength steels. Hence it is possible that the effect of the higher rate of stressing and the cyclic loading at stresses below the normal limit of proportionality increased the stress at the limit of proportionality. A typical stress-strain curve for the prestressing steel is shown in fig. 7.4 where the off-loading and re-loading curves are assumed to be parallel to the elastic portion of the stress-strain curve, (in practice there will be a hysteresis effect). It is likely that the concrete surrounding the steel and also the prestressing load would have affected the properties of the steel and the stress-strain curve.

7.5.2 Moment - Curvature Relationships.

The curvature of a section is a measure of the strains produced in the concrete and steel within the beam by the applied load. Consider the stresses and strains produced across the section of prestressed concrete beams during a static test and the n^{th} cycle of a dynamic test as shown in fig. 7.5. In the analysis it is assumed that the bond conditions are the same in both the static and dynamic cases and that plane sections remain plane.

For the static test the curvature at a particular load is ϕ_s

where $\phi_s = \frac{e_{cs} + e_{ss}}{D'}$ ... 7.10

and under the same load the curvature in a dynamic test is ϕ_d

where $\phi_d = \frac{e_{cd} + e_{sd}}{D'}$ ... 7.11

By combining equations 7.10 and 7.11 and putting

$$e_{cd} - e_{cs} = d(e_c)$$

and

$$e_{sd} - e_{cd} = d(e_s)$$

the ratio of the two curvatures will be

$$\frac{\phi_d}{\phi_s} = 1 + \frac{d(e_c) + d(e_s)}{e_{cs} + e_{ss}} \quad \text{... 7.12}$$

Equation 7.12 may be applied to any section along a beam and if the stress-strain relationships for the concrete and steel under both dynamic and static conditions are known then it is possible to find the effect of the fatigue loading. The above analysis may also be applied to the beams tested as the steel in the upper half of the beam resisted only approximately 14% of the positive moments on the beam and hence the effect of this steel on the behaviour of the beam would have been negligible.

During the second stage of behaviour of prestressed concrete elements, i.e. after the flexural cracks have formed

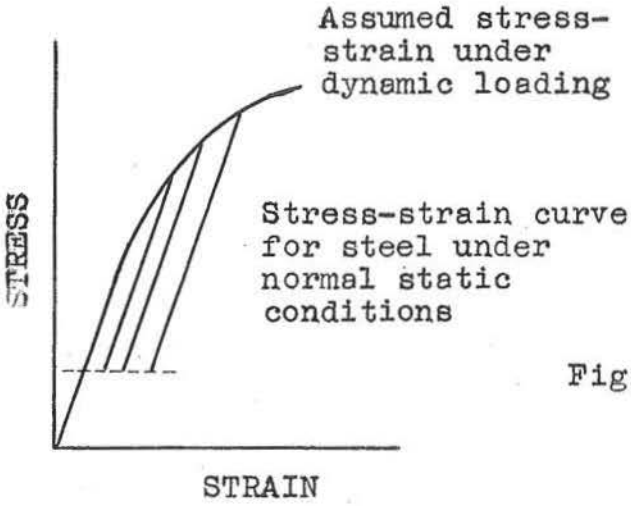

Fig. 7.4 STRESS-STRAIN CURVES FOR PRESTRESSING STEEL.

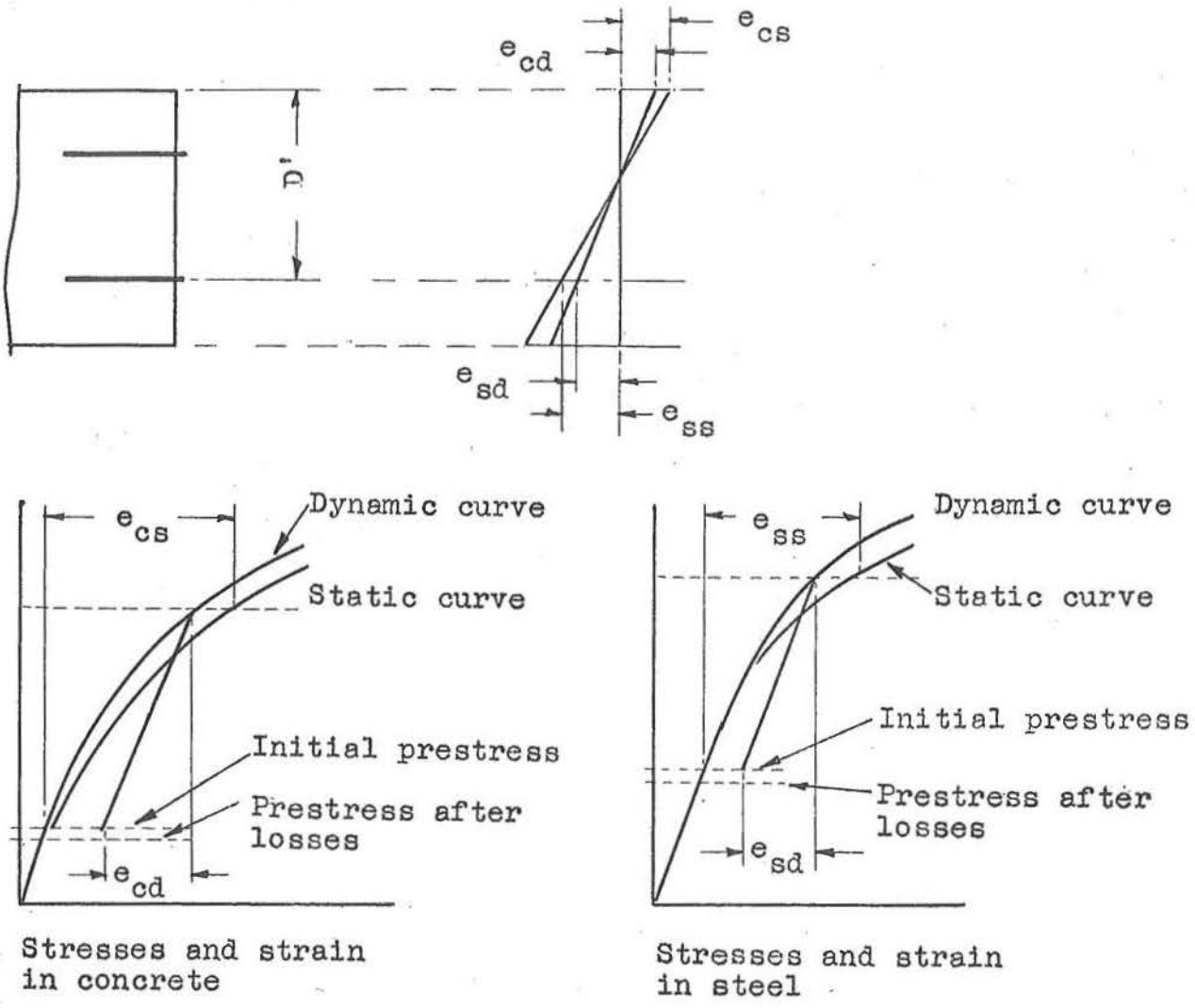

Fig. 7.5 TYPICAL STRESSES AND STRAINS WITHIN THE AVERAGE BEAM OF THE BEAMS TESTED AFTER CRACKING HAS OCCURRED

but before the steel yields, the difference in the curvatures , ϕ_d and ϕ_s, is caused by the change in the stress-strain curve of the concrete which also produces a shift of the neutral axis. As the strain in the extreme compression fibre and the strain in the steel control the position of the neutral axis it follows that the reduction of curvature due to the dynamic loading is also influenced by the steel stress. Under normal static conditions the steel stress increases as the depth to the neutral axis decreases and hence the ratio of the curvatures ϕ_d and ϕ_s, will increase as the depth to the neutral axis increases providing the reduction in the concrete strain is constant.

The stress-strain curve for the concrete shown in fig. 7.5 (c), although idealized, shows that the range of strain from zero to maximum load is greater for a static test than for the n^{th} cycle of a dynamic test. Therefore the change in the strain, $d(e_c)$, is negative and as the change of steel strain, $d(e_s)$, is zero

$$\frac{\phi_d}{\phi_s} < 1$$

During the third stage of behaviour of prestressed concrete, i.e. after the steel has yielded, the range of strain in the steel from zero to maximum load is lower for the dynamic case than the static case because of the absence of the effect of the permanent strains, see fig. 7.5 (d). Therefore the change of the range of strain in the steel $d(e_s)$ will be negative and the ratio of the dynamic and static curvatures will be reduced further. Since the curvature of a section of

a beam is inversely proportional to the stifness of the beam the dynamic stiffness of a prestressed concrete beam will be greater than the static stiffness.

The loss of prestress which occurs in prestressed concrete beams under cyclic loading will tend to increase the range of strains in the concrete and steel. Thus the curvature will increase but unless the loss is large the curvature will not increase to that for the static case.

As the number of cycles increases the concrete in the external fibres begins to creep causing a redistribution of stress across the section and an increase in the curvature. When the load level increases the redistribution of stress increases, the range of curvature increases because of the increase in the range of the strains and the stiffness of the beam decreases. Since the stress-strain properties of the steel and concrete under cyclic loading are very complex and generally unknown it is not possible to discuss in greater detail the mechanism of the increase of curvature and reduction of stiffness of the prestressed concrete beams as the tests proceeded and as failure was approached.

In a prestressed concrete beam the stress distribution varies over the region between the cracks, as shown in fig. 7.6, and thus the stress-strain curve for the concrete and steel will also vary. Since the steel and concrete stresses are lower at the section midway between the cracks the change in the ratio of the curvatures, ϕ_d and ϕ_s, will be different to that at the cracks.

7.6. Loss of Prestress.

A loss of prestress occurs in prestressed concrete beams when the concrete and steel are overstrained and permanent strains occur within the two materials. As the maximum load increases the prestress loss increases.

The stress-strain curves for the steel shown in fig. 7.7 assume, for simplicity, that the curves for all cycles except the first are the same. It is also assumed that:

1. the maximum positive and negative moments and their respective curvatures are the same,
2. plane sections remain plane,
3. there is no breakdown of the bond.

If the stresses and strains in a beam before the start of a test were "a" and "p" on the stress-strain curves for the concrete and steel respectively then at the end of the first cycle, if there is no yielding of the steel, the concrete and steel stresses will be "f" and "u" respectively. The reason is that if the stresses in the concrete at the completion of the first cycle had become the same as initially, i.e. "c", the permanent strains in the concrete would have produced a lower strain in the steel and therefore the concrete compressive forces would have been greater than the tensile steel forces. Similarly if the concrete strain had become the same as the initial strain "d" then the tensile steel forces would have been greater than the compressive forces. Thus the actual conditions must lie somewhere between the two cases, i.e. "f" and "u".

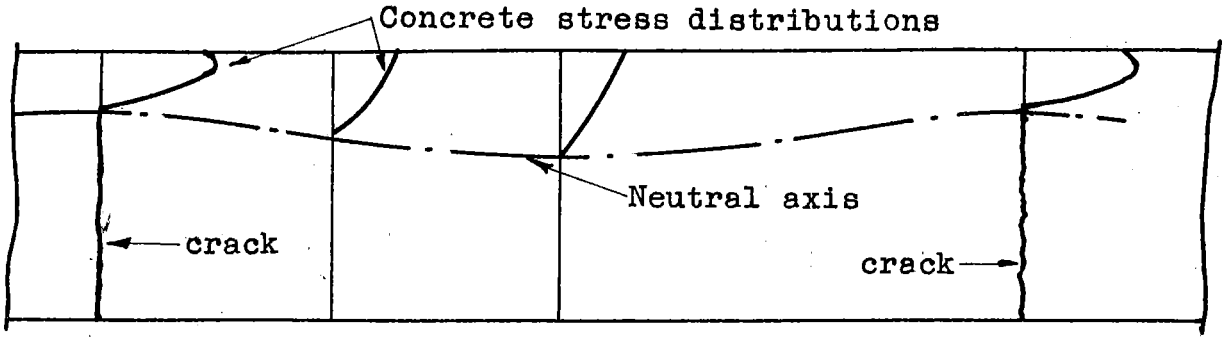

Fig. 7.6 VARIATION OF COMPRESSIVE STRESSES IN CONCRETE BETWEEN CRACKS.

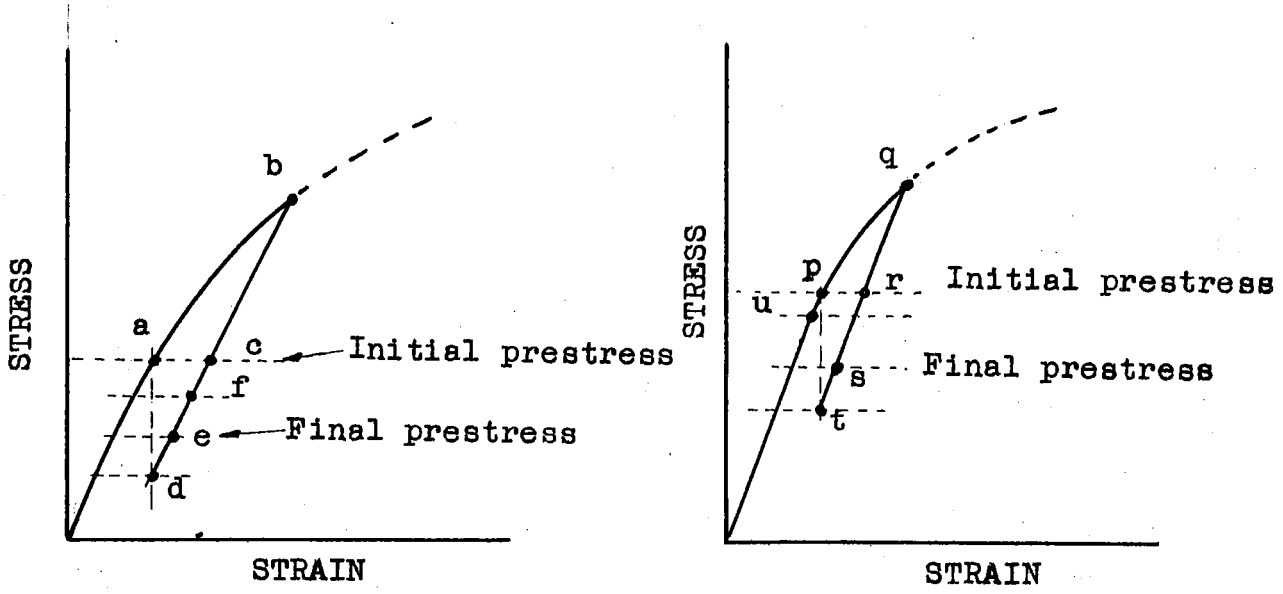

Stress-strain curve for the concrete in the beam

(a)

Stress-strain curve for the steel

(b)

Fig. 7.7 CHANGES OF STRESS AND STRAIN IN BEAMS CAUSED THROUGH LOSSES OF PRESTRESS

When the maximum load also causes yielding of the steel it may be shown by a similar method that there will be a further loss of prestress and hence the final conditions will correspond to "e" and "s" for the concrete and steel respectively. As the load increases the maximum stresses increase causing an increase in the permanent strains and an increase in the loss of prestress. At the higher load levels the permanent strains in the steel increase and become greater than those in the concrete and thus at higher loads the major portion of the loss of prestress is due to overstraining of the steel.

In the dynamic tests the effect of the cyclic loading would have caused creep in the concrete, as found in the tests reported by Leonhardt[32], and possibly in the steel as well. Thus when creep occurs in either the concrete or steel the loss of prestress will increase.

When a beam is loaded there is a stress gradient across the section and as the largest stresses are produced in the external fibres the greatest prestress losses will also occur in the same fibres. The typical redistributions of prestress shown in fig. 7.8 indicate that the loss of prestress in the central fibres of the beam is small because the stresses in these fibres are relatively low. Since the stress distribution in a beam is not uniform over the region between the cracks there will also be a variation in the loss of prestress along the beam and as the greatest stresses occur at the cracks the greatest losses will also occur at the cracks.

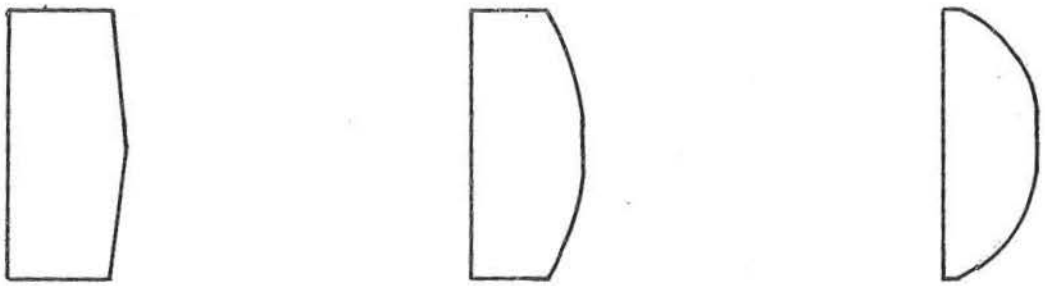

Distribution of prestress after low loads (i.e. within the elastic range).

Distribution of prestress after intermediate loads.

Distribution of prestress after high loads have been applied.

Fig. 7.8 PROBABLE TYPICAL DISTRIBUTIONS OF STRESS IN BEAMS AFTER PRESTRESS LOSSES

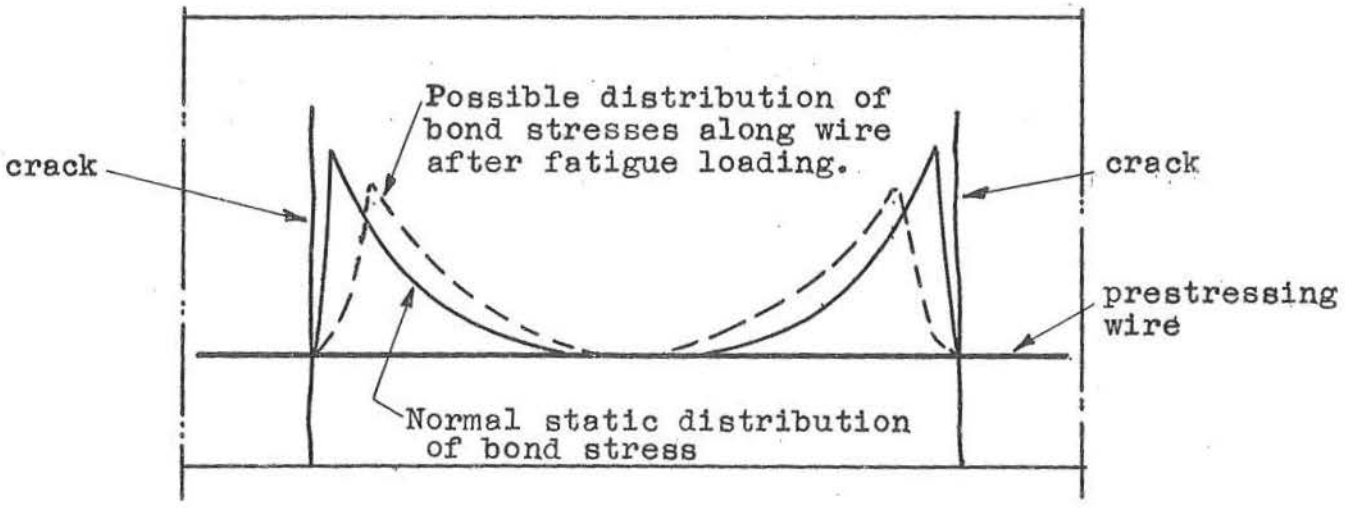

Fig. 7.9 COMPARISON OF DISTRIBUTIONS OF BOND STRESS BETWEEN CRACKS OF A STATICALLY TESTED BEAM AND A DYNAMICALLY TESTED BEAM.

The effect of the loss of prestress will cause an increase in the range of strains in the beams and hence an increase in the range of curvature. Therefore cyclic loading will tend to have two opposing effects on prestressed concrete elements; the first tends to increase the stiffness of the beams by the removal of the effect of the permanent strains while the second tends to decrease the stiffness through the loss of prestress.

7.7. Bond.

In the fatigue tests at the increments of load after the cracks had formed the deflections of the beams did not become stable until 50 - 200 cycles after each increase of load. For Beams 3 and 4 it was 400 - 500 cycles after the final increment of load before the deflections became stabilized and this indicates that the number of cycles before the deflections became stable increased as the magnitudes of the loads increased.

The increase of deflection would have been primarily caused by the destruction of the steel - concrete bond at the cracks. As the tests progressed the deflections continued to increase but this would have been primarily due to the reduction in the stiffness of the beams as discussed in the previous sections although further smaller losses of bond would have occurred.

The bond in concrete beams is caused by the friction developed by the slip between the steel and the concrete. Thus in the fatigue tests the reversed cyclic loading would have caused a continual "to and fro" slipping of the steel

in the concrete which would have pulverized the layer of cement grout on the wires adjacent to the cracks. As a result much of the bond in the region of the cracks would have been lost although the curvature of the beam would have forced one surface of the wire into contact with the concrete aggregate particles and allowed the bond stresses to build up slowly. Hence the cyclic loading would have reduced the maximum bond stress and also changed the distribution of the bond stresses along the wire. Typical bond stress distributions between two cracks for static and fatigue type loadings are shown in fig. 7.9.

As little is known of the properties of the steel concrete bond in concrete beams subjected to fatigue loading a great deal of further research on this topic is necessary.

7.8. Ductility Factors.

The ductility factor for prestressed concrete beams should be used with discretion because with different types of loading both the maximum deflections and the deflections at the flexural cracking loads can be different as was found in the case of the beams tested; see Table 6.2.

The ductility of a small section of a beam is the ratio of the curvature of the section at a particular load to the curvature at the flexural cracking load and will not necessarily be the same as the ductility of the whole beam. In the prestressed concrete beams tested the ductility of the complete beam would have been less than the ductility of the zone of pure flexure as shown by the curvature. In the analysis of a structure it is possible that the ductility of a section will

be more applicable and it is likely that the ductility factor of the complete structure will be different from the ductility factors of both the individual components and the sections of the components. This is because the ductility factor of a structure is influenced by the number of indeterminants within the structure as well as the properties of the components; however this is a topic which requires a great deal of further research. Also the topic of the individual components alone requiries much further research to determine the shape of the section, the level of prestress and the position and area of steel to give the maximum economic ductility factor. Nevertheless the dynamically tested beams have shown that prestressed concrete can exhibit a relatively large ductility factor under dynamic loading conditions.

7.9 Cracking Patterns.

The general formation and the crack spacing for the statically and dynamically tested beams were similar as shown in figs. 7.10 - 7.14. The cracks in the zones of pure flexure of the dynamically tested beams appeared to form in bands across the beams, and the reason is probably related to the concentration of curvature at the cracks across the compression zone. The permanent compressive strains in the concrete would have produced a concentration of curvature and thus a virtual hinge at the terminal point of the compressive zone crack as shown in fig. 7.15. Consequently the cracks forming at the opposite face would have tended to develop towards the concentration of curvature at the base of the crack.

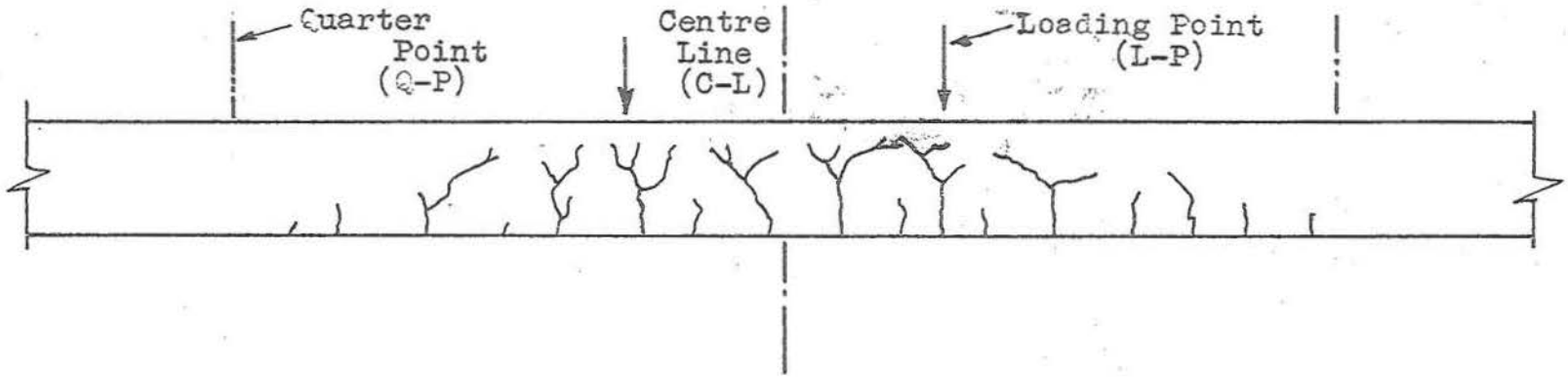

Fig. 7.10 CRACKING PATTERN FOR BEAM 1 (Static test)

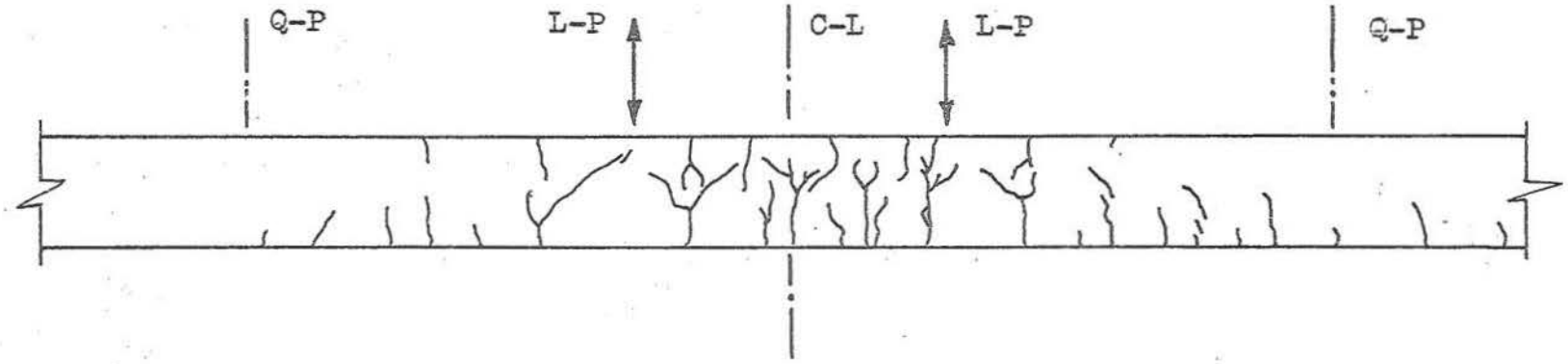

Fig. 7.11 CRACKING PATTERN FOR BEAM 2 (Static test with reversal of loading)

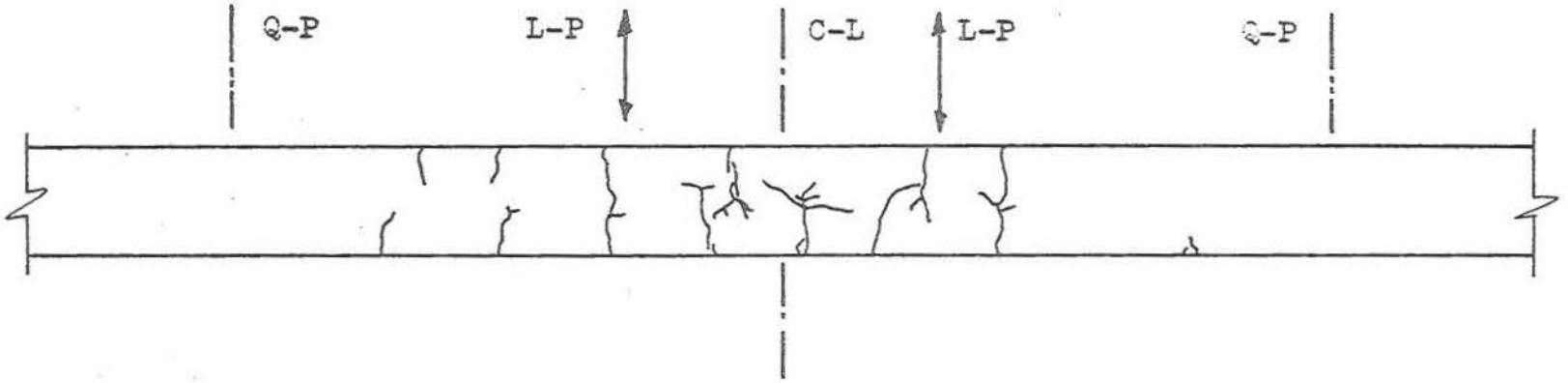

(a) After fatigue test

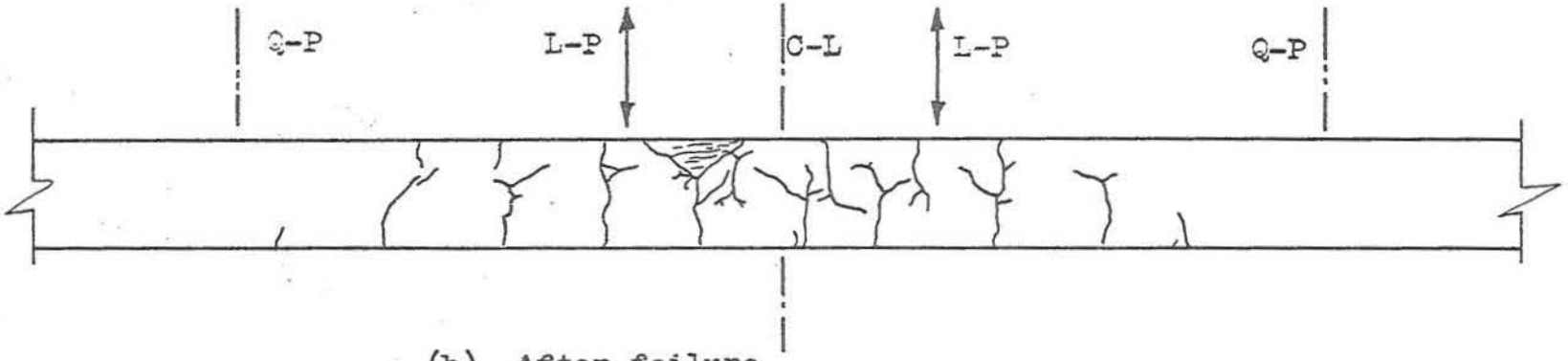

(b) After failure

Fig. 7.12 CRACKING PATTERN FOR BEAM 3 AFTER FATIGUE TESTS AND AFTER FAILURE.

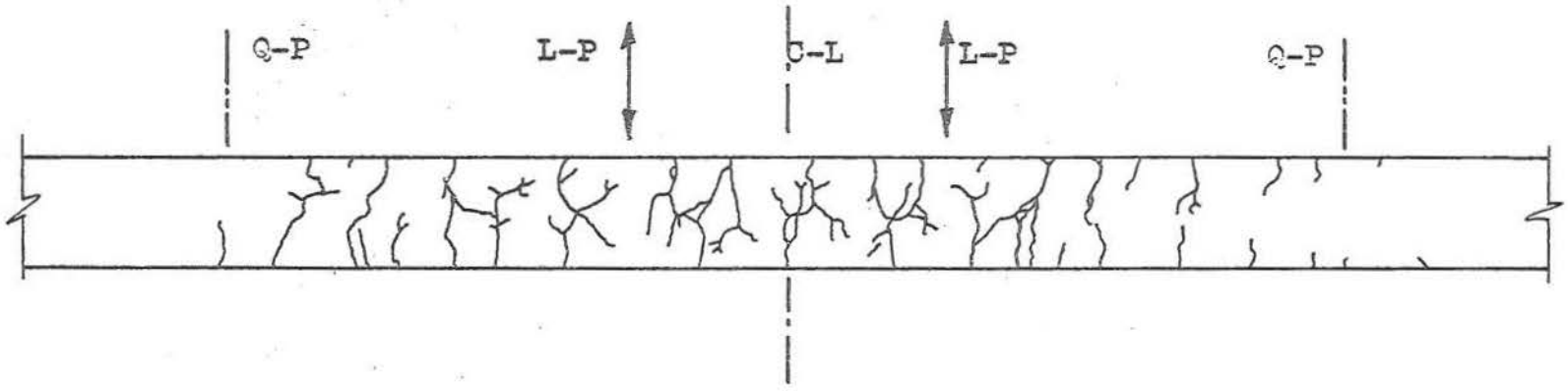

(a) After fatigue test

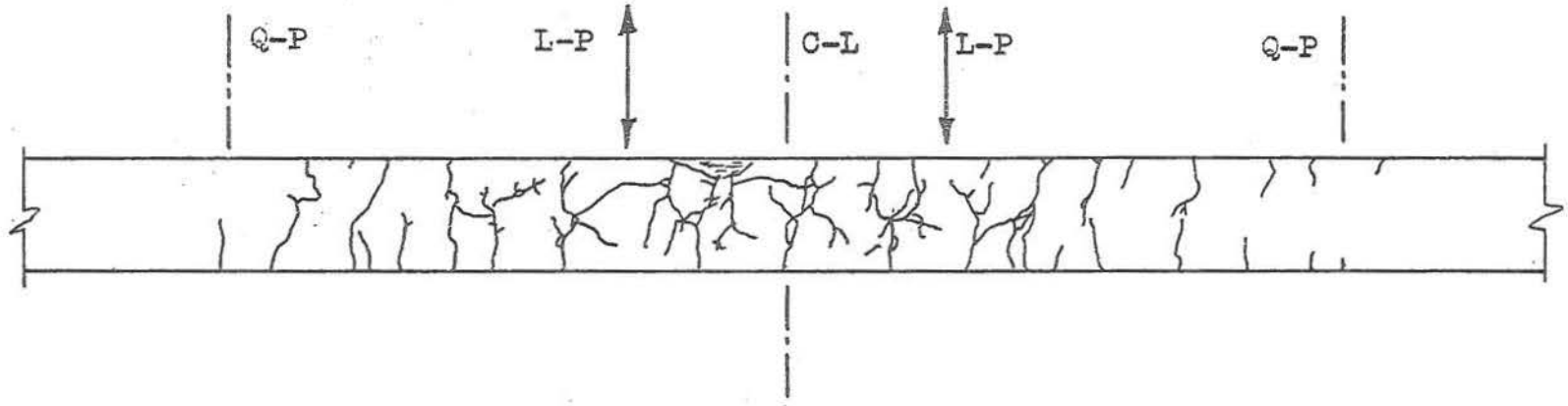

(b) After failure

Fig. 7.13 CRACKING PATTERN FOR BEAM 4 AFTER FATIGUE TESTS AND AFTER FAILURE

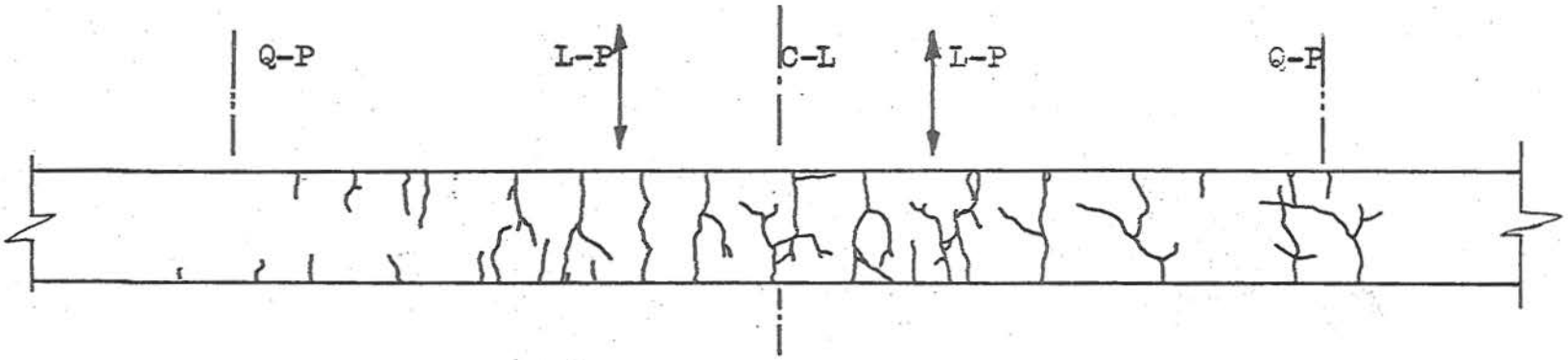

(a) After fatigue test

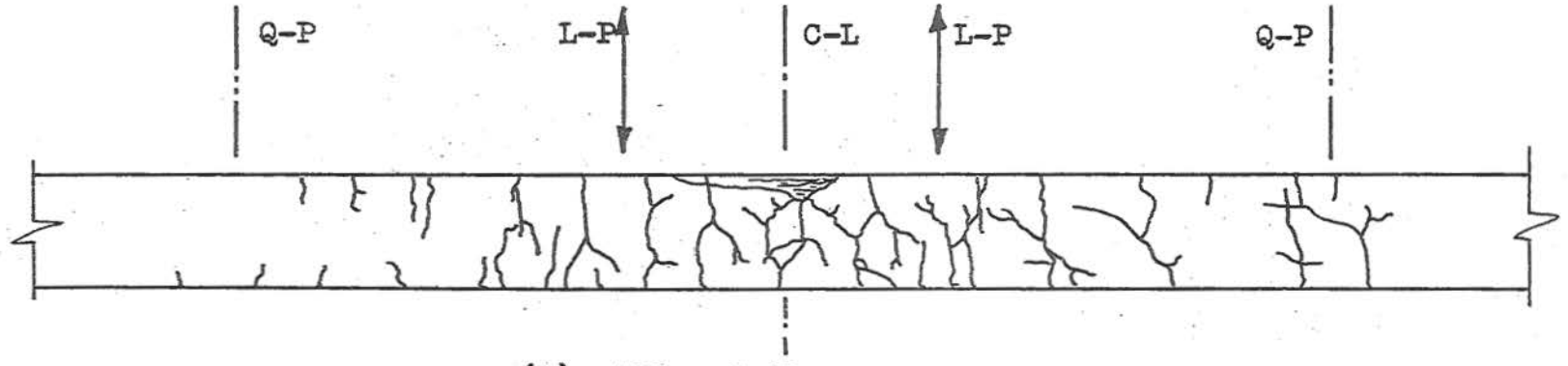

(b) After failure

Fig. 7.14 CRACKING PATTERN FOR BEAM 5 AFTER FATIGUE TESTS AND AFTER FAILURE.

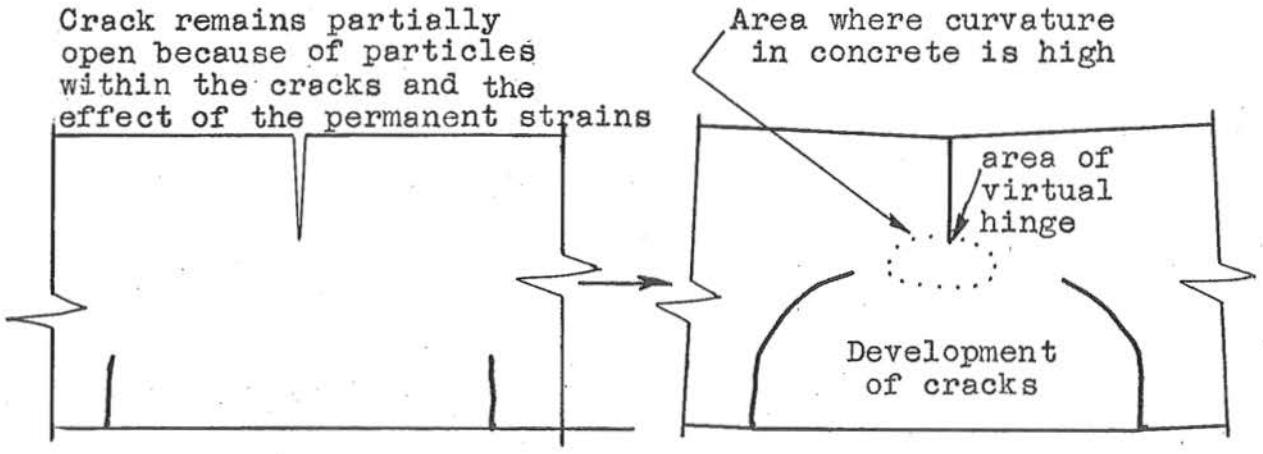

At zero load during a fatigue test

(a 1)

Following a further increment of load during the test
(Beams subjected to positive load)

(a 2)

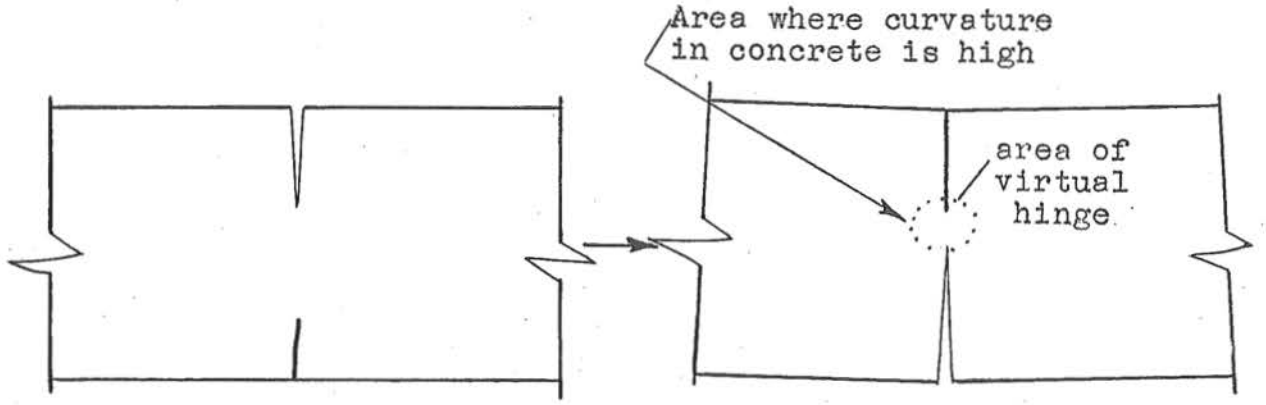

At zero load during a fatigue test

(b 1)

Following a further increment of load during the test
(Beams subjected to positive load)

(b 2)

In both cases the cracks developing on the lower face of the beam develope towards the area of high concentration of curvature.

Fig.7.15 A DIAGRAMATIC REPRESENTATION OF THE DEVELOPMENT OF THE CRACKS FOR TWO DIFFERENT CRACKING CONDITIONS

The width of the larger cracks appeared to increase as the fatigue tests progressed but after the maximum load for the test was reached there was only a limited increase in the length of the cracks. It is thought that the shear force acting across the beam increased the interaction between the cracks in the shear zone.

The absence of shrinkage cracks in Beam 3 may be attributed to autogenous healing of the cracks during the extended curing period.

7.10 Dynamic Mode of Failure.

Both Beams 4 and 5 were close to the point of failure at the end of the fatigue test and both beams failed at loads less than the estimated ultimate load in the subsequent static test. If it is assumed that the mode of failure in the fatigue test would have been the same as in the static test then if the fatigue tests had not been stopped before failure Beam 4 would have failed through the fracture of one wire and Beam 5 would have failed through crushing of the concrete. The trend of these results together with the mode of failure for Beam 3 were similar to the results from the beams tested by Venuti[27].

It is apparent that the mode of failure of prestressed concrete beams is dependent on the magnitude of the maximum applied load because as the maximum load increases the probability of a tension failure decreases while the probability of a compression failure increases. The change of the mode of failure is due to the change of the ratio of the steel and

concrete stresses and the increasing breakdown of the bond as the load increases. The analysis of the stresses in the beams (see section 6.6) shows that at the intermediate load levels i.e. 50% - 60% of ultimate, the ratio of the maximum concrete compressive stress to the maximum crushing stress of the concrete is considerably lower than the ratio of the steel stress in the lower wires to the ultimate steel stress but as the load level increases the increase of the concrete stress ratio is more rapid and at loads close to the static ultimate load of the beams the two ratios are practically the same. Since there was a loss of bond at the higher load levels as discussed in section 7.7 the maximum concrete stresses in the beams would have been greater than those indicated by the analysis.

At the conclusion of the fatigue test on Beams 4 and 5 small sections of the concrete on the upper face of the cracks had been crushed as shown in Plates, 17 and 18. The crushing of the concrete was caused by the high stresses in the concrete and by high local tensile stresses which were caused by small aggregate particles in the cracks. The loss of bond and creep in the concrete would have caused the cracks to open wider than the cracks in a normal static test and would have tended to dislodge the aggregate particles in the two crack surfaces. When the cracks close the particles would have been forced back into the crack surfaces producing high local radial stresses around each particle. As this was likely to have occurred over most of the depth of the crack the strength of the

concrete adjacent to the cracks would have been reduced. The strength of the concrete in the upper surface would have been reduced at a faster rate than predicted by fatigue tests on plain concrete and the probability of a failure due to crushing of the concrete would have been increased further at the higher loads. For Beam 5 the crushed concrete would have caused a reduction of the overall depth of the beam which alone would result in a reduction of the strength of the beam.

7.11 Secondary Static Tests.

The behaviour of the three dynamically tested beams in the static tests indicates the degree of overstressing and damage to the concrete and steel. The fatigue loading caused a reduction of the stiffness of the beams and was greatest for Beam 5 which was subjected to the largest applied load. The ultimate loads of Beams 4 and 5 were reduced by the fatigue loading but the deflections of the three beams when they finally collapsed were of the same order as the deflections of the two statically tested beams at failure. However, the deflection of Beam 4 when the one wire fractured was approximately half the deflection when the beam finally collapsed.

The reduction of the stiffness of the beams produced by the fatigue loading would have been due to a combination of:

1. a change in the stress-strain properties of the concrete,
2. a change in the distribution of prestress across the section,
3. the loss of bond,

4. the loss of prestress,
5. the presence of particles and cement dust in the cracks of the beam,
6. general damage and a reduction of the strength of the concrete accompanied by microcracking of the concrete.

For Beam 3 the shape of the static load-deflection curve up to the maximum load applied in the fatigue test was probably close to the shape of the dynamic load-deflection curves for the beam and also close to the shape of the curves for Beams 4 and 5 before they began to lose strength and started to fail. The shape of the lower portion of the static curve for Beam 3 was similar to the shape of the curves found by Venuti when testing prestressed concrete beams cyclicly without reversing the load and was also similar to the shape of the moment-curvature curves found by Spencer[35] while testing prestressed concrete beams subjected to reversed cyclic loading. All the curves consisted of two almost linear portions and show that after the beam has been loaded into the plastic range the stiffness in the elastic or linear range will be reduced. For Beam 3, the reduction of stiffness over the elastic range after the beam had been loaded into the plastic range was approximately 50% of the stiffness of the beams during the dynamic elastic range tests.

The change in shape of the moment-curvature curves for Beams 4 and 5 would have been caused by the change in the stress-strain properties of the concrete as found by two early investigations [6,7] and for slower rates of loading by Sinha,

Gertsle and Tulin[8]. The curves became concave upwards for some gauge lengths on Beam 4, but became only linear for Beam 5 although the latter was subjected to larger applied loads than Beam 4. It is thought that because the larger loads applied to Beam 5 produced greater losses of prestress and bond the beam acted as a reinforced concrete beam at low loads with the result that the properties of the concrete did not directly influence the behaviour of the beam to the same degree as Beam 4. Both Beams 4 and 5 showed that a wide variation of the moment-curvature relationships occurred over the zone of pure flexure for all stages of loading, the greatest curvature being in the region at which failure occurred.

The cracking patterns of Beams 4 and 5 were practically fully developed by the fatigue loading and consequently during the static tests there was very little extension of the cracks. As Beam 3 was not severely cracked the positive moment cracks, i.e. the cracks which formed while a positive moment acted on the beam, and also to a lesser extent the negative moment cracks, extended during the static test when the moment was positive. Since the negative moment cracks below the neutral axis of Beam 3 reopened and extended because of the tensile stresses in the concrete it is reasonable to assume that the negative moment cracks in Beams 4 and 5 also reopened during the static test. A number of secondary cracks branching out from the primary cracks formed on Beams 4 and 5 but did not form on Beam 3 and it is thought that these secondary cracks give an indication of the "damage" to the beam caused by the fatigue loading.

The strains measured on the faces of Beams 4 and 5 and shown in fig 5.16 and 5.21 show that the neutral axes of the beams remained practically stationary for large portions of the static tests. This is probably partially caused by the permanent compressive strains in the concrete and the non-closure of the cracks which resulted in the formation of virtual hinges at the junction of the cracks across the compressive zone and the position of the neutral axes when the maximum positive load acted on the beam during the fatigue test. As a virtual hinge is the idealization of the area of the beam about which adjacent sections rotate the neutral axis would have been close to the hinge. Since the position of the virtual hinges would have been practically stable the neutral axes would have remained in almost stationary positions. However, it was found that when there was a loss of bond or when a wire fractured the neutral axis rose slightly.

The static load-deflection curves for Beams 4 and 5 were practically linear and as the neutral axes were found to have been almost stationary during the tests it would confirm that the stress-strain curves for the steel and concrete in the beam were modified by the fatigue loading so that they became almost linear. The bi-linear load-deflection curves for Beam 3 and for the beams tested by Venuti and Spencer represent the behaviour of the beams in the elastic and plastic ranges.

Beam 3 failed when the concrete in the compression zone was crushed at a load greater than the estimated ultimate load and the maximum deflection was greater than that for Beam 1. Venuti also found that some beams which did not fail in the fatigue test failed statically at loads greater than the mean ultimate

load found for the beams tested statically only. Since Venuti found that the mean ultimate load of beams tested statically after a fatigue test where the load was not reversed was only slightly less than that for beams tested statically without previous fatigue testing it is probable that if more beams had been tested then there would have been a negligible difference in the mean ultimate loads of beams tested statically with and without previous fatigue testing where the load was reversed. However, this will not apply to beams which have been badly damaged by the fatigue testing. The stiffness of Beam 3 was greater than the stiffness of Beam 1 after the load in the static test had exceeded the maximum load in the fatigue test. As this occurred within the plastic range of the beam where the behaviour of the beam is controlled principally by the steel it is thought that the fatigue loading caused strain-hardening of the steel as discussed in secion 7.5.1.

Beam 4 failed initially when one of the lower wires fractured and finally collapsed after the load had caused large strains in the remaining wire which resulted in an uplift of the neutral axis and crushing of the concrete in the compression zone. The first wire fractured at a load lower than the estimated ultimate load and therefore the average steel stress was lower than the normal ultimate steel stress. Since the fractured wire was badly corroded in the region of the crack where the fracture occurred it is possible then the breakdown of bond on the fractured wire was not as great as for the unfractured wire. Therefore before the initial failure the stress in the fractured wire could have been greater than the stress in the

unbroken wire but the stress would still have been less than the normal ultimate stress. However the fatigue loading on the corroded and pitted wire probably produced stress concentrations which led to a gradual reduction of strength of the wire. It has been suggested that the strain in the wire during the period between the fatigue test and the static test could have resulted in inter-crystalline corrosion and a further decrease of the ultimate strength of the wire.

The failure of Beam 5 was due to a breakdown of the steel-concrete bond resulting in crushing of the concrete. The fatigue testing severely damaged portions of the compression zone and in the region where the beam failed the top fibres of the concrete were crushed and practically destroyed as shown in Plate 18.

7.12 A General Note for Aseismic Design.

The few accelograph records for earthquakes of large magnitude show that strong ground motions rarely last longer than a minute although vibrations of lower magnitude may last longer periods. Since the large deformations of a building are associated with long periods, i.e. low frequency, the number of repetitions of loads of high intensity will be relatively low and not likely to be greater than a hundred. Hence the total number of repetitions of high load during the life of a structure in an active earthquake zone will not be large and consequently for prestressed concrete components loads considerably greater than the normal design load may be permissible for aseismic design. Nevertheless the increase of the design stresses for aseismic design must be chosen on the basis of economics and the philosophy for the condition of the building after the earthquake. For example, the building

housing the communications or other essential services for a city or town during an earthquake must be safe and practically undamaged after the earthquake whereas it may be more economical to accept the possibility that a commercial building could be unsafe following a large earthquake and need to be demolished and rebuilt. It would also be necessary to consider the state of the building or structure at the conclusion of an earthquake of intermediate intensity. However it is essential, whatever philosophy is adopted, that the structure is erect after the earthquake to allow the occupants to escape from the building and prevent loss of life.

The tests have shown that there is a reduction of the stiffness of prestressed concrete elements after reversed cyclic loading of high magnitude and hence if a prestressed concrete structure survives on earthquake with a minimum of damage there is the possibility that the reduced stiffness of the components will cause a reduction of the natural frequency of the structure. Thus extra stiffness may need to be provided; on the other hand the reduced stiffness could be beneficial as long as the strength of the building was unimpaired. However this will depend on the type of building and the foundation conditions.

The tests have also shown that after an earthqake unless a beam within the frame has completely collapsed it is probable that it will still be capable of supporting the full design load although the ultimate load may have been reduced. For a beam there will be the beneficial effect of the end restraints which

would tend to improve the ultimate load.

The mode of failure of a beam is likely to be influenced by the bond conditions and since the loss of bond decreases as the mechanical bond capacity increases the use of wires where the mechanical bond, as distinct from the bond due to friction, is improved is recommended. The use of rusted and pitted wires which have been found to improve the static bond should also be avoided because of the detrimental effects of the corrosion and the possibility of internal changes in the crystalline structure of the wire which could lead to a reduction of the ultimate stress. Possibly the use of steel with small surface deformations results in the best performance of prestressed concrete elements under cyclic loading since a limited loss of bond could be beneficial whereas at the cracks the peak stresses in steel with large surface deformations may become excessive and cause the wire to fracture after a low number of cycles.

8. CONCLUSIONS

The tests conducted on the prestressed concrete showed that prestressed concrete is capable of withstanding reversals of cyclic loading of large magnitude without failing and that as the magnitude of the maximum load increases the number of cycles before failure decreases.

The effect of the reversal of loading was small both before cracks appeared and when the cracks were small but as the cracks increased in length and width the possibility of detrimental effects due only to the reversal of loading increased.

The overall stiffness of prestressed concrete beams subjected to reversed cyclic loading was initially greater than for similarly over-loaded beams for all ranges of loading although after the load exceeded that for the linear range of the beams the stiffness over the elastic range decreased.

The ductility of the beams was relatively large but as little is known of the relationship between the ductility of a component of a structure and the overall ductility of the structure it is not known whether the ductility found is sufficient for aseismic design. An aspect which requires further research is the determination of the relationship between the ductility of a section of a beam, the overall ductility of the beam and the ductility of the complete structure.

Fatigue loading produces a greater breakdown of the bond than static loading. Further research on the behaviour of flexural bond under fatigue loading is necessary.

The mode of failure of prestressed concrete beams is complex and is related to the magnitude of the maximum applied

load and the breakdown of bond. At no stage should the possibility of a shear failure be excluded.

Further research on the properties of plain concrete subjected to compressive cyclic loading and prestressing steel subjected to tensile cyclic loads are necessary as they are directly related to the the response of a prestressed concrete element to cyclic loading. Parameters which need further investigation are the stress-strain curves and the permanent strains and how they are affected by the repeated loading and the loading intensity.

Prestressed concrete has been shown to be capable of resisting large dynamic loads and is recommended as a suitable material for use in aseismic design. Nevertheless care should be taken in the design to check the shear and bond strengths of the components as the possibility of a premature bond or shear failure is greater under dynamic, and hence aseismic, conditions.

BIBLIOGRAPHY

1. Housner G.W. "Reporters Summary of Theme II 'Analysis of Structural Response'." Proceedings Third World Conference on Earthquake Engineering, New Zealand, 1965.

2. Despeyroux J. "The Use of Prestressed Concrete in Earthquake Resistant Design". Proceedings Third World Conference on Earthquake Engineering, New Zealand, 1965.

3. Van Ornum J.L. "The Fatigue of Cement Products" Transactions A.S.C.E. Vol. 51 Dec. 1903.

4. Nordby G.M. "Fatigue of Concrete - A Review of Research". Proceedings A.C.I. Journal Vol. 55, Aug. 1958.

5. Bate S.C.C. "The Strength of Concrete Members under Dynamic Loading". Proceedings of a Symposium on the Strength of Concrete Structures, London, May 1956.

6. Van Ornum J.L. "The Fatigue of Concrete". Transactions A.S.C.E. Vol. 58, June 1907.

7. Probst E. "The Influence of Rapidly Alternating Loading on Concrete and Reinforced Concrete". The Structural Engineer. Vol. 9, p 410, 1931.

8. Sinha B.P., Gertsle K.H., Tulin L.G. "Stress - Strain Relations for Concrete under Cyclic Loading". Proceedings A.C.I. Journal Vol. 61, Feb. 1964.

9. Kesler C.E. "Effect of Speed of Testing on Flexural Fatigue of Plain Concrete". Proceedings Highway Research Board Vol. 32, 1953.

10. Ople F.S. and Hulsobos C.L. "Probable Fatigue Life of Plain Concrete with a Stress Gradient." Proceedings A.C.I. Journal Vol. 63 Jan, 1966.

11. Lea F.C. "Repeated Stresses on Structures". The Structural Engineer Vol. 18 No.2 1940 p.511.

12. Muhlenbruch C.W. "The Effect of Repeated Loading on the Bond Strength of Concrete". Proceedings A.S.T.M. Vol.45 1945.

13. Muhlenbruch C.W. "The Effect of Repeated Loading on the Bond Strength of Concrete II". Proceedings A.S.T.M. Vol. 48 1948.

14. Saliger R. "Austrian Fatigue Tests of Reinforced Concrete Beams" Engineering News Record Vol. 114 May 16, 1935.

15. Chang T.S. and Kesler C.E. "Static and Fatigue Strength in Shear of Beams with Tensile Reinforcement". Proceedings A.C.I. Journal Vol. 54, June, 1958.

16. Chang T.S. and Kesler C.E. "Fatigue Behaviour of Reinforced Concrete Beams." Proceedings A.C.I. Journal Vol. 55 Aug. 1958.

17. Verna J.R. and Stelson T.E. "Failure of Small Reinforced Concrete Beams Under Repeated Load". Proceedings A.C.I. Journal Vol. 59, Oct. 1962.

18. Verna J.R. and Stelson T.E. "Repeated Loading Effect on Ultimate Static Strength of Concrete Beams." Proceedings A.C.I. Journal, June 1963.

19. Freyssinet E. "A Revolution in the Technique of the Utilization of Concrete." The Structural Engineer, Vol.14 May 1936.

20. Abeles P.W. "Prestressed Reinforced Concrete Sleepers Tested as Simply Supported Beams." Concrete and Constructional Engineering, Vol. 42 No.4 April 1947, and No. 5 May 1947.

21. Abeles P.W. "Static and Fatigue Tests on Partially Prestressed Constructions." Proceedings A.C.I. Journal Vol. 51 Dec. 1954.

22. Hanson N.W. Discussion of a Paper by J.R. Janney, "Nature of Bond in Pretensioned Prestressed Concrete". Proceedings A.C.I. Journal Vol. 50, May 1954, p.736-7.

23. Ozell A.M. and Ardaman E. "Fatigue Tests of Prestressed Concrete Beams." Proceedings A.C.I. Journal Vol. 53, Oct. 1956.

24. Bate S.C.C. "The Relative Merits of Plain and Deformed Wires in Prestressed Concrete Beams Under Static and Repeated Loadings." Proceedings Inst. of Civil Engineers, Vol. 10, August 1958.

25. Bate S.C.C. "An Experimental Study of Strand in Prestressed Concrete Beams Under Static and Fatigue Loading." Proceedings Inst. of Civil Engineers Vol. 23, Dec. 1962.

26. Bate S.C.C. "A Comparison Between Prestressed-Concrete and Reinforced-Concrete Beams under Repeated Loadings."

Proceedings Inst. of Civil Engineers, Vol. 24, March 1963.

27. Venuti W.J. "A Statistical Approach to the Analysis of Fatigue of Prestressed Concrete Beams." Proceedings A.C.I. Journal Vol. 62, No. 11, Nov. 1965.

28. Hognestad E, Hanson N.W. and McHenry D. "Concrete Stress Distribution in Ultimate Strength Design." Proceedings A.C.I. Journal, Vol. 52, Dec. 1955.

29. Barnard P.R. "Researches into the Complete Stress-Strain Curve for Concrete." Magazine of Concrete Research Vol. 16, No. 49, Dec. 1964.

30. Rogers G.L. "An Introduction to the Dynamics of Framed Structures." published by John Wiley & Sons.

31. McHenry D. and Shideler J.J. "Review of Data on Effect of Speed in Mechanical Testing". Symposium on Speed of Testing A.S.T.M. Special Publication No. 185, 1956.

32. Leonhardt F. "Prestressed Concrete Design and Construction." Translated by C. van Amerogen, published by Wilhelm Ernst & Sohn, Berlin, Munich.

33. Aladapo I.O. "Dynamic Loading of Prestressed Concrete Beams." Magazine of Concrete Research Vol. 14, No. 40, March 1962.

34. Clark D.S. and Woodhead D.S. "The Time Delay for the Initiation of Plastic Deformation at Rapidly Applied Constant Stress." Proceedings A.S.T.M. Vol. 49, 1949.

35. Spencer R.A. "The Damping and Flexural Properties of Prestressed Concrete Members Subjected to Reversed Cyclic Loading". Ph.D. thesis University of Auckland, New Zealand, 1966.

APPENDIX A.

Motion of Beam.

If the elastic shortening of the components and the lack of fit between the components in the linkage system are assumed to be negligible then the vertical motion of the beam will be identical to that of the head of the conrod. The vertical motion of the head of the conrod and therefore of the beam is given by equation A.1

$$y_{wt} = r \sin wt + \sqrt{l_c^2 - r^2 \cos^2 wt} - \sqrt{l_c^2 - r^2} \quad \ldots \text{A.1}$$

where y_{wt} is the displacement of the head of the conrod,

wt is the angle through which the crankpin has travelled after time t,

r is the throw of the crankpin,

l_c is the length of the conrod.

The velocity, V_{wt}, and acceleration, A_{wt}, of the beam at the loading points may be found by differentiating equation A.1 with respect towt once and twice respectively

Therefore:

$$V_{wt} = r \cos wt - \tfrac{1}{2} \frac{r^2 \sin 2wt}{\sqrt{l_c^2 - r^2 \cos^2 wt}} \quad \ldots \text{A.2}$$

$$A_{wt} = -r \sin wt - \tfrac{1}{2} \frac{r^2 \cos 2wt}{\sqrt{l_c^2 - r^2 \cos^2 wt}} + \tfrac{1}{2} \frac{r^4 \sin^2 wt}{(l_c^2 - r^2 \cos^2 wt)^{3/2}} \quad \ldots \text{A.3}$$

The effective length of the conrod was 25.3" and the maximum throw of the conrod during any test was 1" and therefore under these conditions equations A.1 - A.3 become

$$y_{wt} = \sin wt + \sqrt{640 - \cos^2 wt} - \sqrt{639} \quad \ldots \text{A.4}$$

$$V_{wt} = \cos wt - \tfrac{1}{2} \frac{\sin 2wt}{\sqrt{640 - \cos^2 wt}} \quad \ldots \text{A.5}$$

$$A_{wt} = -\sin wt - \tfrac{1}{2} \frac{\cos 2wt}{\sqrt{640 - \cos^2 wt}} + \tfrac{1}{2} \frac{\sin^2 wt}{(640 - \cos^2 wt)^{3/2}} \quad \ldots \text{A.6}$$

By inspection it may be seen that the motion of the beams described by equations A.4 - A.6 is very close to being sinusodial. When the throw of the crankpin is decreased, i.e. r decreases, the motion of the beams becomes even closer to being sinusodial and therefore for all practical purposes it may be said that the motion of the beams during the dynamic tests was sinusodial.

Torque Applied by the Dynamic Loading Unit.

The design of the unit was based on the assumption that the load-deflection curves of the beams to be tested would be cubic parabolas. Thus the load deflection curves were assumed to be

$$P = p\left(\left(\frac{y}{r}\right)^3 - 3\left(\frac{y}{r}\right)^3 + 3\frac{y}{r}\right) \qquad \ldots \text{ A.7}$$

where p is the load applied to the beam at a deflection of y,

P is the maximum load applied during a test,

r is the throw of the crankpin (as above)

The resulting torque is T

where $T = p.l'$ ... A.8

where l' is the lever arm of the crankpin for the vertical load

since it has been shown that the motion is practically sinusoidal

$$\sin wt = \frac{y}{r}$$

and as $l' = r \cos wt$

equation A.7 becomes

$$T = P.r\ (\sin^3 wt - 3 \sin^2 wt + 3 \sin wt) \cos wt \qquad \ldots \text{ A.9}$$

The torque-angle diagram may be derived directly from equation A.9 and is shown in fig. A.1. The maximum Torque is T_m

where $T_m = .758\ P.r$ ... A.10

and occurs when the angle, wt, is $30^\circ\ 12'$

The coefficient .758 is known as the Beam Factor and is the maximum value of f(wt), (see equation A.11), for the cubic parabola load deflection curve assumed.

$$f(wt) = (\sin^3 wt - 3 \sin^2 wt + 3 \sin wt) \cos wt \quad \ldots A.11$$

The mean Torque over any range of loading was found by integrating equation A.9 with respect to t and dividing by the angle through which the crankpin has travelled.

For the first quarter of a cycle the mean torque was .477 P.r

If the load deflection curve had been a square parabola the Torque angle diagram would have been described by:

$$T = P.r \sin 2wt \ (1 - \tfrac{1}{2} \sin wt) \quad \ldots A.12$$

The corresponding torque angle diagram is shown in fig. A.2 where the maximum torque is

$$T_m = .67 \ P.r \quad \ldots A.13$$

i.e. a Beam Factor of .67

If the load-deflection curve had been linear the torque angle diagram would have been given by:

$$T = .50 \ P.r \sin 2wt \quad \ldots A.14$$

and the maximum torque would have been:

$$T_m = .50 \ P.r \quad \ldots A.15$$

i.e. a Beam Factor of .50

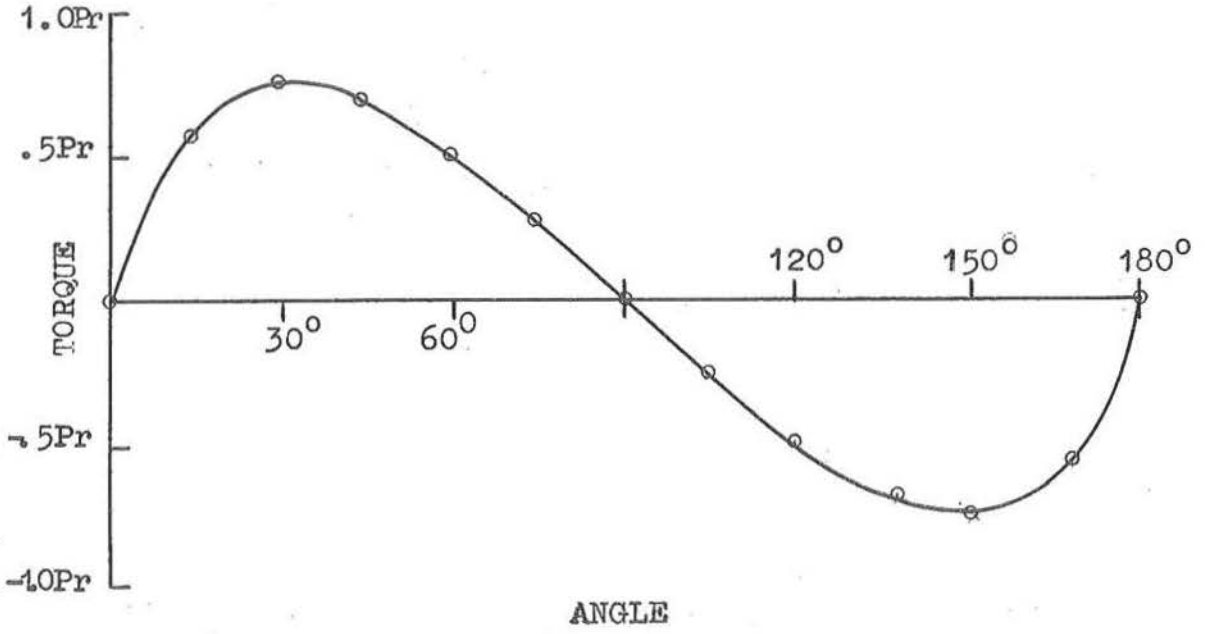

Fig. A.1 TORQUE-ANGLE DIAGRAM FOR CUBIC LOAD-DEFLECTION CURVE

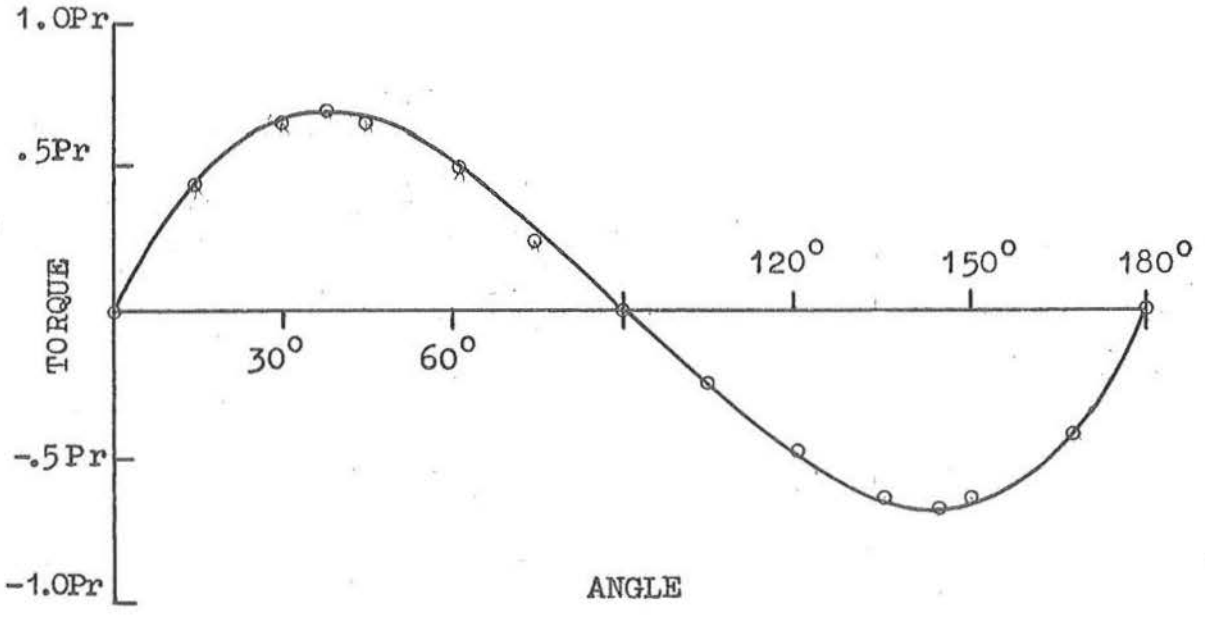

Fig. A.2 TORQUE ANGLE DIAGRAM FOR PARABOLIC LOAD-DEFLECTION CURVE

In practice the shape of the load-deflection curves changed during the dynamic testing. For the elastic range tests the curves would have been practically linear whereas they would have changed in shape and tended to become similar to a cubic parabola in shape as the load increased. In the fatigue tests it is likely that the load-deflection curves were practically bi-linear until the stage when the beams began to fail. The Torque angle diagram for the bi-linear curve is discussed below.

The shape of the typical bi-linear load-deflection curve shown in fig. A.3 is described by:

$$P_1 = \frac{m}{r} \cdot \frac{y}{r} \quad P \qquad \text{from } 0 - mp \qquad \ldots \text{ A.16}$$

and

$$P_2 = \frac{1}{1-k} \quad (m-k) + \frac{y}{r} \quad (1-m) \quad \text{from } mp - P \qquad \ldots \text{ A.17}$$

as $T = p.l'$

where $l' = r \cos wt$

and $\frac{y}{r} = \sin wt$

$$T_1 = P.r \frac{m}{k} \frac{1}{2} \sin 2wt \qquad \ldots \text{ A.18}$$

$$T_2 = P.r \frac{1}{1-k} \quad (m-k) + \sin wt \ (1-m) \sin wt \qquad \ldots \text{ A.19}$$

consider the special case where $m = 2/3$, $k = 1/3$

$$T_1 = P.r \sin 2wt \qquad \ldots \text{ A.20}$$

$$T_2 = P.r \frac{1}{2} (1 + \sin wt) \cos wt \qquad \ldots \text{ A.21}$$

The corresponding Torque-Angle diagram is shown in fig. A.4

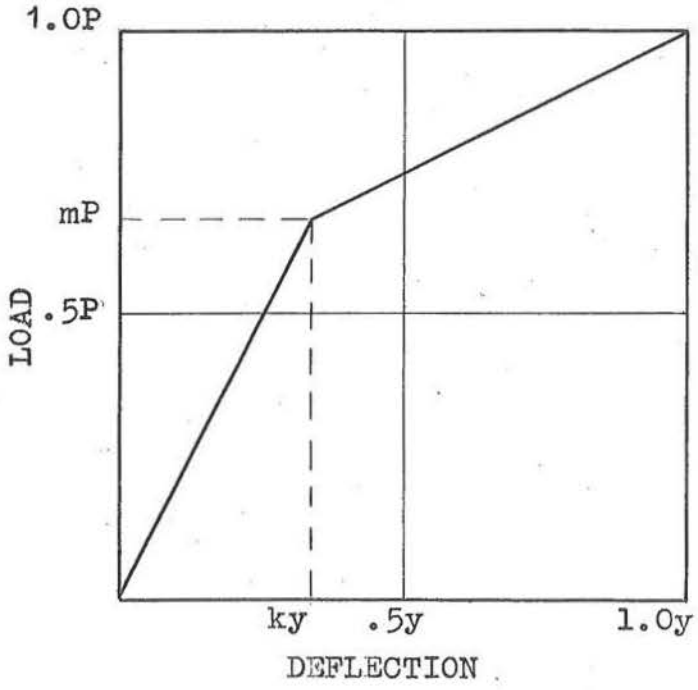

Fig. A.3 BI-LINEAR LOAD DEFLECTION CURVE

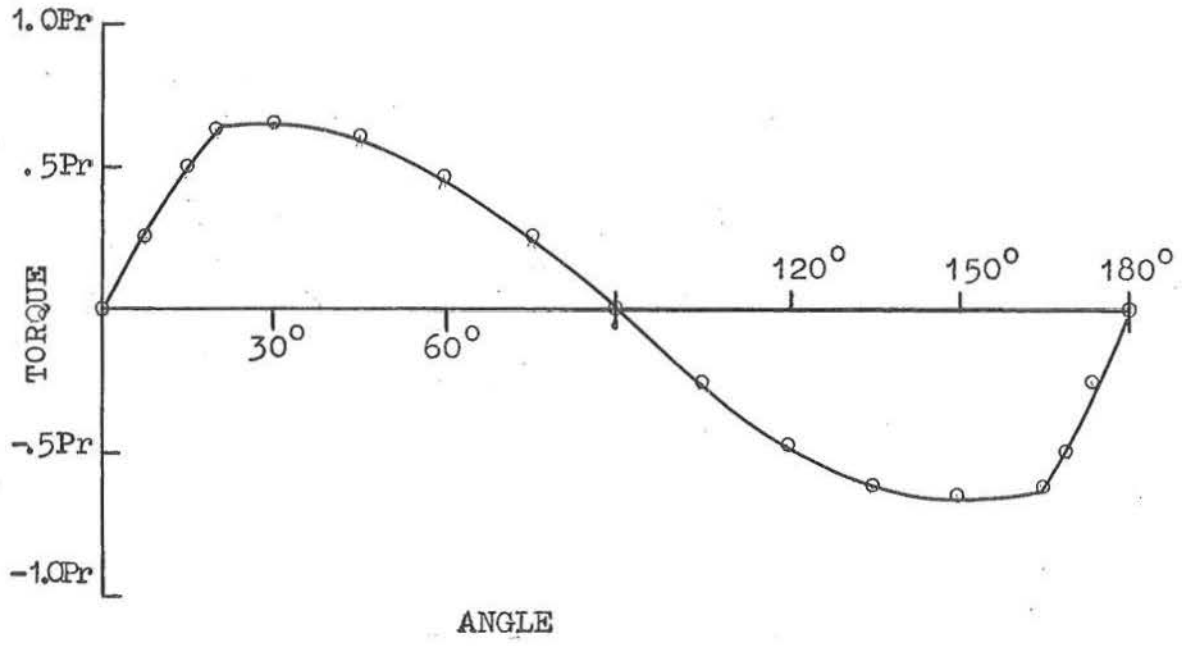

Fig. A.4. TORQUE-ANGLE DIAGRAM FOR BI-LINEAR LOAD DEFLECTION CURVE

The above discussion shows that the shape of the torque angle diagram is a function of the load-deflection curve of the beams and hence the Beam Factor is also a function of the Load-deflection curve of the beam. If it is assumed that the load-deflection curve of a beam cannot be concave then the minimum Beam Factor is given by equation A.15 and is .50. The upper limit for the Beam Factor is unity but this can only occur for the special case of the bi-linear load-deflection curve when m = 1 and k = 0 which is impractical. Hence it was assumed for the design of the Dynamic Loading Unit that the upper limit for the Beam Factor would be given by a cubic parabolic load-deflection curve.

The analysis above also shows that as the load-deflection curve becomes more concave towards the X axis the Beam Factor increases and thus the maximum limit for the product of the applied load and the throw of the crankpin , P.r , decreases.

Energy Capacity of Flywheels.

The Kinetic energy capacity of a flywheel is given by

$$K.E. = \tfrac{1}{2} I_f . w^2 \qquad \ldots A.22$$

where I is the moment of inertia of the flywheel ($in.lb/sec^2$)

w is the angular velocity (sec^{-1})

If there is a change of the speed of rotation of the flywheel the change of the kinetic energy is given by

$$d(K.E.) = \tfrac{1}{2} I_f . (w_1^2 - w_2^2) \qquad \ldots A.23$$

where w_1 and w_2 are the initial and final angular velocities respectively

If $$\frac{w_1 - w_2}{w_1} = \bar{C}$$

equation A.23 becomes

$$d\,(K.E.) = \tfrac{1}{2}\, I_f . w_1^2\, (2\bar{C} - \bar{C}^2) \qquad \ldots \text{A.24}$$

As $\bar{C}$ is small $\bar{C}^2$ may be neglected and hence

$$d\,(K.E.) = J_f . w_1^2 . \bar{C} \qquad \ldots \text{A.25}$$

The moment of inertia of the flywheels incorporated in the Dynamic Loading Unit was 34.6 in.lb/sec^2 and therefore

$$d\,(K.E.) = 34.6\, w_1^2\, \bar{C}$$

The fluctuations of the energy of the Unit are given by the Torque-angle diagrams and it was found that under most conditions the coefficient of speed variation, $\bar{C}$, was greater than 1% which is the normal figure assumed for design.

APPENDIX B

f_c (p.s.i.)	e_c	k_1	k_2	k_3	$k_1 k_3$
6800	.0029	.70	.39	.94	.66
6890	.0027	.69	.37	.94	.65
7000	.0025	.66	.37	.94	.61
7100	.0023	.64	.37	.94	.60
7140	.0021	.60	.36	.94	.57
6920	.0019	.59	.36	.91	.53
6320	.0016	.57	.35	.83	.47
4920	.0011	.53	.35	.64	.34
3780	.0008	below e_c = .001 assume a triangular distribution of stress k_2 = .34			
2030	.0004				

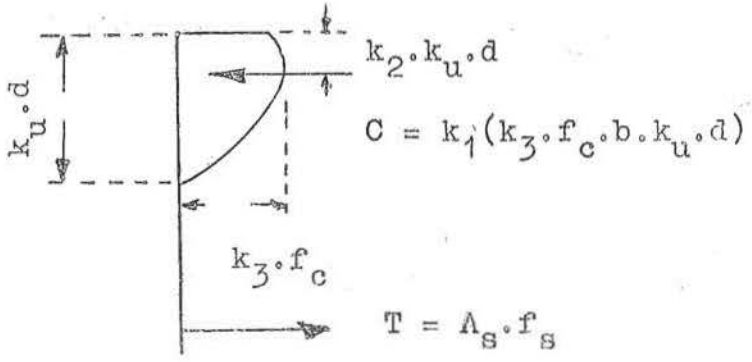

k_1 = ratio of average stress to maximum stress

k_2 = ratio of maximum stress to cylinder strength f'_c

k_3 = ratio of depth to resultant of compressive stress and depth to neutral axis.

Table B.1. Coefficients for the Stress-Strain Curve of Concrete

APPENDIX C

Increment Number	Applied Load (lbs)	Deflections (inches)				
		A	B	Centre	D	E
1	330	.013	.016	.016	.015	.014
2	570	.025	.028	.029	.028	.025
3	850	.041	.045	.047	.045	.040
4	1090	.058	.065	.067	.064	.057
5	1400			.097		
6	1630			.133		
7	1890			.197		
8	2210			.362		
9	2535			.621		
10	2650			.787		
11	2875			1.217		
12	3045			1.882		

Table C.5.1 Load - Deflection results from Beam 1.

N.B. Gauges B, D 10" from centre line.

Gauges A, E 20" from centre line.

(ref. fig. 5.3)

Increment Number	4	6	7	8	10		4	6	7	8	10
Applied Load (lb)	1100	1640	1810	2215	2665		1100	1640	1810	2215	2665
Gauge A1	-130	-260	-380	-520	-1000	Gauge D1	-160	-290	-390	-570	-980
A2	- 60	-120	-140	-190	- 90	D2	- 90	-140	-160	-200	-120
A3	10	10	80	240	470	D3	- 10	10	60	390	1130
A4	70	180	460	1260	3880	D4	60	160	390	1050	3360
A5	140	420	830	1960	5870	D5	100	350	860	2430	4890
Gauge B1	-140	-280	-390	-580	-920	Gauge C1	-140	-280	-400	-570	-940
B2	- 70	-160	-180	-180	- 70	C2	- 70	-130	-180	-190	- 80
B3	-	50	160	420	1140	C3	10	30	100	500	1680
B4	90	280	590	1340	3230	C4	90	220	420	1330	3490
B5	170	530	1010	2170	4930	C5	170	440	820	2190	5330
1	-140	-280	-390	-560	-960		The strains shown in the opposite panel are the average of the strains in the zone of pure flexure, derived from the strains shown above.				
2	- 70	-140	-170	-190	- 90						
3	0	20	100	380	1100						
4	80	210	460	1250	3490						
5	150	440	880	2190	5250						

Table C.5.2 Strains produced in Beam 1 over the region of pure flexure.
Units of strain : micro-strains (ref. fig. 5.2)

Increment Number		4	6	7	8	9	10	11	12
Load (lbs)		1100	1640	1915	2210	2540	2670	2880	3070
Gauge	1	130	280	420	690	1170	1480	2190	3110
	2	170	350	530	830	1210	1490	2080	2880
	3	140	300	440	750	1130	1390	1960	2800
	4	150	290	410	660	1030	1260	1860	2640
	5	130	290	440	780	1180	1420	2020	2660
	6	140	270	340	680	1040	1290	1820	2460
	7	130	290	400	650	1100	1360	1950	2720
Average strain		140	290	430	720	1120	1380	1980	2750

Table C.5.3. Compressive strains on the top face of Beam 1 over the region of pure flexure.

Units of strain : micro-strains.

(ref. fig. 5.4)

Increment Number	Applied Load (lbs)	Deflection (inches)						
		Centre	3A	2A	1A	1B	2B	3B
1	290	.015	.011	.013	.015	.015	.013	.011
2	600	.031	.021	.026	.030	.030	.027	.021
3	920	.050	.035	.043	.048	.048	.043	.035
4	1140	.067	.047	.058	.065	.065	.057	.046
5	1440	.092						
6	1705	.124						
Zero	-	.014						
7	-300	-.010						
8	-600	-.027						
9	-900	-.045						
10	-1200	-.064						
11	-1500	-.083						
12	-1800	-.109						
13	-2100	-.140						
Zero	-	.001						
14	870	.059						
15	1650	.130						
16	1950	.187						
17	2260	.333						
Zero (1)	-	.035						
Zero (2)	-	.028						

Increment Number	Applied Load	Deflection on centre
18	-1200	-.055
19	-2100	-.130
20	-2400	-.189
21	-2700	-.270
Zero	-	.003
22	910	.077
23	1770	.214
24	2320	.325
25	2590	.515
26	2850	.953
27	3265	1.544

Table C.54. Load - Deflection results from Beam 2.

N.B. Gauges 1A. 1B 10" from centre.

Gauges 2A, 2B 20" from centre.

Gauges 3A, 3B 30" from centre.

Increment number	4	6	Zero	15	16	17	Zero (1)	Zero (2)	24	24	26	27
Applied Load (lb)	1150	1710		1670	1990	2290			2340	2600	2850	3000
A1	-120	-220	-10	-220	-290	-430	-60	-40	-430	-680	-910	-1140
A2	-80	-140	-20	-140	-180	-220	-70	-60	-220	-220	-100	210
A3	-10	20	0	20	60	280	0	0	310	650	1910	
A4	70	160	30	180	230	450	50	30	490	800		
A5	100	190	20	200	290	570	10	30	620	1000		
B1	-160	-260	-40	-260	-330	-590	-110	-80	-590	-770	-1060	-1370
B2	-100	-150	-20	-150	-200	-210	-60	-40	-170	-130	10	530
B3	- 40	- 40	10	- 40	- 20	270	-20	0	360	760	1990	
B4	40	100	10	100	190	660	30	30	1030	1660		
B5	100	130	10	100	110	610	0	10	780	1370		
B6	150	300	30	300	330	1800	120	120	2160	3690		
C1	-180	-280	-30	-300	-390	-630	-120	- 90	-650	-820	-1190	-1550
C2	-120	-180	-30	-180	-200	-240	- 70	- 60	-210	-170	- 110	540
C3	- 40	- 50	-20	- 40	0	110	- 40	- 50	140	210	440	
C4	10	110	0	110	200	340	- 20	- 10	220	1490		
C5	90	290	40	380	490	1170	- 20	70	1090	1850		
C6	140	280	30	360	440	1310	0	-10	140	160		
D1	-130	-210	- 50	-220	-290	-430	- 60	- 30	-440	-590	-890	-1150
D2	- 90	-140	- 20	-160	-180	-220	- 40	- 40	-210	-110	- 70	240
D3	0	20	- 10	20	70	120	- 20	- 20	220	300	350	
D4	90	140	20	120	150	160	- 10	10	140	150		
D5	110	150	10	140	50	120	- 10	0	120	90		

Table C.5.5. Strains produced in Beam 2 over region of pure flexure
Units of Strain : micro-strain (ref. fig. 5.5)

Increment Number	Average Load (lbs)	Deflections (inches)			Average Load (lbs)	Deflections (inches)			Average Load (lbs)	Deflections (inches)		
		C	B	D		C	B	D		C	B	D
-	38	.001	.003	.001	55	.002	.003	.001	60	.002	.003	.001
1	197	.008	.009	.007	197	.008	.009	.007	181	.007	.008	.006
2	410	.016	.019	.016	384	.016	.017	.014	384	.015	.017	.014
3	612	.026	.029	.025	626	.026	.028	.024	611	.025	.028	.024
4	831	.037	.042	.036	858	.036	.039	.034	845	.035	.039	.035
5	1026	.043	.052	.044	1072	.044	.050	.042	1079	.043	.049	.041
Speed $\frac{1}{2}$ c.p.s.					Speed 1 c.p.s.				Speed $1\frac{1}{2}$ c.p.s.			
300 revs / increment					300 revs / increment				900 revs / increment			

Table C.5.6 Load - Deglection results from Dynamic elastic range tests on Beam 3.

Number of cycles	Average Load (lbs)	Deflections (inches)		Number of cycles	Average Load (lbs)	Deflections (inches)	
		B	C,D			B	C,D
0- 150	-	-	-	4200-4600	2355	.359	.300
150- 260	760	.034	.037	4600-5000	2355	.359	.300
260-400	1260	.060	.053	5000-5250	2355	.359	.297
400- 550	1760	.079	.069	5250-5440	2355	.359	.297
550-660	1930	.109	.092	5440-5800	2420	.371	.310
660- 840	2100	.141	.120	5800-6200	2420	.371	.310
840-980	2240	.269	.222	6200-6600	2420	.377	.313
980-1090	2215	.280	.230	6600-6900	2420	.371	.313
1090-1160	2270	.311	.262	6900-7200	2420	.377	.313
1160-1390	2270	.332	.262	7200-7600	2355	.371	.313
1390-1560	2270	.338	.279	7600-8000	2355	.371	.313
1560-2000	2355	.346	.289	8000-8400	2355	.371	.313
2000-2400	2295	.346	.286	8400-8730	2355	.371	.310
2400-2800	2295	.346	.287	8730-9100	2420	.385	.322
2800-3020	2295	.346	.283	9100-9500	2420	.385	.322
3020-3400	2355	.359	.300	9500-9900	2420	.392	.324
3400-3800	2355	.359	.300	9900-10,300	2420	.385	.322
3800-4200	2355	.359	.300				

Table C.5.7 Results from Fatigue Test on Beam 3

N.B. The Deflections shown in column C,D are the average of the deflections obtained from gauges C and D. (ref. figs. 5.7, 5.8, 5.9)

Increment Number	Applied Load (lbs)	Deflections (inches)		
		C	B	D
1	300	.019	.023	.019
2	600	.039	.045	.038
3	900	.063	.075	.062
4	1200	.096	.116	.094
5	1500	.150	.184	.147
6	1800	.228	.284	.225
7	2100	.305	.381	.301
8	2400	.385	.483	.381
9	2700	.532	.665	.521
10	3000	.908	1.147	.893
11	3150	1.179	1.496	1.157
12	3300	1.667		1.734
	Failure load 3440 lb.			

Table C.5.8 Results from static Test on Beam 3.

(ref. fig. 5.7, 5.10)

Increment Number	Average Load (lbs)	Deflections (inches)			Average Load (lbs)	Deflections (inches)			Average Load (lbs)	Deflections (inches)		
		C	B	D		C	B	D		C	B	D
1	198	.008	.009	.007	198	.008	.009	.007	198	.008	.010	.007
2	389	.016	.018	.016	368	.016	.018	.016	368	.016	.018	.016
3	565	.025	.027	.024	572	.024	.027	.025	559	.024	.027	.025
4	800	.034	.037	.035	788	.034	.038	.034	789	.034	.038	.035
5	994	.042	.049	.043	981	.042	.048	.043	994	.042	.049	.043
Speed 1 c.p.s.					Speed $1\frac{1}{2}$ c.p.s.				Speed $\frac{1}{2}$ c.p.s.			
200 cycles / increment					430 cycles / increment				150 cycles / increment			

Table C.5.9 Load - Deflection results from Dynamic elastic range tests on Beam 4.

Number of cycles	Average Load (lbs)	Deflections (inches)		Number of cycles	Average Load (lbs)	Deflections (inches)	
		B	C,D			B	C,D
0- 60	-	-	-	4800-4950	2690	.465	.408
60-252	326	.019	.019	4950-5150	2630	.465	.414
252-444	810	.042	.037	5150-5350	2690	.484	.429
444-636	1170	.057	.053	5350-5650	2690	.505	.446
636-828	1670	.087	.080	5650-6100	2690	.523	.463
828-908	2420	.215	.188	6100-6250	2630	.543	.478
908-1020	2420	.238	.199	6250-6650	2630	.555	.493
1020-1100	2570	.287	.255	6650-6850	2630	.576	.503
1100-1212	2520	.300	.255	6850-7350	2630	.603	.525
1230	2570	.371	-	7350-7535	2690	.628	.541
1240-1350	2690	.371	.315	7535-7650	2690	.655	.567
1350-1600	2690	.394	.340	7650-7770	2690	.684	.582
1600-1800	2690	.394	.340	7770-8220	2690	.688	.593
1800-2050	2690	.399	.358	8220-8820	2630	.706	.603
2050-2300	2740	.419	.367	8820-9120	2630	.726	.623
2300-2450	2690	.419	.364	9120-9340	2630	.745	.642
2450-2950	2690	.419	.367	9340-9580	2690	.778	.660
2950-3350	2690	.427	.379	9580-9760	2630	.810	.688
3350-3600	2740	.440	.392	9760-10,060	2630	.837	.719
3600-4000	2690	.460	.392	10,060-10,300	2690	.867	.743
4000-4500	2740	.460	.399	10,300-10,550	2630	.867	.743
4500-4800	2740	.465	.414	10,550-10,920	2570	.867	.743

Table C.5.10 Results from Fatigue Test on Beam 4.

N.B. The Deflections shown in column C,D are the average of the deflections obtained from gauges C and D. (ref. figs. 5.11. 5.13. 5.14)

Increment Number	Applied Load (lbs)	Deflections (inches)		
		C	B	D
1	-	-	-	-
2	310	.045	.052	.048
3	605	.128	.164	.126
4	915	.226	.282	.220
5	1210	.322	.401	.314
6	1520	.478	.595	.461
7	1830	.590	.732	.569
8	2120	.737	.914	.710
9a	2310			
b	1490	.864	1.062	.794
10	1810	1.110	1.360	.998
11	2030	1.478	1.825	1.309

Table C.5.11 Load - Deflection results from static test on Beam 4.

(ref. figs. 5.11, 5.15)

Increment Number	1	4	6	8	9B	10	11
Applied Load (lbs)	-	915	1520	2120	1480	1810	2030
Gauge A1	60	-280	-530	-710	-650	-810	-940
A2	170	250	450	670	1520	2310	3400
A3	470	1440	2560	3520	6060	9310	14010
A4	1310	5230	9140	12210			
A5	1670	6640	11530	150			
B1	100	-150	-430	-590	-550	-620	-780
B2	190	-170	-290	-460	-620	-740	1090
B3	280	930	1810	2750	2980	3090	3230
B4	380	1890	3500	5210			
B5	1070	2340	4210	6210			
C1	-100	-340	-840	-1020	-640	-710	-750
C2	- 20	- 40	60	130	210	190	220
C3	240	580	1090	1720	1770	1840	1880
C4	260	2050	2040	2990			
C5	260	1360	2040	3710			
Gauge 1	20	-260	-600	-770	-610	-710	-820
2	110	130	270	420	780	1080	1570
3	330	980	1820	2660	3600	4750	6370
4	650	3060	4890	6800			
5	1000	3450	5930	3360			

Table C.5.12 Strains produced in Beam 4 in static test

Units of strain : micro-strains
(ref. figs. 5.12, 5.16)

crement Number	Average Load (lbs)	Deflections (inches)			Average Load (lbs)	Deflections (inches)			Average Load (lbs)	Deflections (inches)			Average Load (lbs)	Deflecti (inches	
		C	B	D		C	B	D		C	B	D		C	B
-	55	.002	.002	.001	45	.002	.002	.001	50	.002	.003	.001	41	.001	.002
1	163	.006	.007	.005	157	.006	.007	.005	161	.006	.007	.005	161	.006	.007
2	368	.015	.016	.014	364	.015	.016	.014	358	.015	.016	.014	352	.014	.016
3	541	.023	.025	.023	531	.022	.025	.023	546	.023	.024	.022	525	.023	.025
4	785	.032	.035	.032	778	.032	.036	.033	772	.033	.035	.032	753	.032	.035
5	994	.039	.046	.041	980	.041	.047	.041	981	.039	.046	.040	963	.041	.045
Speed $1\frac{1}{2}$ c.p.s.					Speed $\frac{1}{2}$ c.p.s.				Speed 1 c.p.s.				Speed 2 c.p.s		
450 cycles / increment					150 cycles/increment				300 cycles/increment				480 cycles/increm		

Table C.5.13. Load - Deflection Results from Dynamic elastic range tests on Beam 5.

Number of cycles	Average Load (lbs)	Deflections (inches)		Number of cycles	Applied Load (lbs)	Deflections (inches)	
		B	C,D			B	C,D
0- 60	-	-	-	1790	2990	.593	
60- 300	430	.025	.021	1800	2990	.593	.516
300- 540	810	.039	.035	1810-1850	2950	.608	.541
540- 730	1190	.057	.050	1850-1900	2950	.644	.578
735	1440	.069		1900-1950	2900	.677	.608
740-1020	1560	.078	.069	1975	2950	.710	
1020-1260	1980	.117	.103	2000-2025	2950	.738	
1270	2250	.126		2025-2075	2900	.803	.700
1290	2420	.177		2075-2125	2840	.833	
1300	2310	.180	.155	2125-2175	2780	.841	.732
1300-1500	2250	.180	.155	2175-2225	2740	.845	
1510	2470	.242		2225-2275	2740	.841	.727
1520	2630	.279		2300	2690	.853	.740
1530	2690	.315		2325	2740	.905	
1540-1740	2630	.353	.310	2350	2690	.936	.812
1750	2780	.419		2375	2690	.994	
1760	2900	.426		2400	2690	1.020	.864
1770	2990	.486		2425	2570	1.020	
1780	2990	.563					

Table C.5.14 Results from Fatigue Test on Beam 5.

N.B. The Deflections shown in column C,D are the average of the deflections obtained from gauges C and D. (ref. figs. 5.11, 5.18, 5.19)

Increment Number	Applied Load (lbs)	Deflections (inches)		
		C	B	D
1	220	.056	.083	.064
2	390	.143	.199	.154
3	595	.223	.310	.244
4	780	.297	.413	.328
5	995	.386	.532	.431
6	1225	.489	.674	.550
7	1420	.580	.797	.655
8	1615	.666	.913	.753
9	1800	.764	1.043	.863
10	1990	.878	1.198	.998
11	2170	.972	1.323	1.103
12	(2370 (2180	1.066	1.463	1.247
13	2390	1.159	1.586	1.355
14	(2620 (2400	1.294	1.792	1.519

Table C.5.15 Load - Deflection results from static test on Beam 5

(ref. figs. 5.11, 5.20)

Increment number	Zero	3	6	8	9	10	11	13	14
Applied Load (lb)	-	595	1215	1610	1800	1990	2170	2390	2395
Gauge A1	-70	-320	-490	-610	-670	-720	-790	-850	-800
A2	170	150	220	290	330	380	410	440	310
A3	180	540	1090	1400	1600	2800	2960	2190	2610
A4	420	1130	1650	2120		3540			
A5	820	2260	3620	4820	6040				
B1	430	-110	-530	-750	-870	-990	-1190	-1460	-1400
B2	-40	- 60	- 40	- 30	- 10	- 10	- 10	- 30	- 120
B3	470	1080	1870	2310	2530	2720	2910	3230	3050
B4	680	1760	3140	3770		4520			
B5	1090	3410	5730	6950		8520			
C1	30	-540	-900	-1030	-1210	-1410	-1530	-1800	-1930
C2	810	1060	1430	1710	1820	1990	2100	2210	2040
C3	1100	2940	4700	5590	6100	6840	7680	9010	11220
C4	1400	2820	6150	7390		9180			
C5	1140	3280	5530	6670		8400			
D1	30	-290	-500	-610	- 700	-760	-840	- 940	-610
D2	290	350	410	470	540	520	520	600	310
D3	820	1980	3030	3600	4980	5230	6650	7340	7410
D4	1350	2360	6850	8310		9860			
D5	1810	5450	7730	10250		12150			
Gauges 1	105	-315	-605	-750	-860	-970	-1090	-1260	-1185
2	305	375	505	610	670	720	755	805	635
3	640	1635	2670	3225	3800	4400	5050	5440	6070
4	960	2017	4445	5395		6775			
5	1215	3600	5650	7170		8780			

Table C.5.16 Strains produced in Beam 5 in static Test.

Units of strain : micro-strains (ref. figs. 5.17, 5.21)

APPENDIX D.

Position	$\frac{dR}{dy}$ (lb/in)	x (in)	f(x)	E x 10^{-6} (p.s.i.)	E_{av} x 10^{-6} (p.s.i.)
A	9600	40	59,300	4.90	
B	8410	50	66,700	4.84	
Centre	8330	60	69,200	4.96	5.01
D	9000	50	66,700	5.16	
E	10200	40	59,300	5.21	

Table D.6.1 Calculations for the Modulus of elasticity (E) for the concrete in Beam 1, for the definition of $\frac{dR}{dy}$ and f(x) refer to section 6.1

Position	$\frac{dR}{dy}$ (lb/in)	x (in)	f(x) (in^3)	E x 10^{-6} (p.s.i.)	E_{av} x 10^{-6} (p.s.i.)
Centre	9080	60	69,200	5.42	
1A & 1B	9380	50	66,800	5.40	5.43
2A & 2B	10600	40	59,300	5.41	
3A & 3B	13250	30	48,000	5.48	

Table D.6.2 Calculations for the Modulus of Elasticity (E) for the Concrete in Beam 2.

Position	Speed (c.p.s.)	$\frac{dR}{dy}$	x	f(x)	E x 10^{-6}	E_{av} x 10^{-6}	Standard Deviation
B		9620	60"	69200	5.74		
C	$\frac{1}{2}$	11800	40"	59300	6.03	5.84	.13
D		11250	40"	59300	5.75		
B		10900	60"	69200	6.50		
C	1	11630	40"	59300	5.95	6.19	.23
D		11980	40"	59300	6.12		
B		10850	60"	69200	6.47		
C	$1\frac{1}{2}$	11900	40"	59300	6.08	6.16	.23
D		11600	60"	59300	5.93		

Table D.6.3 Calculations for the Dynamic Modulus of Elasticity (E) for the concrete in Beam 3.

Position	Speed (c.p.s.)	$\frac{dR}{dy}$	x	f(x)	Ex 10^{-6}	E_{av} x 10^{-6}	Standard Deviation
B		10450	60"	69200	6.23		
C	1	11360	40"	59300	5.81	5.94	.21
D		11300	40"	59300	5.78		
B		10200	60"	69200	6.08		
C	$1\frac{1}{2}$	11430	40"	59300	5.84	5.81	.23
D		10780	40"	59300	5.51		
B		10110	60"	69200	6.03		
C	$\frac{1}{2}$	11400	40"	59300	5.82	5.84	.14
D		11110	40"	59300	5.68		

Table D.6.4 Calculations for the Dynamic Modulus of Elasticity (E) for the Concrete in Beam 4.

Position	Speed (c.p.s.)	$\frac{dR}{dy}$	x	f(x)	E x 10^{-6}	E_{av} x 10^{-6}	Standard Deviation
B		10630	60"	69200	6.34		
C	$1\frac{1}{2}$	12030	40"	59300	6.15	6.16	.14
D		11730	40"	59300	6.00		
B		10440	60"	69200	6.23		
C	$\frac{1}{2}$	11730	40"	59300	6.00	6.01	.18
D		11330	40"	59300	5.79		
B		10710	60"	69200	6.39		
C	1	12030	40"	59300	6.15	6.28	.10
D		12350	40"	59300	6.31		
B		10710	60"	69200	6.39		
C	2	11480	40"	59300	5.89	5.96	.33
D		10950	40"	59300	5.60		

Table D.6.5 Calculations for the Dynamic Modulus of Elasticity (E) for the Concrete in Beam 5.

	Increment Number	4	6	7	8	10
	Applied Load	1.10	1.64	1.81	2.22	2.67
	Moment	27.5	41.0	45.3	55.4	66.6
Set A	Depth to N.A.(in.)	2.75	2.82	2.47	2.18	1.60
	e_c	170	320	480	680	1460
	Curvature	60	110	190	310	910
Set B	Depth to N.A.(in.)	3.00	2.72	2.33	2.00	1.59
	e_c	180	340	500	760	1380
	Curvature	60	130	220	380	870
Set C	Depth to N.A.(in.)	2.85	2.63	2.30	2.00	1.58
	e_c	180	360	510	750	1390
	Curvature	60	140	220	380	880
Set D	Depth to N.A.(in.)	2.95	2.50	2.22	2.03	1.62
	e_c	180	370	510	740	1430
	Curvature	60	150	230	360	880
	Average Curvature	60	130	220	360	870

Table D.6.6 Moment Curvature Relationships for Beam 1

Note: Units - Load : Kips
Moment : Kip-ins
e_c : Micro-strains
Curvature : Rad./in x 10^6

	Increment Number	4	6	16	17	24	25	26	27
	Applied Load	1.14	1.71	1.95	2.26	2.32	2.59	2.85	3.02
	Moment	28.5	42.7	48.7	56.5	58.0	64.7	71.2	75.5
Set A	Depth to N.A.(in.)	3.00	2.80	2.65	2.17	1.91	2.07	1.60	1.36
	e_c	160	250	330	510	800	900	1350	1830
	Curvature	50	90	120	230	420	430	840	1350
Set B	Depth to N.A.(in.)	3.50	3.20	2.95	2.13	1.93	1.69	1.42	1.23
	e_c	200	300	400	730	730	1040	1620	2300
	Curvature	60	90	140	340	380	620	1140	1870
Set C	Depth to N.A.(in.)	3.60	3.20	2.75	2.30	2.15	2.03	1.75	1.25
	e_c	190	320	450	820	820	1180	1700	2770
	Curvature	50	100	160	360	380	580	970	2220
Set D	Depth to N.A.(in.)	2.80	2.70	2.60	2.44	2.25	1.05	1.69	1.32
	e_c	170	260	350	530	530	810	1300	1830
	Curvature	60	100	130	220	240	440	770	1390
	Average Curvature	60	100	140	290	330	520	930	1710

Table D.6.7 Moment Curvature Relations ships for Beam 2

Note: Units - Load : Kips
Moment : Kip - ins
e_c : Micro-strains
Curvature: Rad/in x 10^6

	Increment Number	1	4	6	8	9b	10	11
	Applied Load	-	.92	1.52	2.12	1.48	1.81	2.03
Set A	Depth to N.A.(in.)	-	1.03	1.04	1.01	.80	.76	.72
	e_c	-	540	1000	1380	1720	2360	3060
	Curvature	-	520	960	1370	2150	2980	4150
Set B	Depth to N.A.(in.)	-	.99	1.12	1.07	.97	.97	.93
	e_c	-	290	770	1090	1110	1320	1700
	Curvature	-	290	690	930	1050	1360	1830
Set C	Depth to N.A.(in.)	-	1.63	1.45	1.39	1.28	1.31	1.28
	e_c	-	590	1400	1580	1060	1150	1270
	Curvature	-	360	960	1140	830	880	990
	Average Curvature	-	390	870	1150	1340	1740	2320
	Moment	-	22.9	38.0	53.0	37.0	45.2	50.7

Table D.6.8 Moment Curvature Relationships for Beam 4 following the fatigue test.

Note: Units - Load : Kips
Moment : Kip - ins
e_c : Micro-strains
Curvature: Rad./in x 10^6

	Increment Number	3	6	8	9	10	11	13	14
	Applied Load	.60	1.22	1.61	1.80	1.99	2.17	2.39	2.40
Set A	Depth to N.A.(in.)	1.18	1.17	1.17	1.17	1.17	1.17	1.16	1.22
	e_c	530	820	1050	1190	1300	1390	1520	1340
	Curvature	450	700	900	1020	1110	1190	1300	1120
Set B	Depth to N.A. (in.)	1.58	1.50	1.50	1.50	1.50	1.50	1.50	1.56
	e_c	140	810	1020	1310	1480	1780	2170	2020
	Curvature	90	540	680	870	990	1190	1450	1290
Set C	Depth to N.A.(in.)	.84	.89	.87	.90	.91	.92	.93	1.00
	e_c	1320	2020	2380	2610	3070	3310	3830	3860
	Curvature	1570	2300	2740	2900	3380	3600	4120	3860
Set D	Depth to N.A.(in.)	.96	1.04	1.06	1.06	1.08	1.11	1.10	1.18
	e_c	600	940	1140	1330	1410	1530	1740	1080
	Curvature	640	900	1080	1250	1300	1380	1580	920
	Average Curvature	690	1110	1350	1510	1700	1840	2110	1800
	Moment	14.9	30.4	40.3	45.0	49.8	54.3	59.8	59.9

Table D.6.9 Moment Curvature Relationships for Beam 5 following the fatigue test.

Note: Units - Load : Kips
Moment: Kip - ins
e_c : Micro-strains
Curvature: Rad./in x 10^6

Moment Kip - ins	Per cent of ult. Moment	Depth to N.A. (in.)	Strain in extreme compressive fibre e_c	Stress in extreme compressive fibre f_c (p.s.i.)	$\frac{f_c}{f_c'}$ (%)	f_{s2} (k.s.i.)	f_{s1} (k.s.i.)	$\frac{f_{s1}}{f_{su}}$	Curvature ϕ
83.7	100	1.37	.0029	7190	94.0	181	233	93.2	.00212
78.9	94.2	1.47	.0020	7000	91.5	165	223	89.2	.00133
76.1	90.8	1.58	.0017	6550	85.6	160	217	86.8	.00108
75.0	89.6	1.63	.0016	6320	82.5	159	215	86.0	.00098
70.2	83.9	1.84	.0013	5580	72.9	153	206	82.4	.00071
63.8	76.2	2.10	.0011	4920	64.3	147	193	77.2	.00052
60.3	72.0	2.36	.0009	4190	54.7	147	184	73.6	.00038
55.7	64.0	2.63	.0007	3360	43.9	144	175	70	.00027

Table D.6.10 Stresses and Strains in the steel and concrete of the beams tested.

Note: f_c' is the cylinder crushing strength

f_{s1} is the stress in the bottom steel

f_{s2} is the stress in the top steel

f_{su} is the ultimate steel stress.